PDR

EGG-CAAD-5857

May, 1982

TRAC-BD1 VERSION 11 CODE ASSESSMENT CALCULATIONS OF GENERAL ELECTRIC TLTA ECC/NO ECC TESTS 6425 AND 6426

NRC Research and/or Technical Assistance Rept

E. Holcomb

U.S. Department of Energy
Idaho Operations Office • Idaho National Engineering Laboratory

This is an informal report intended for use as a preliminary or working document

Prepared for the
U.S. Nuclear Regulatory Commission
Under DOE Contract No. DE-AC07-76ID01570
NRC FIN No. A6047

EG&G Idaho

EG&G Idaho, Inc.

FORM EG&G 398
(Rev. 03-82)

INTERIM REPORT

Accession No. _____

Report No. EGG-CAAD-5857

Contract Program or Project Title: NRC Technical Assistance Program Division

Subject of this Document:

TRAC-BD1 Version 11 Code Assessment Calculations of General Electric TLTA ECC/No ECC Tests 6425 and 6426

Type of Document:

Technical Report

Author(s):

E. Holcomb

Date of Document:

May, 1982

Responsible NRC Individual and NRC Office or Division: F. Odar

This document was prepared primarily for preliminary or internal use. It has not received full review and approval. Since there may be substantive changes, this document should not be considered final.

EG&G Idaho, Inc.
Idaho Falls, Idaho 83415

Prepared for the
U.S. Nuclear Regulatory Commission
Washington, D.C.
Under DOE Contract No. DE-AC07-76ID01570
NRC FIN No. 6047

INTERIM REPORT

ABSTRACT

In this report, the results of TRAC-BD1 Version 11 code assessment calculations for the General Electric Two Loop Test Apparatus ECC/NO ECC tests are documented. The predictive capability of the code is assessed by comparison of calculated results to experimental data. Evaluation of and probable causes for the differences in the experimental behavior with and without ECC injection are given. The study described in this report has been performed as part of the Idaho National Engineering Laboratory's support to the Nuclear Regulatory Commission for the independent assessment of advanced, best estimate, reactor safety analysis computer codes.

Prepared for the
U.S. Nuclear Regulatory Commission
Under DOE Contract No. DE-AC07-76ID01570
NRC FIN No. 6047

SUMMARY

In this report, calculations are documented for the purpose of assessing the Transient Reactor Analysis Code, TRAC-BD1 Version 11, and to aid in the understanding of the differences in experimental behavior with and without emergency core cooling. TRAC-BD1 Version 11 is an advanced best estimate computer program which was developed at the Idaho National Engineering Laboratory for the purpose of simulating the thermal-hydraulic behavior of boiling water nuclear reactors. The tests chosen for the calculations documented herein were General Electric (GE) integral systems Tests 6425 and 6426, experiments performed in the subscale, non-nuclear Two Loop Test Apparatus (TLTA) in San Jose, California. These calculations were part of the EG&G Idaho, Inc., Code Assessment and Applications Division's program for the overall assessment of TRAC-BD1.

The overall results of these calculations were qualitatively good. TRAC-BD1 answered the important question why the NO Emergency Core Coolant (ECC) test depressurized faster than the ECC test. It was found that the slower depressurization rate in the ECC test was directly correlatable to the jet pump exit pipe void fraction. As the lower plenum refilled, the liquid carryover to the drive side break was greater. This reduced the volumetric break flow substantially, and the ensuing vessel depressurization rate was slower.

Relative to the code assessment objective of this study, we believe the results herein show TRAC-BD1 is an advancement in the basic capability of best estimate computer codes for BWR safety analysis in that the code correctly modeled the qualitative behavior of the subscale experiment. However, the study did identify several specific limitations as described below.

The break flow model contained in Version 11 requires further improvement for subcooled and two phase flow conditions. Single phase vapor break flow was well calculated by the code and the importance of the choking model was demonstrated.

The high void fraction heat transfer characterization of the code is considered to be adequate; however, the calculation of the heater rod temperature response during reflood was not. The results of this study were not sufficient to determine if this response was dominated by the heat transfer or hydraulic calculations or a combination of both. Further code development and assessment effort is required in this regard.

The code characterization of subcooled ECC injection was found to be atypical of the experiment. No general modeling solution within the Version 11 capabilities was found. Such a solution may exist with the Version 12 control system capability and further work in this area should be performed.

The results herein indicate consistency in the initial system conditions is influential in the transient calculations. From an operational view point the lack of an automatic steady state initialization feature in Version 11 is a significant limitation. Resolution of this limitation is likely with the control system capability of Version 12 and should be effected.

ACKNOWLEDGEMENT

The author is indebted to Messrs. R. J. Dallman, R. W. Shumway, J. W. Spore, and P. D. Wheatley, whose development of the TLTA model laid the foundation for the work described herein.

CONTENTS

FIGURES

TABLES

1. INTRODUCTION

The primary purpose of Tests 6425 and 6426 was to measure the effects of ECC injection on the behavior of the subscale, non-nuclear TLTA system in a design basis accident blowdown under conditions of average initial bundle power.

The purposes of this study were to use the TRAC-BD1 computer code to help understand the experimental results and to assess the quality of the code's calculations by comparison to the test data.

Originally, the intended scope of this project was to perform a rapid assessment calculation which would answer the question why the NO ECC Test 6426 depressurized faster than the ECC Test 6425. However, the project scope had to be expanded due to the difficulties encountered in running Version 11 of TRAC-BD1. Therefore, the information documented herein includes the additional break flow and initialization sensitivity studies required to perform the calculations, as well as the transient calculation results required by the key code assessment parameter list desired by the Nuclear Regulatory Commission (NRC).

Section 2 of this report condenses the General Electric TLTA facility description given in Reference 4. Section 3 opens with a discussion of the TRAC-BD1 model of the TLTA facility. Initialization of the model is next discussed, beginning with the break flows and the blowdown system in Section 3.1.1. In Section 3.1.2, the modeling of the delayed opening of the recirculation pump discharge valve in Test 6426 is discussed. Detailed information regarding this equipment problem can be found in Appendix J of Reference 3, which also contains the data for Tests 6425 and 6426 in Appendices E and G. Section 3 concludes with a summary of the limitations of the calculational model of the TLTA facility which was used for these assessments.

In Section 4, the transient calculation results are presented. In Section 4.1, comparisons are made with the sequences of the test events, the ECC mass flow rates, and the vessel differential pressures, the last for purposes of level definition. In Section 4.2, the break inlet conditions are discussed preparatory to a discussion of the break flow comparisons in Section 4.3. The depressurization calculations are presented in Section 4.4. In Section 4.5, the ECC modeling is discussed. In Section 4.6, the rod temperature comparisons are made. Specific conclusions and recommendations resulting from these assessment calculations are given in Section 5. Finally, the references for this report are listed in Section 6.

2. A DESCRIPTION OF THE TLTA FACILITY

The purpose of this section is to give the reader a brief description of the TLTA facility preparatory to a discussion of the TRAC-BD1 model of the installation. For a detailed facility description, the reader is referred to Reference 4.

The General Electric Two Loop Test Apparatus is a non-nuclear scaled facility whose primary mission is the simulation of the thermal-hydraulic phenomena of a BWR/6-218 boiling water reactor (BWR).

The reference BWR/6 had 624 fuel rod bundles. Since the TLTA facility had one heater rod bundle, the primary scaling factor became 1/624 for dimensions, volumes, and power levels in the TLTA installation. Proper scaling of the TLTA configuration was a primary design criterion and was rigidly adhered to as far as was practicable.

A schematic of the TLTA facility is shown in Figure 1. The principal components were the vessel, heater rod assembly, jet pumps, recirculation loops, blowdown lines, feedwater and ECC injection systems, and instrumentation system.

Demineralized feedwater was supplied to the test apparatus by the feedwater pump. Flow into the vessel was regulated by a flow control valve which was operated by temperature probes in the vessel downcomer. Fluid discharge from the system was normally through the main steam line at the top of the vessel. The TLTA steam discharge system had three separate configurations which allowed the simulation of a design basis accident (DBA), a steam line break, or a small break situation. In the DBA configuration, a pressure control valve and a pressure regulator acted in tandem to simulate the closing of the main steam isolation valve and the turbine control valve in the reference BWR/6.

The ECC injection system consisted basically of the High Pressure Core Spray (HPCS), Low Pressure Core Spray (LPCS), and Low Pressure Coolant Injection (LPCI) multistage turbine injection pumps and attendant piping.

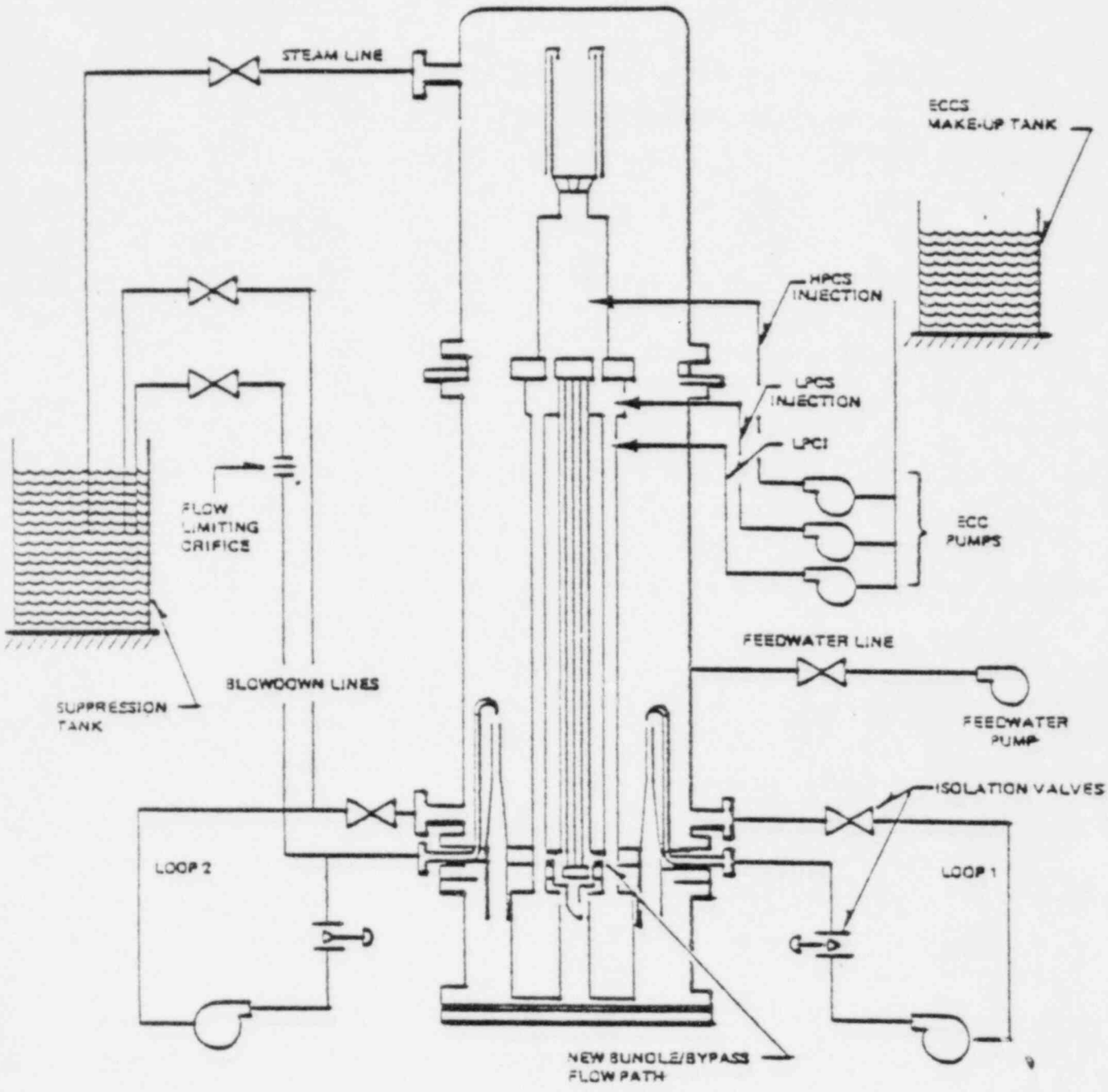

Figure 1. *Two-Loop Test Apparatus Configuration 5A (TLTA-5A) with Emergency Core Cooling Systems*

The proper scaled flow rate was provided in each case by a network of control valves and bypass lines. LPCI fluid entered the vessel at the top of the core bypass tubes at an elevation of 4.95 meters above the vessel base for BWR/6 simulations. The HPCS and LPCS injection lines discharged into the upper plenum and the mixing plenum, at elevations of 5.82 meters and 5.24 meters, respectively, in the TLTA-5A configuration. Vessel penetrations existed to plumb both of these systems for injection into the mixing plenum if desired. The ECC systems were activated by timers in TLTA, and injection into the vessel began when it depressurized below the rated head of the injection pumps.

The TLTA recirculation loops contained a centrifugal drive pump, a downstream orifice for flow measurement, valves for flow control and pump protection and interconnecting piping. The recirculation loop valves were automatically closed during a LOCA test by timing circuits which tripped the valve actuators.

Each recirculation pump drove its own jet pump. The drive flow entered the vessel at the 1.37 meter elevation and continued upward through the drive line riser to the top of the jet pump, near the 2.0 meter elevation. It then made a 180 degree turn through the ramshead and entered the jet pump through the drive nozzle. Upon exit from the nozzle the drive flow combined with jet pump suction flow from the downcomer; both were diffused and discharged into the vessel lower plenum.

The two TLTA blowdown lines extended from the suction and discharge sides of the broken loop recirculation pump to a suppression tank. Blowdown discharge exited through globe valves, which were opened by independent actuators to initiate a DBA test. These blowdown valves opened in less than 0.1 second. The recirculation pump discharge side blowdown line had a small diameter restricting orifice to reduce the flow out the jet pump drive line to the proper scaled value. The recirculation pump suction side blowdown line had a flow nozzle installed adjacent to the vessel. The flow nozzle had a 0.178 meter long throat to aid in establishment of thermodynamic equilibrium of the flow.

The vessel was cylindrical, 0.41 meter inside diameter, and approximately 7.85 meters tall from the base of the lower plenum to the top of the steam dome. The lower plenum contained four identical guidetubes of 0.135 meter inside diameter. Flow from the lower plenum entered each guidetube near its top through a small side entry orifice which was 0.00432 meter in diameter. The guidetubes connected the lower plenum to the fuel rod bundle bypass region. This bypass region consisted of four tubes of elliptical cross section which connected to the mixing plenum near the top of the core.

The heater rod assembly consisted of an 8 x 8 bundle with 62 electrically heated rods of 0.0123 meter diameter. Two 0.0150 meter unheated rods simulated BWR water rods, but no flow was permitted through these in the TLTA facility. The rods were arranged in a square lattice with a pitch of 0.0162 meter. The rod bundle was housed inside a 0.0072 meter thick square alumina channel which was itself sheathed in a 0.0188 meter thick stainless steel channel. The rods were spaced internally with GE prototype BWR spacers.

The rods were 4.08 meters long and were heated over 3.81 meters of their length. Excluding the water rods, three rod types existed within the bundle with separate local/average power peaking factors to simulate the power distribution of the reference BWR/6. The TLTA bundle followed a chopped cosine axial power profile with an axial power peaking factor of 1.387.

There was a plenum at the base of the stainless steel rod housing channel with a flow tube which protruded into the vessel lower plenum. The flow tube had a 0.062 meter diameter entry orifice which admitted lower plenum flow to the rod bundle. The channel base plenum also had four small holes (0.0075 meter diameter) which connected the fuel rod bundle to the bypass tubes. The top of the heated rod bundle terminated near the upper tie plate. This tie plate was located at the base of the mixing plenum and served as a restrictor for channel flow.

The downcomer was formed by the space between the vessel, the heater rod assembly, and the bypass tubes. It extended from the jet pump support

plate, which separated the downcomer from the lower plenum, to the top of the upper plenum. Radial flow was prevented across this interval. There were three intervals of interest in the downcomer. The lowest interval was the region between the jet pump support plate and the jet pump suction inlet. Here the recirculation pump suction lines entered the vessel opposite the jet pump diffuser, made a downward 90° turn, and picked up fluid at the base of the downcomer. The lower downcomer was a crowded region. It housed the jet pumps, the recirculation pump suction inlets, and the four heater rod bypass tubes.

The central downcomer section consisted of the region above the jet pump suction and below the feedwater sparger. Subcooled feedwater entered the downcomer approximately 0.4 meter above the jet pump suction and mixed with saturated liquid flowing downward from the overlying separation regions. The third downcomer region was the annulus above the feedwater inlet. It extended to the top of the upper plenum and provided a flow path for liquid discharged from the steam separator.

The steam/water mixture generated in the heater rod assembly flowed through the bundle tie plate and the upper plenum and entered the steam separator. Steam continued upward to the vessel dome, while a swirling motion was imparted to the liquid by static vanes near the separator base. The liquid was thrown outward and was diverted back to the downcomer at several elevations along the separator by a system of concentric annuli and entrainment flanges.

The TLTA system was heavily instrumented with differential pressure cells and thermocouples. Static pressure instruments were located in the steam dome, the upper and lower plenums, and in the broken loop recirculation pump suction line. Most of the automatic valves in the facility had positioners which provided signal input data. Each recirculation pump had a tachometer.

Virtually all flows, densities, fluid levels, and void fractions reported in the TLTA data were derived from the differential pressure cells. The only places where independent flow information was available in

the facility were on the broken loop recirculation pump suction and drive lines. There were a turbine meter and a drag disc at both of these locations. There was no gamma densitometer in the installation.

3. THE TRAC-BD1 MODEL OF THE TLTA FACILITY

The TRAC-BD1 model of the TLTA facility is shown in Figure 2. The full model consisted of 28 components and 33 junctions and represented the vessel, recirculation loops, feedwater and ECC injection systems, and the steam and blowdown lines. The full component model was used for the steady-state calculations. For the transient calculations, Valves 22 and 23 were removed from the model to reduce the computational costs.

Feedwater was supplied to the vessel from a constant velocity fill which delivered subcooled liquid to a 1.0 meter long feedwater pipe. The feedwater flow was ramped linearly to zero within 0.5 second of the onset of the transient calculation. The HPCS, LPCS, and HPCI systems were modeled similarly, with the important exception that these fills employed pressure-velocity tables for control of ECC injection. Thus, the accuracy of the ECC timing calculation was dependent upon the accuracy of the vessel depressurization calculation.

The flow out the top of the vessel was controlled by the pressure at Break 19, which was fixed at 7.1 MPa. Flow could also be controlled by Valve 18, but a fully open configuration was used in this assessment calculation, with no attempt made to model restrictions near the vessel. For the transient calculation, this valve was closed by 9 seconds, ramped linearly to the shut position according to differential pressure data and the valve positioner signal.

The recirculation loops contained the drive pumps, piping, and valving. Two valves were used in the intact loop, one each on the pump discharge and suction sides. A single valve was used in the broken loop on the discharge side of the recirculation pump. These valves were all fully open for the steady-state calculation. They were closed during the transient calculation, again according to differential pressure or valve positioner data. Valves 1 and 48 isolated the intact loop by 21 seconds. Valve 6 was closed within 1.2 seconds for Test 6425. In Test 6426 this valve malfunctioned and remained open for the first 25 seconds of the

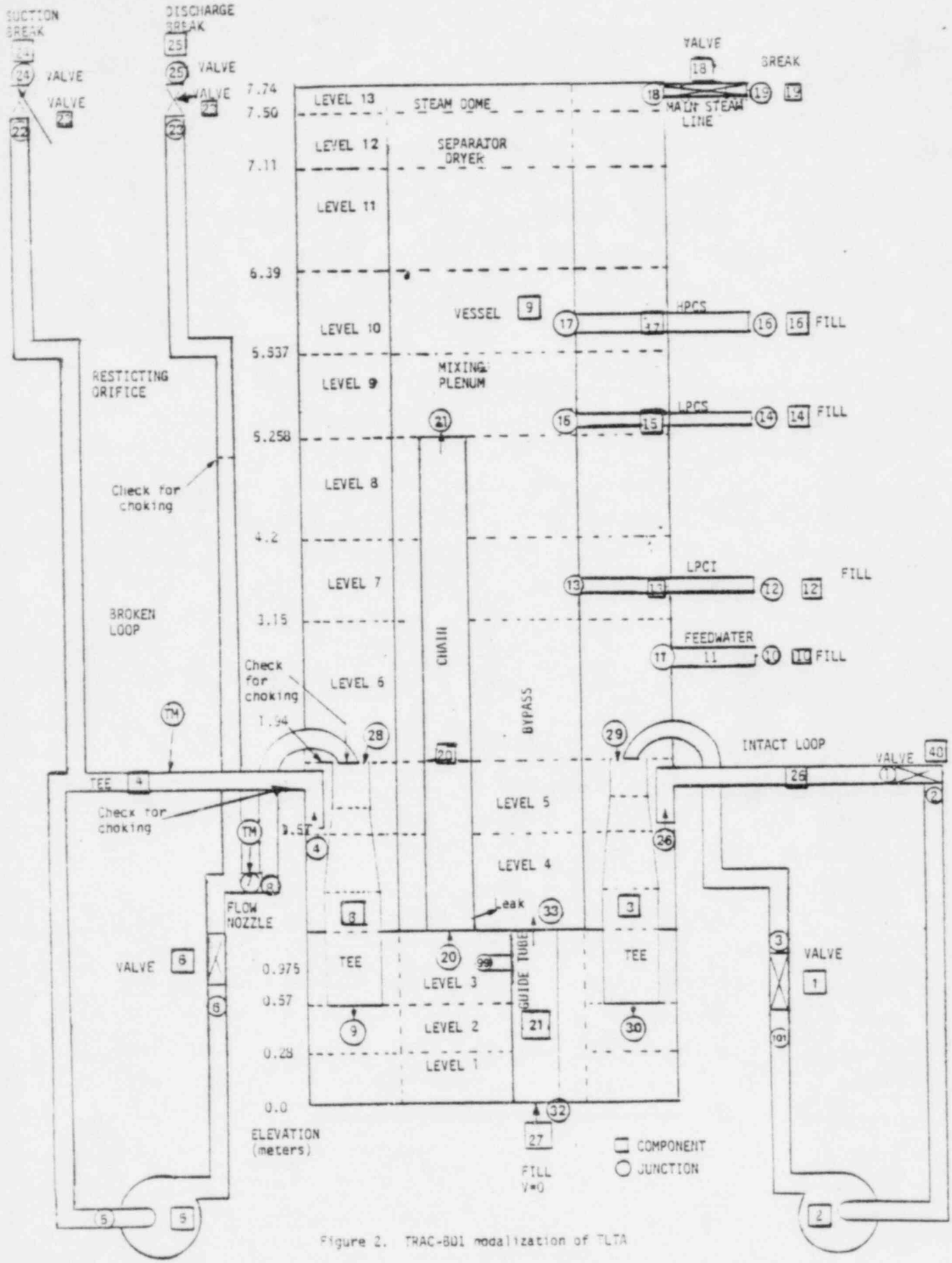

Figure 2. TRAC-B01 modalization of TLTA

test. The modeling of this behavior is further discussed in Section 3.1.2. The recirculation pumps had their speeds adjusted to achieve proper jet pump flows during the steady-state calculation. The pump speeds followed tables for the transient calculation which were derived from the tachometer data. These tables were normalized to the adjusted pump speeds from the steady-state calculation.

The TLTA blowdown system was modeled by the side legs of Tees 4 and 7, which were connected to the blowdown valves. As mentioned, Valves 22 and 23 were used for the steady-state calculation only, during which they remained closed. These blowdown valves were removed from the model at the onset of the transient calculation. The main reason for doing this was that it was very difficult to open these valves in TRAC-BD1. The blowdown valves in the TLTA facility were designed to open within 0.1 second. Initial upstream pressures were over 7.2 MPa, while the downstream sides of the valves were at atmospheric conditions. To open these valves in the TRAC model, timesteps of 0.01 millisecond would have been necessary, independent of whether the choking option was employed or not. This would have been very expensive, particularly since multiple runs were necessary in the transient calculation initialization process. Consequently, Breaks 24 and 25 were employed at the ends of Tees 4 and 7, with pressures which were ramped to atmospheric during the first half second of the transient calculation. This modeling method had two disadvantages. First, the pressure profile was not correct. Second, the system saw the full pipe area open to flow immediately at the break, which was not the actual case. In reality, the valves opened rapidly, but not instantaneously to an area which was less than the full bore of the blowdown pipe, and this behavior was not modeled.

The drive side blowdown line had a restriction orifice which was modeled by the last cell face in the secondary of Tee 7. The actual flow area was used, and this face was coupled directly to Break 25. Use of the choking option at this face gave best results. The long throat flow nozzle, located adjacent to the vessel in the broken loop recirculation pump suction line, was modeled by Cells 1 and 2 in the primary side of Tee 4. The actual throat flow area was used, with the choking option

invoked at the minimum area cell face. The downcomer suction pipe, the nozzle converging section, and the nozzle throat were combined into one cell. On the downstream side, one cell was used for pressure recovery in expanding the flow area from the throat to the 0.08 meter nominal pipe size.

The TLTA vessel was treated as a cylindrical geometry in axisymmetric flow. There were 13 axial levels, two radial rings, and one azimuthal segment for a total of 26 vessel cells. The lower plenum was modeled by the first three axial levels. Four guidetubes provided the flow path from the lower plenum to the bypass. The guidetubes were combined into one flow path of equivalent area for modeling purposes. The guide tube side entry orifices were modeled by the single-celled secondary of Tee 21. The vessel-to-tee heat transfer option (IPVHT = 1) was invoked for both the primary and secondary of Tee 21. There were a total of five primary cells in the guidetube, three of which were in vessel Level 3.

The downcomer was modeled by Levels 4 through 11 in the outer radial ring. The only communication between the lower plenum and the downcomer was through the two jet pumps. The standard, five-celled TRAC-BD1 jet pump model was used without modification.

The electrically heated bundle was modeled in TRAC by an eight-celled Chan component which extended from vessel levels 3 to 9. The protrusion connecting the lower plenum to the bundle was modeled in TRAC-BD1 by the first cell of the Chan component. The 0.062 meter diameter bundle inlet orifice was used for the flow area of the first Chan cell face. Actual hydraulic diameters were used in the Chan component for the bundle inlet orifice, the bundle itself, and the upper tie plate. However, the bundle hydraulic diameter did not take the grid spacers into account, and the flow through the bundle had to be regulated by the FRIC parameter. The bundle flow, pressure drop, and the lower plenum pressure were quite sensitive to the FRIC value used in the Chan. The FRIC parameter was set to zero across the bundle inlet orifice. The total FRIC value input to the Chan component was apportioned between the bundle and the upper tie plate according to the differential pressure data.

The lowest Chan level was unheated . There were three heat transfer nodes in the channel wall. The Biasi or CISE-GE-Xc correlation was used for the critical heat flux calculation. Wall-to-fluid heat transfer from the outside channel wall was ignored in this calculation due to a coding error in TRAC-BD1 Version 11.

Each fuel rod was divided into five radial nodes. The innermost node was 304 stainless steel, followed by the gap, then three Inconel 718 nodes. The metal-water and fuel-cladding interactions were turned off. No fine mesh calculation was performed.

The channel was comprised of five rod groups for modeling the single 8 x 8 bundle. The rod-to-rod power distribution, CPOWR, was unity for all rods. The axial power distribution, ZPOWR, followed a cell-centered chopped cosine profile. The centerline-to-surface radial power distribution, RDPWR, lumped the power generation in the outermost cell for all rods.

A radiation heat transfer calculation between rod groups was performed every 100 timesteps. Steam and droplets were ignored in this calculation. View factors were corrected for anisotropic reflection.

3.1 Initialization of the TRAC-BD1 Model

In this section, initialization of the TRAC-BD1 model is discussed. As used herein, initialization can refer both to the steady-state and transient calculations. Although separate initialization procedures were necessary for both calculational modes, iteration between the two often proved necessary. For example, an apparently good steady-state calculation would produce erroneous transient results, necessitating recalculation of the steady state. Because of the interrelationship between the two modes, the initialization discussion in the sequel will couple both the steady-state and transient modes.

Steady state operating conditions were not established prior to running TLTA Tests 6425 and 6426. The water level in the downcomer was dropping at the start of each test. Additionally, the power level was increased from 2MW to 5MW prior to starting the test, as the 5 MW power level could not be tolerated for long periods because of insufficient feedwater pump capacity. These test conditions necessitated the duplication of instantaneous test conditions in the TRAC-BD1 steady-state runs rather than initialization of the code to stable pre-test measurements. The transient pre-test operating conditions made it extremely difficult to initialize the code.

The first attempts to initialize Test 6425 made use of the differential pressure (DP) data because these were believed to be the most accurate. By opening the main steam valve, adjusting the pressure in Break 19, reducing the feedwater flow rate, and adjusting the bundle FRIC values, an acceptable initialization was obtained. The steady-state vessel pressure distribution was quite good and generally within the data uncertainties, so the Test 6425 transient calculation proceeded.

Test 6426 was next initialized and run for the first 25 seconds of the transient. Agreement with the vessel depressurization data was much better than Test 6425, and it was discovered that the transient results were highly dependent upon the downcomer void fractions calculated from the steady-state run.

Attempts were next made to reinitialize the downcomer voids for Test 6425. This proved to be a trial and error process. Due to the transient pre-test operating conditions discussed above, it was found that the steady-state calculated void fractions and subcooling in the downcomer were dependent on the initial voids input to TRAC-BD1 at time zero and also on the duration of the steady-state run. The downcomer voids proved especially sensitive to their initial input values, and effecting an initialization in this manner was time consuming and expensive.

The results of the Test 6426 initialization suggested that a revised vessel noding be attempted. A cell was added at the 2.50 meter level, just

above the feedwater injection point. While this improved the water level definition, the voids were once again determined by the initial conditions, and the subcooling in the downcomer was not correct.

The final attempt at the steady-state initialization of Test 6425 involved running TRAC-BD1 in the transient mode and made use of the downcomer level trip option. Based on differential pressure data, the water level at time zero was 2.16 meters above the base of the downcomer, the latter defined by Level 3 in the vessel model. This assumed a sharp liquid-vapor interface in the downcomer, neglected the velocity of the falling water level, and assumed there was no vapor carryunder to the lower levels. These assumptions appeared reasonable based on the data, and an initialization run was made for 25 seconds.

The results of several downcomer void fraction initialization attempts are summarized in Table 1. Case A was a steady-state run in which the downcomer voids were left as calculated by TRAC-BD1. In Case B the void fractions were manually set to the values shown. Case C was reached with the downcomer level trip option invoked. The differences in voids between Cases A and C were sufficient to render the Case C vessel internal pressure distribution incorrect. Also, neither Case A nor C produced an accurate transient calculation. No calculational solution could be effected which would yield the correct downcomer void fractions. Manual initialization was necessary, and the Case B values were believed reasonable in terms of the data with the exception of Level 6. The dependency of the transient results on the Level 6 void fraction is further discussed in Appendix A.

In summary, the manual reset procedure of Case B was necessary because of the uneconomical trial and error procedures involved in initialization of the downcomer conditions. It is recommended that the control system now employed in Version 12 of the TRAC-BD1 code be used for future initializations of TLTA tests, and that a calculational solution be attempted for the downcomer initialization. However, successful use of the control system presumes that true steady-state conditions are established prior to starting a test.

TABLE 1. TLTA TEST 6425 VOID FRACTION INITIALIZATION

Level	Data	TRAC Case A	TRAC Case B	TRAC Case C[a]
1	0.0	0.0	0.0	0.0
2	0.0 - 0.1	0.095	0.0	0.06
3	0.0 - 0.3 (Guidetube)	0.0/0.14 GT/LP	0.0	0.096
4	0.0 (Bypass)	0.05	0.0	0.089
5	--	0.33	0.0	0.21
6	0.0	0.31	0.89	0.196
7	--	0.90	0.89	0.88

a. Downcomer level trip set at 2.16 m.

The remainder of the initialization for Tests 6425 and 6426 is shown in Tables 2 and 3. In general, the pressure data were more important than the flow data because the former were direct measurements whereas the latter were generally derived from differential pressure cells.

The Test 6425 initialization was generally quite good. The approach was to input the actual values of flow area and hydraulic diameter as closely as these were known from physical drawings of the TLTA facility. To calculate the correct bundle pressure distribution, bundle FRIC values calculated from Reference 1 were proportioned according to the DP cell measurements and adjusted uniformly until the correct pressure drop was calculated. The resultant total bundle FRIC value used for Tests 6425 and 6426 was 0.09.

A trial and error approach was necessary in the adjustment of the FRIC parameter, but it was methodical and without the problems discussed in the downcomer initialization. Use of the FRIC parameter in the bundle and a pressure boundary condition at the main steamline were two of the most important items in achieving the correct vessel internal pressure distribution.

Upon examination of the last four initialization parameters in Tables 2 and 3, it was evident that Test 6425 was better initialized than Test 6426 as far as the vessel pressure drops were concerned. The correct vessel pressure distribution depended on the calculated void fractions and the degree of subcooling in the downcomer, i.e., the vessel water level. Accordingly, varying the steady-state time zero voids (α) and liquid temperatures (TL) affected the vessel pressure drops. As α and TL were changed in attempts to improve the 6425 downcomer initialization, so changed the vessel pressure distribution. Test 6425 was first initialized to obtain the correct vessel pressure drops as the supporting data were more precise than the water level measurement. However, correct initialization of the downcomer void fraction proved to be the more important factor for the transient calculation. Test 6426 was initialized after 25 seconds of the Test 6425 transient calculation were run. Because of the transient results, more attention was paid to downcomer initialization in Test 6426 at the expense of the vessel pressures. The

TABLE 2. INITIALIZATION OF TLTA TEST 6425

Parameter	TLTA	TRAC-BD1
Bundle power	5.02 - 5.08 MW	5.05 MW
Steam dome pressure	7.164 - 7.233 MPa	7.215 MPa
Lower plenum pressure	7.350 - 7.419 MPa	7.357 MPa
Lower plenum enthalpy	1216.4 - 1239.6 kJ/kg	1247.5 kJ/kg
Feedwater enthalpy	90.4 - 99.6 kJ/kg	94.0 kJ/kg
Bundle DP	0.076 - 0.079 MPa	0.083 MPa
Steam flow	2.27 - 3.18 kg/s	2.63 kg/s
Feedwater flow	0.50 - 0.77 kg/s	0.51 kg/s
Intact loop drive pump flow	3.68 - 4.58 kg/s	4.40 kg/s
Broken loop drive pump flow	3.36 - 4.27 kg/s	4.05 kg/s
Intact loop jet pump flow	9.07 - 10.89 kg/s	9.47 kg/s
Broken loop jet pump flow	8.17 - 10.0 kg/s	8.55 kg/s
Bundle inlet flow	15.43 - 19.96 kg/s	17.82 kg/s
Flow nozzle DP	0.146 MPa	0.420 MPa
Core bypass inlet DP	0.051 MPa	0.050 MPa
Bundle inlet orifice DP	0.033 - 0.044 MPa	0.032 MPa
Core bypass DP	0.034 MPa	0.035 MPa
Lower plenum/Guidetube DP	0.075 - 0.089 MPa	0.077 MPa

TABLE 3. INITIALIZATION OF TLTA TEST 6426

Parameter	TLTA	TRAC-BD1
Bundle power	5.02 - 5.08 MW	5.06 MW
Steam dome pressure	7.164 - 7.233 MPa	7.219 MPa
Lower plenum pressure	7.329 - 7.398 MPa	7.337 MPa
Lower plenum enthalpy	1211.7 - 1235.0 kJ/kg	1244.8 kJ/kg
Feedwater enthalpy	148.3 - 157.6 kJ/kg	153.6 kJ/kg
Bundle DP	0.075 - 0.076 MPa	0.071 MPa
Steam flow	2.27 - 3.18 kg/s	2.68 kg/s
Feedwater flow	0.45 - 0.73 kg/s	0.46 kg/s
Intact loop drive pump flow	3.27 - 4.17 kg/s	3.54 kg/s
Broken loop drive pump flow	3.36 - 4.27 kg/s	3.97 kg/s
Intact loop jet pump flow	6.35 - 8.17 kg/s	7.37 kg/s
Broken loop jet pump flow	8.17 - 9.98 kg/s	8.63 kg/s
Bundle inlet flow	12.70 - 17.24 kg/s	15.91 kg/s
Flow nozzle DP	0.170 MPa	0.368 MPa
Core bypass inlet DP	0.048 MPa	0.039 MPa
Bundle inlet orifice DP	0.029 - 0.041 MPa	0.025 MPa
Core bypass DP	0.036 MPa	0.035 MPa
Lower plenum/Guidetube DP	0.068 - 0.077 MPa	0.060 MPa

initial vessel pressure distribution could possibly have been improved in Test 6426 were the bundle FRIC parameter adjusted differently from Test 6425. This was not deemed appropriate, because FRIC was a geometrical parameter, and the geometry was the same for both tests.

Inspection of Table 3 reveals that the initialization of Test 6426 for the TRAC-BD1 calculation was generally very good. The calculated lower plenum enthalpy was too high, reflecting the calculation of too little lower plenum subcooling. The feedwater flow rate was purposely set at the low end of the tolerance to bring the water level down to the correct level in the 12-seconds run time allowed for this initialization calculation. Minor problems were apparent in the calculated pressure drops in the vessel and heated bundle. Although the bundle flow was within tolerance, the calculated pressure drop was slightly low. Likewise, calculated pressure drops across the bypass inlet, the bundle inlet orifice, and from the lower plenum to the guidetube were also too low. These miscalculations were attributed in part to the uncertainties in the data, but the vessel internal pressure drops were in general more sensitive to the calculated water level (void distribution) in the downcomer.

3.1.1 Break Flow Initialization

In this section the break flow initialization is discussed. During these assessment calculations, errors were discovered in the TRAC-BD1 Version 11 steam flow choking calculation. The differences between the calculated and measured single-phase break flows could not be explained in terms of the coding errors. The coding errors would have affected the calculation only when the void fraction at the break reached unity, but not during the initialization. The possible ramifications of these errors are discussed in greater detail in Section 4.3. The necessary corrections to the code have been implemented in the current Version 12.

The most significant pressure initialization problem in the two tests occurred at the recirculation pump suction line flow nozzle, located adjacent to the vessel. As shown in Tables 2 and 3, with the nozzle flows correctly initialized, the flow nozzle pressure drop was overcalculated by factors of as much as 2.88 for the steady state case with single phase

flow. This behavior persisted in the transient calculations, as exemplified in Figure 3. Similar behavior was observed at flow restrictions elsewhere in the model. For example, when the broken loop recirculation pump discharge orifice, with an orifice-to-pipe diameter ratio of 0.8, was initialized to the correct flow, TRAC overcalculated the pressure drop through this restriction by about 50 percent compared to the data.[a]

In general, the calculated pressure drop through the flow nozzle was incorrect, and the miscalculation was independent of the flow regime and the Mach number. This suggested that the flow nozzle may have been modeled improperly. However, TRAC-BD1 was known to have a problem in the treatment of the pressure drop calculation through a flow restriction.

The flow nozzle configuration used for this calculation is compared to the actual nozzle configuration in Figure 4B. The correct geometric values of flow area and hydraulic diameter were input at the restriction plane. With FRIC = 0.0, the hydraulic diameter was varied to assess its effect on the break flow calculation. The results in Table 4 show that the flow varied little and that the pressure drop was also insensitive to changes in the hydraulic diameter. The reason for this was that the wall shear was an insignificant portion of the pressure loss through the flow nozzle.

Experiments with TLTA flow nozzles documented in Reference 5 had shown that critical mass flux was dependent on nozzle configuration, but sufficient runs were not made in this calculation to determine if a better model of the flow nozzle could be devised. Configuration C shown in Figure 4 better modeled the actual geometry, but it would not run, regardless of where the choking flag was placed.

---

a. Flow and DP measurements were not independent at the orifice, but there were separate measurements at the flow nozzle.

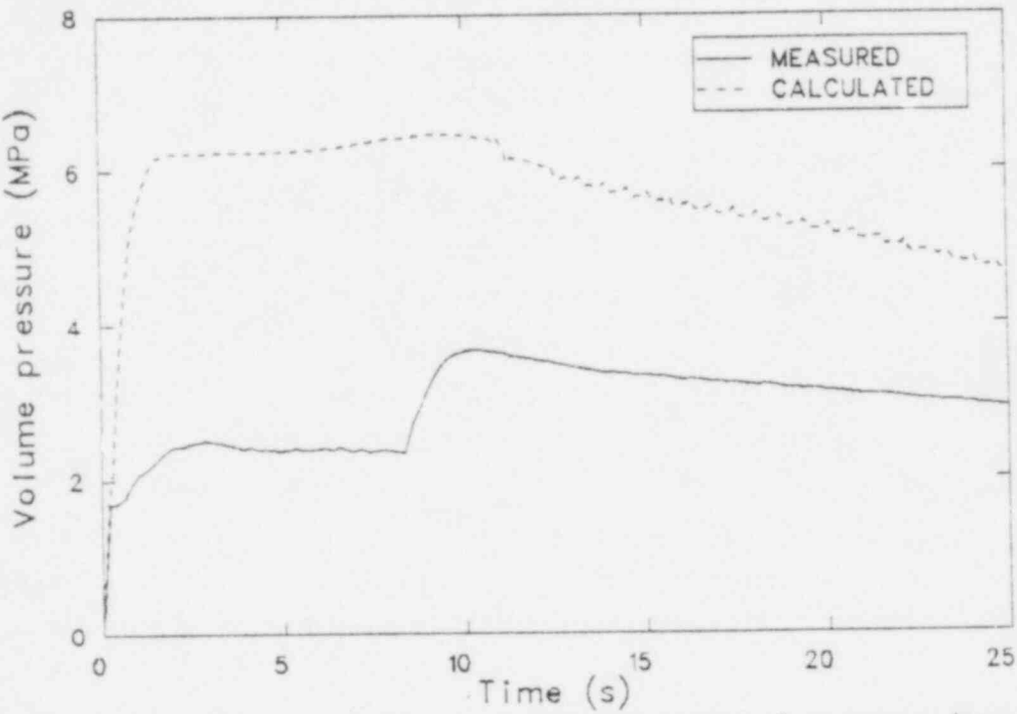

Figure 3. Comparison of calculated and measured pressure drop across the suction line flow nozzle for TLTA Test 6425.

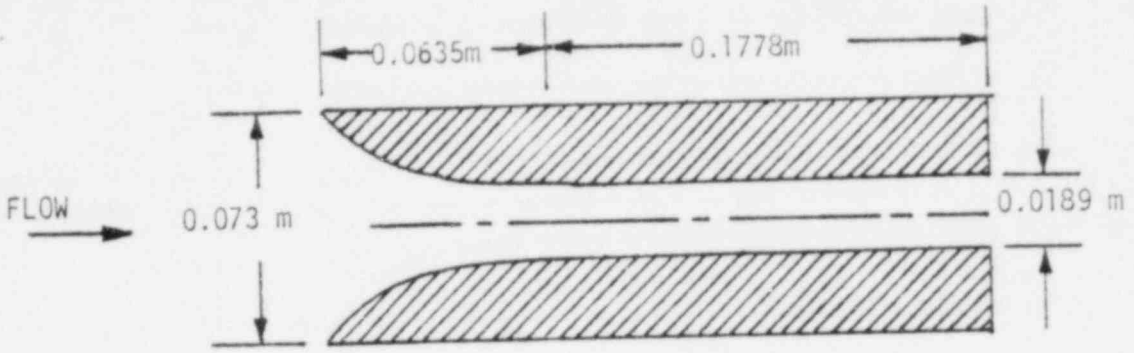

A. ACTUAL CONFIGURATION OF TLTA-5A FLOW NOZZLE

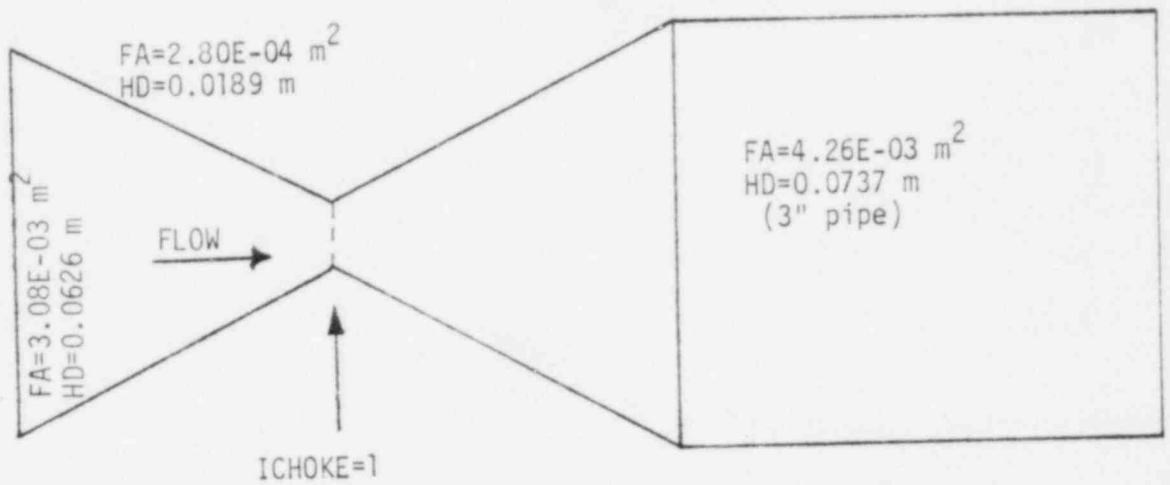

B. TRAC-BD1 MODEL FLOW NOZZLE CONFIGURATION

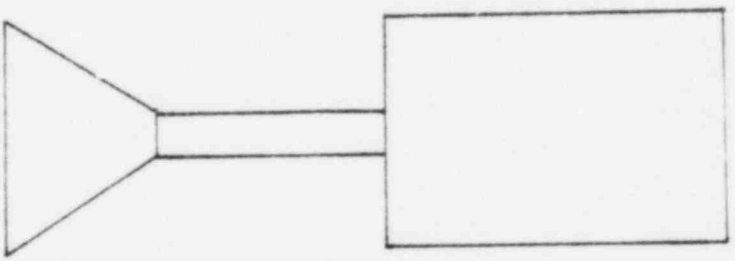

C. ALTERNATE CONFIGURATION

Figure 4. Suction side break nozzle modelling for TLTA TESTS 6425 and 6426.

TABLE 4. SENSITIVITY OF THE FLOW NOZZLE PRESSURE DROP TO CHANGES IN HYDRAULIC DIAMETER UNDER STEADY STATE SINGLE PHASE LIQUID FLOW CONDITIONS

HD[a] (m)	Desired Flow (kg/s)	Calculated Flow (kg/s)	Desired DP (MPa)	Calculated DP (MPa)
0.014	3.36 - 4.27	3.74 - 4.04	0.145	0.436
0.018	3.36 - 4.27	3.76 - 3.96	0.145	0.380
0.040	3.36 - 4.27	3.82 - 3.95	0.145	0.375
0.180	3.36 - 4.27	3.84 - 3.97	0.145	0.366

a. For this sensitivity study, FRIC = 0.0 and FA = 2.8E - 04 m^2 in the flow nozzle.

Fine noding of the nozzle, the well known solution to the problems created by the backward differencing of the flow equations, was not pursued because of the need to assess the choking model in TRAC-BD1. However, this approach may well be warranted if it can be done without severe economic penalties during a 400 second transient.[a]

The break line noding configurations used in this calculation are shown in Figure 5. It was found that the results of the break flow calculation were dependent on the blowdown system noding and the placement of choking flags. Best results were obtained with a choking flag set at each of the exit break planes. The drive side break was placed adjacent to the flow restricting orifice, with the piping downstream of the orifice not modeled. A choking flag set at the end of the suction side blowdown line produced the best results, as expected for this constant cross sectional area pipe.

The restricting orifice in the drive side blowdown line was modeled with a flow restriction equal to the geometric area of the orifice. This model produced good results in the early drive line break mass flow calculation, as shown in Figure 6 for Test 6426. The restriction afforded by the valve at the end of the suction side blowdown pipe was not modeled, and the calculated suction line break mass flow was not in as good agreement with the data as the drive side break flow for the first 30 seconds of the calculation, as shown in Figure 7.

With the drive side results in mind, a flow restriction of 1.1 E-03 m^2 was added at the end of the suction side blowdown line for the purpose of simulating the blowdown valve there. This flow area corresponded arbitrarily to about one-third the valve seat area. In the same run, the break flow nozzle area was increased by 40 percent to see if the pressure drop calculation could be improved at this location. The results of these modeling changes are shown in Figure 8. Note first that

---

a. Subdividing the nodes in Figure 4B in two was of no help in calculating the correct DP-flow relationship through the flow nozzle.

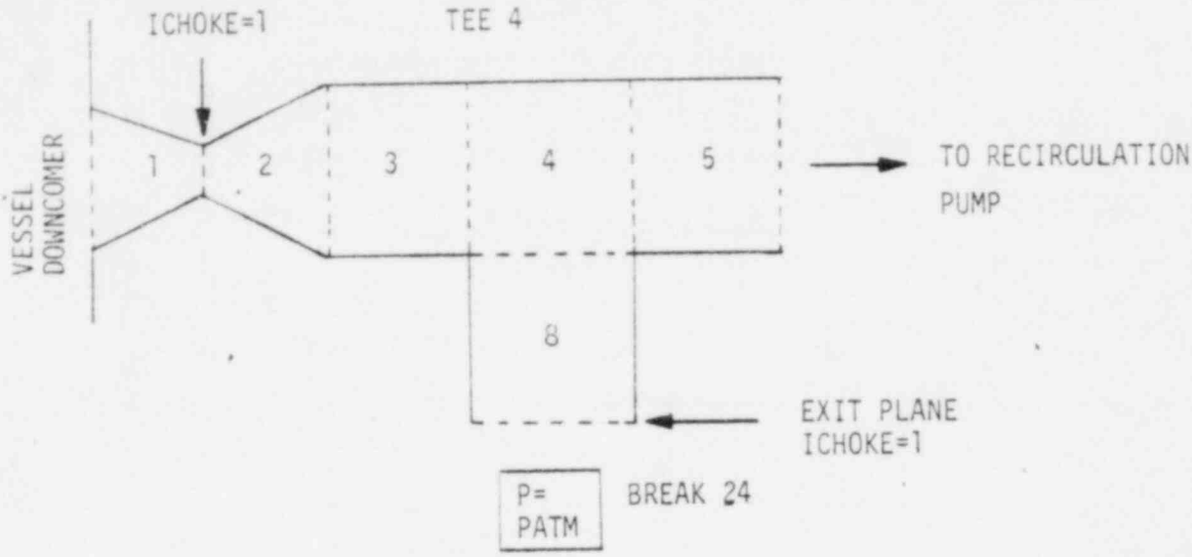

A. SUCTION SIDE

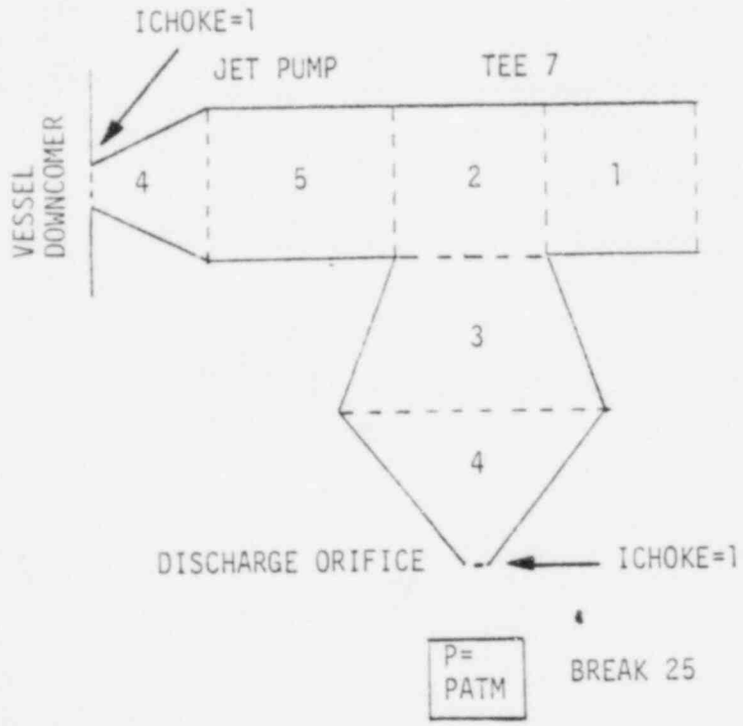

B. DRIVE SIDE

Figure 5. TLTA-5A blowdown line noding configurations for the TRAC-BD1 calculations Tests 6425 and 6426

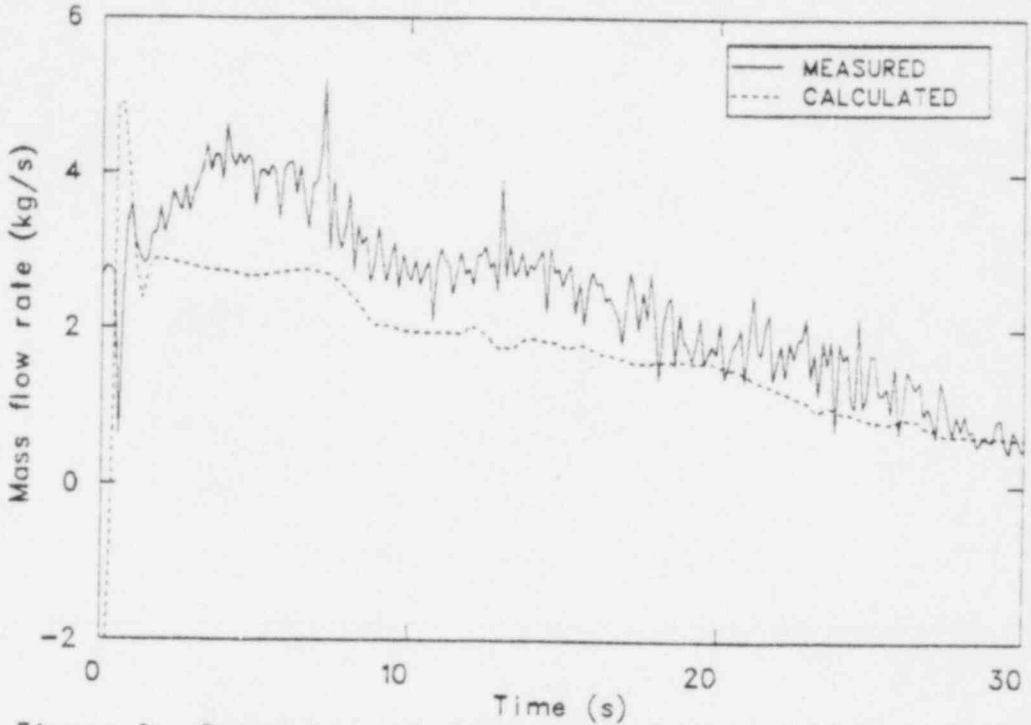

Figure 6. Comparison of measured and calculated drive line blowdown flows for the TLTA Test 6426 early transient.

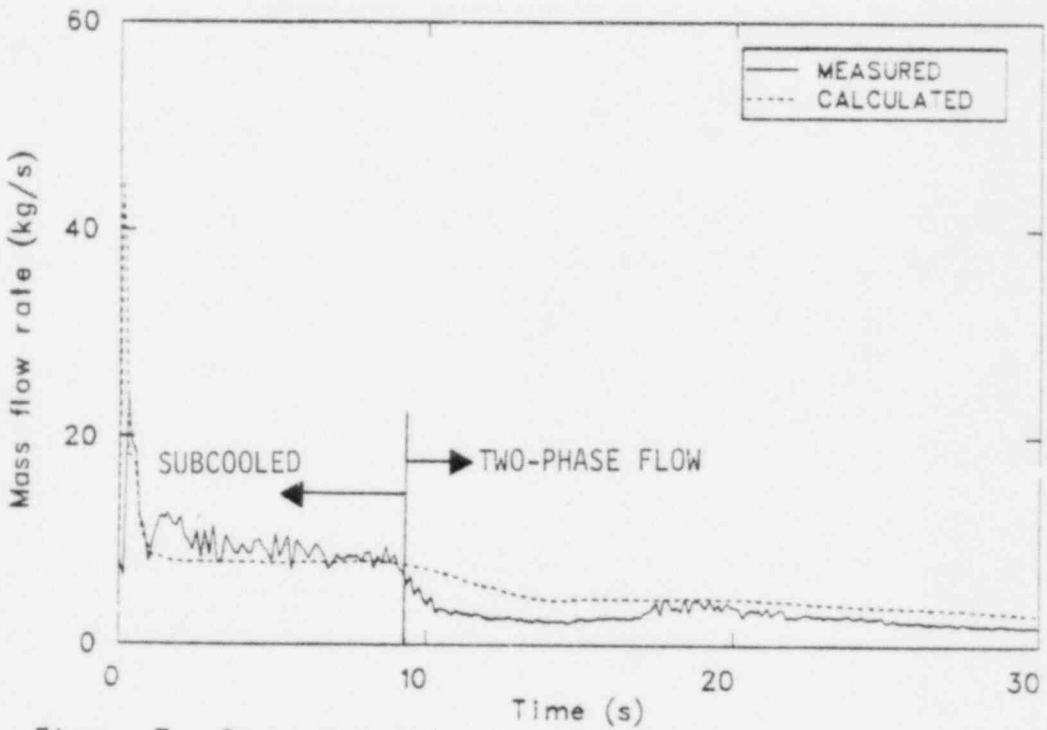

Figure 7. Comparison of measured and calculated suction line blowdown flows for the TLTA Test 6426 early transient.

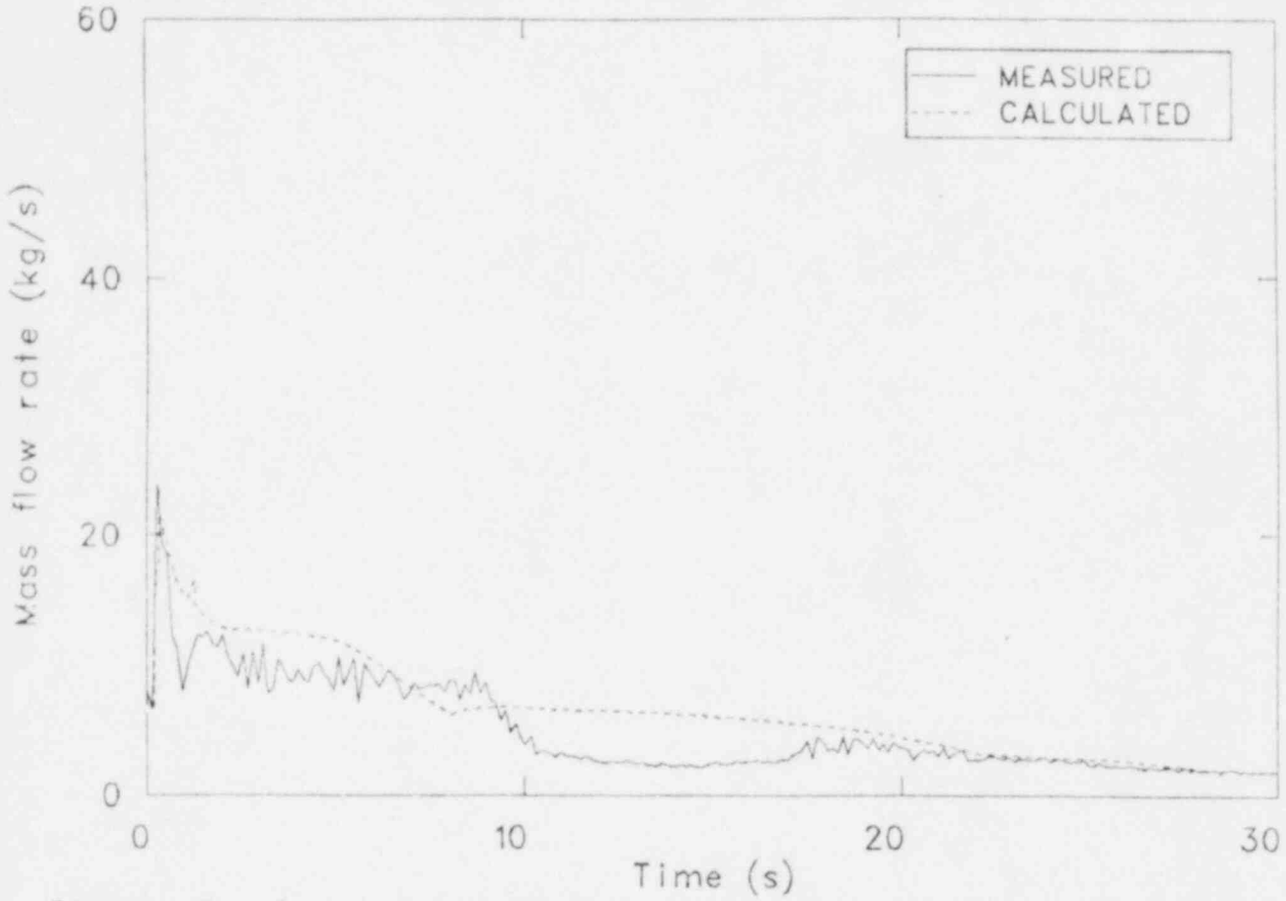

Figure 8. Comparison of calculated and measured suction line break flows with the exit flow area arbitrarily reduced to 1.1E-03 M^2 TLTA Test 6426.

the flow spikes at blowdown initiation no longer appeared. Second, the subcooled blowdown flow was overcalculated, the reverse of Figure 7. Third, the calculation was much improved beyond 18 seconds. The improved break flow calculation in Figure 8 compared to Figure 7 was fortuitous and achieved via methods invalid for code assessment purposes. Indeed, substantial error was apparent in the vessel depressurization calculation for the run used to generate Figure 8, even though the flow remained choked at the enlarged break flow nozzle.

Along with the drive side noding mentioned earlier, Figure 8 suggested that different modeling of flow restrictions downstream of the primary choking plane might improve the break flow results. The artificial methods used for this particular run also implied that modeling techniques might be employed to achieve a better volumetric flow comparison, as the pressure drop calculation at the flow nozzle was improved by opening the break flow area. However, a fully correct flow--DP relationship could not be attained at the break nozzle, irrespective of the modeling technique used. Thus, volumetric break flow comparisons were abandoned, and the geometric break flow area was adhered to for the transient calculations documented herein.

3.1.2 Test 6426 Valve Malfunction

Due to a faulty controller, TLTA Valve 8 (TRAC-BD1 model Valve 6) remained open for the first 25 seconds of the transient. This was evident in the test data. Figure 9 shows the differential pressure measured by DP58 at the broken loop recirculation pump discharge flow orifice for Tests 6425 and 6426. This DP cell indicated that the flow through the orifice reversed at about 1 second and peaked at about 90 percent of the steady-state flow through the recirculation pump.

The broken loop pump speed for the first 30 seconds of Test 6426 is shown in Figure 10. The flow through open Valve 6 drove the pump in reverse between 13.1 and 25.9 seconds. In order for the pump to have reversed speed, impeller-to-casing clearances in the recirculation pump were believed to have been small. Thus, it was postulated that Pump 5

offered a high flow impedance in the connection between the suction and drive side blowdown lines. This connection is shown in Figure 11. The suction side of the blowdown system offered a small flow resistance compared to the drive side due to the presence of the small diameter (0.00813 meter) flow restricting orifice in the drive side blowdown line. Because of high flow resistance offered by this orifice, an open Valve 6 should have caused a substantial reduction in the differential pressure measured across this orifice. Figure 12 shows that the drive side blowdown flow was indeed reduced for Test 6426 as compared to Test 6425, but the reduction was not as much as Figure 11 alone would have implied. Thus, it was attempted to add resistance to Pump 5 in the TRAC-BD1 model to simulate the effects of the open Valve 6.

The TRAC-BD1 input processor would not allow negative values of pump speed. Attempts at reducing the flow area in the recirculation pump failed. Upstream flow area reductions would have starved the pump, while downstream area reductions raised discharge pressures high enough to cause an abort in TRAC subroutine THERMO. The TRAC pump speed calculation was not used due to the lack of two-phase flow curves for the TLTA recirculation pumps.

Because of the aforementioned modeling difficulties with the pump component, the approach ultimately taken in simulating this equipment problem was to close Valve 6 in the TRAC model until the drive side restriction orifice differential pressure fell into the range of the data. This is illustrated in Figure 13 for Test 6426 compared to Test 6425. This approach resulted in a 4.8 percent opening for Valve 6 for the first 20 seconds of the calculation and a linear closing thereafter, with the valve shut by 25 seconds. The small valve open fraction required for the proper flow split between the suction and drive side blowdown legs substantiated the original assumption regarding the high flow impedance offered by Pump 5.

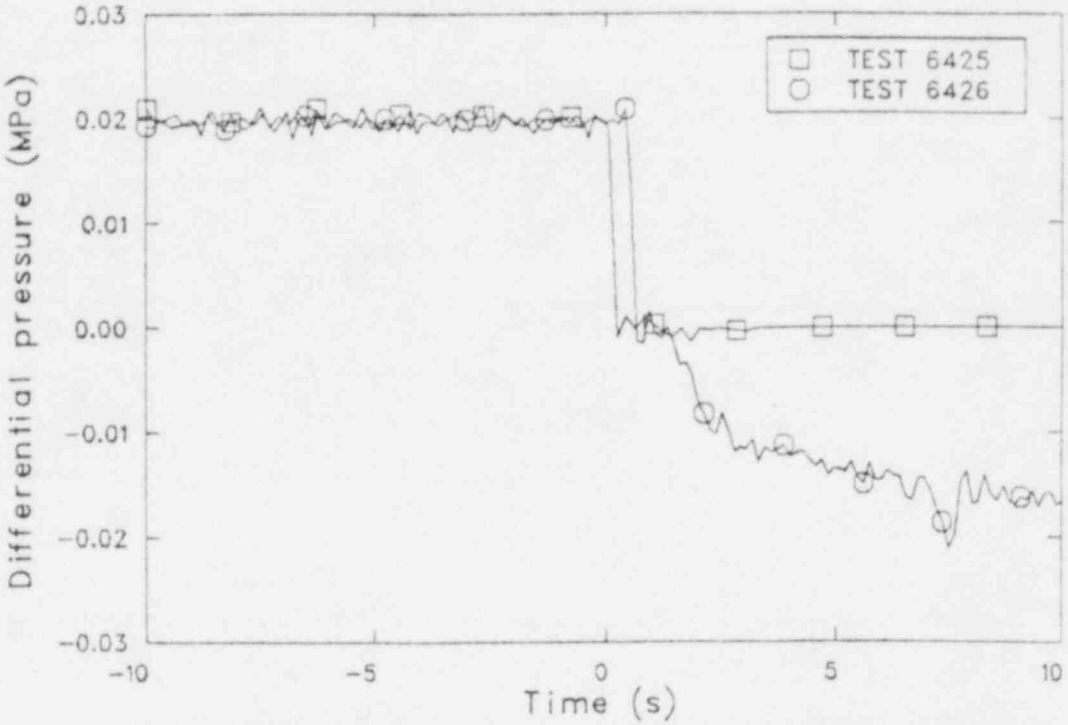

Figure 9. Measured differential pressures across the recirculation pump discharge orifice plate for TLTA Tests 6425 and 6426.

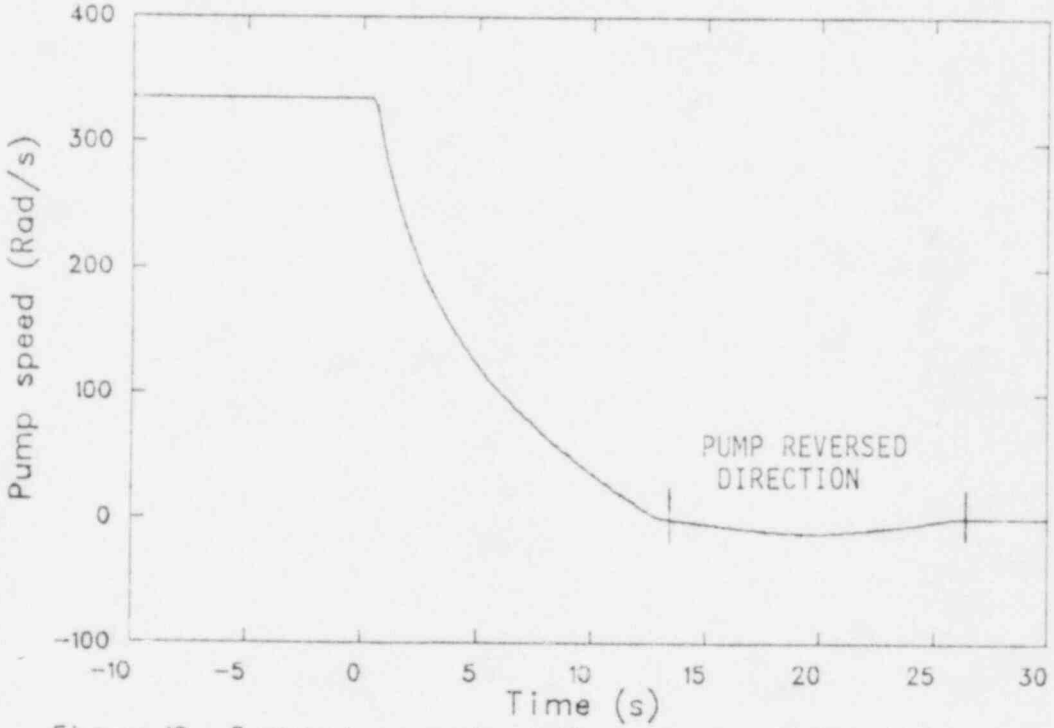

Figure 10. Broken loop recirculation pump speed for TLTA Test 6426.

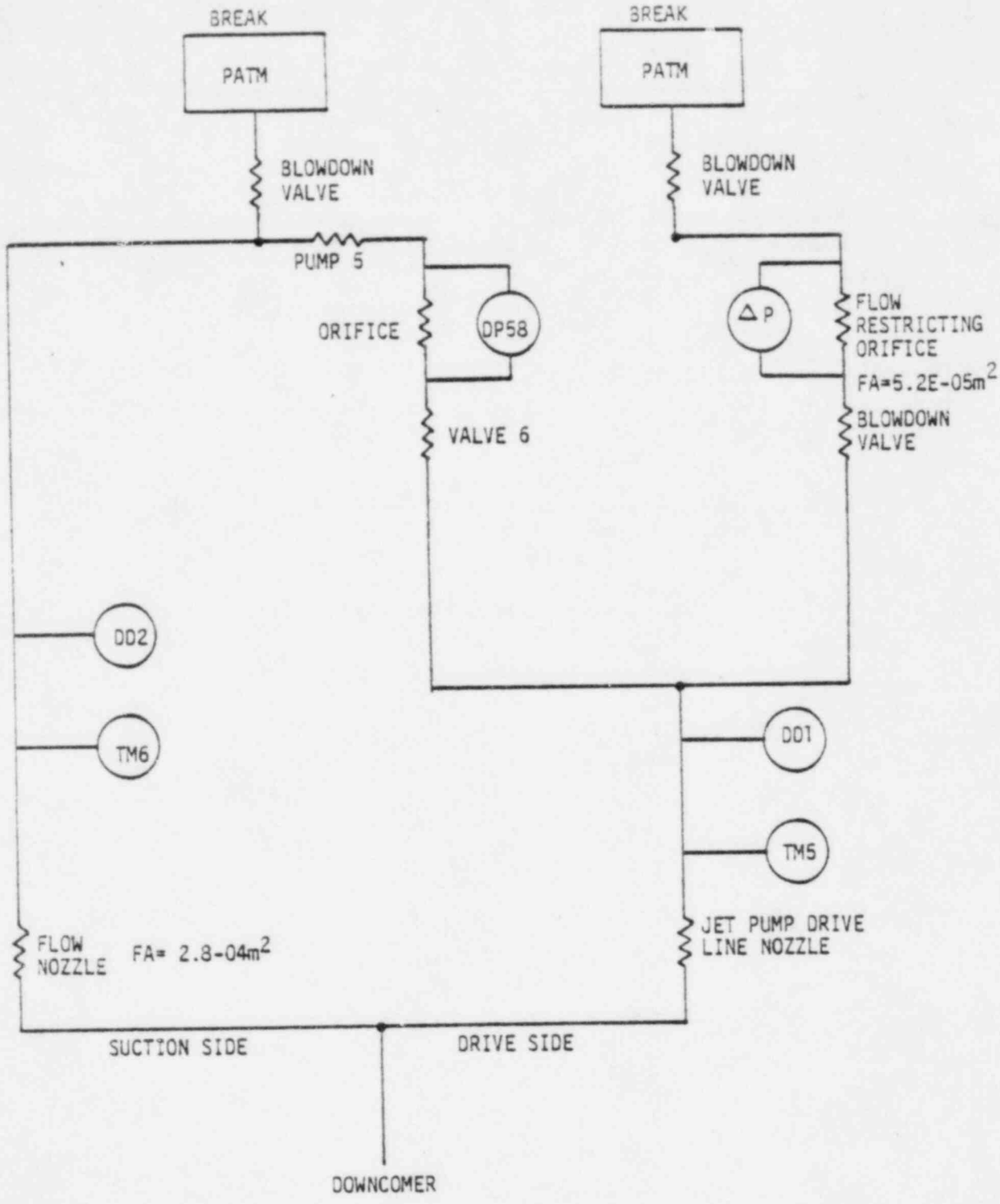

Figure 11. Flow resistance analogy of the TLTA-5A blowdown system.

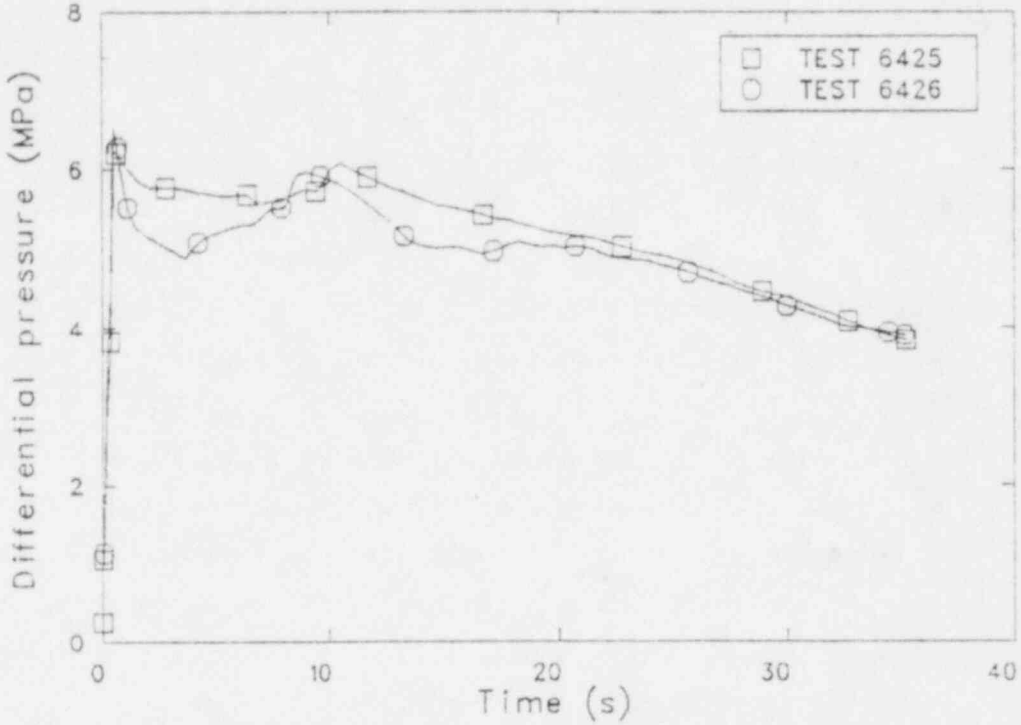

Figure 12. Measured differential pressures across the drive side blowdown line restricting orifice for TLTA Tests 6425 and 6426.

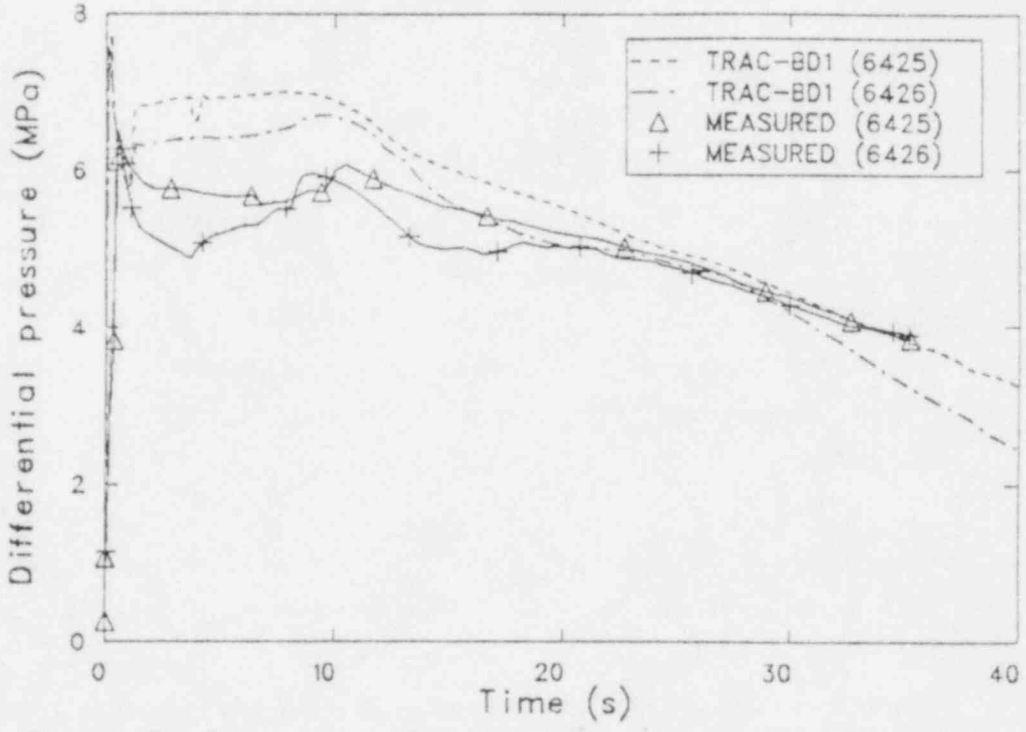

Figure 13. Comparison of calculated and measured differential pressures across the drive side blowdown line restricting orifice for TLTA Test 6425 and 6426.

3.1.3 Model Limitations Summary

The modeling limitations in the TRAC-BD1 deck used for this calculation are summarized below. In addition, several errors have been discovered in TRAC-BD1 Version 11 by the Idaho National Engineering Laboratory (INEL) Code Assessment and Applications Division (CAAD) during its recent code assessment efforts. Those most significantly affecting this calculation are listed below.

1. The blowdown valves were not included in the computational model of the TLTA facility. The effects of this approximation were that TRAC-BD1 immediately saw full downstream pipe flow areas upon the initiation of blowdown. This produced large initial flow spikes several times greater than the data and shortened the calculated duration of the subcooled blowdown.

2. Coding errors were discovered in the TRAC-BD1 steam choking model. It will be shown that these errors did not affect the results of these calculations.

3. The rod-to-rod power distribution within the heated bundle was not modeled. A flat radial power profile was input across the TRAC-BD1 computational rod groups. The effects of this approximation were not quantified, but they had potential to affect the critical power level significantly. To improve calculations of the peak rod temperatures and the time to and location of initial rod dryout, it is recommended that the interrod power distribution be modeled in future TLTA assessment calculations.

4. Due to a Version 11 coding error, there was no heat transfer calculated between the channel wall and the external fluid. This problem would have kept the calculated rod temperatures too high and the fluid in the bypass too cool. There was another coding problem in which the convective heat transfer from the channel wall to the internal fluid was doubly added, tending to keep the

channel wall too cool. These two errors were in opposite directions, but their relative magnitudes were not quantified in these calculations. These errors have been corrected in TRAC-BD1 Version 12.

5. Heat transfer from the bypass tubes to the surrounding fluid was not modeled. This insulated the ECC fluid in the bypass tubes from the hotter fluid in the downcomer. This modeling approximation was expected to have augmented the ECC modeling problems described in Section 4.5.

6. An initialization calculation with the system in a static configuration was not performed. This precaution would have verified the accuracy of the gravity terms input. If errors in input were to exist, the most probable place for them was in the recirculation loops. Therefore, any gravity term error would have had a negligible effect on the calculation beyond 20 seconds, the loop isolation time.

4. TRANSIENT CALCULATION RESULTS

In this section, the transient calculation results for TLTA Tests 6425 and 6426 are presented. In Section 4.1, general comparisons are made for many of the key assessment parameters desired by the NRC. In Section 4.2, the break inlet conditions are established, preparatory to a discussion in Section 4.3 of the break flow results. The vessel depressurization calculations are compared to the data in Section 4.4. Numerous problems were encountered with the simulation of the ECC injection systems in Test 6425, and these are summarized in Section 4.5. Finally, the rod temperature comparisons are presented in Section 4.6.

Due to code instability problems, Test 6425 was run for 137 seconds of the 400 second transient and the calculation terminated. The 6426 calculation was run for the complete 300 second test. Comparisons of the 6426 calculation with the data were generally made for the first 150 seconds of the assessment to facilitate comparison with the 6425 results. However, 300 second plots have been used as necessary where changes in either the data or the calculation beyond 150 seconds warranted their presentation.

4.1 General Comparisons

This section has been divided into three parts for the comparisons that follow. In Section 4.1.1, the calculated times to various important events in the experiments are compared to the actual sequence. In Section 4.1.2, the mass flow calculations are compared to the data for the three ECC systems in Test 6425. In Section 4.1.3, the calculated vessel pressure distributions are compared to the test results.

4.1.1 Time to Critical Events

Summaries of the test events compared to the TRAC-BD1 calculations are shown in Tables 5 and 6, for Tests 6425 and 6426, respectively. The test data in these tables were taken from Reference 3. There were some small differences in the feedwater and valve timing events which arose primarily

TABLE 5. SEQUENCE OF EVENTS FOR TEST 6425

Event	Measured Time (s)	Calculated Time (s)
Blowdown valves open	0.0	0.0
Bundle power decay initiated	0.5	0.65
Blowdown loop jet pump flow reverses	0.5	0.3
Feedwater flow stops	0.5	0.65
Jet pump suction uncovers	6.7	5.9
Steamline valve completely closed	9.0	8.8
Recir. suction line begins to uncover	9.4	7.4
Lower plenum bulk flashing	11	14.6
Core inlet uncovers (SEO center line)	20	20.6
Loop 1 isolated	20	20.8
HPCS injection begins	26.6	25.5
Lower plenum mixture level reaches jet pump exit plane	35	25.4
LPCS flow begins	63.2	52.0
LPCI flow begins	75	56.1
Peak cladding temperature	75	112
Bypass/guide tube region begins to refill	85	72
CCFL breaks down at bypass outlet	95	91
Bundle begins to refill	114	115
Bypass region refilled	125	116
CCFL breaks down at upper tie plate	125	118
Bundle quenched	150	124
End of test/calculation	400	137

TABLE 6. SEQUENCE OF EVENTS FOR TEST 6426

Event	Measured Time (s)	Calculated Time (s)
Blowdown valves open	0.0	0.0
Bundle power decay initiated	0.5	0.68
Blowdown loop jet pump flow reverses	0.1	0.3
Feedwater flow stops	0.5	1.9
Jet pump suction uncovers	6.5	8.4
Steamline valve completely closed	7.9	9.1
Recir. suction line begins to uncover	9.2	8.8
Lower plenum bulk flashing	13.3	7.4
Core inlet uncovers (SEO center line)	20	28
Lower plenum mixture level reaches jet pump exit plane	33	33
Peak Cladding Temperature	294	294
End of test/calculation	300	300

from subjectivities in the interpretation of the data. For Test 6425, significant departures were evident in the time to peak cladding temperature and the bundle quenching time. The timings of these events are discussed in conjunction with the rod temperature comparisons in Section 4.6.

Although they led the data, calculations of the jet pump uncovery and flashing events compared well with the experiment. The time to jet pump suction uncovery for Test 6425 was determined from the void fractions shown in Figure 14. TRAC-BD1 calculated this event at 5.9 seconds compared to 8.1 seconds from the data via the same method. The difference between this last figure and the time listed in Table 5 was believed to be interpretive in nature. The recirculation pump suction line was calculated to uncover at 7.4 seconds compared to 9.4 seconds in the experiment, as shown in Figure 15. Based on the lower plenum level 3 void fraction, the jet pump discharge was calculated to uncover after 25.4 seconds compared to 33.4 seconds in Test 6425, as shown in Figure 16. This last number differed slightly from the 35-second time picked by General Electric in Table 5, again due to the subjectivity of the interpretation.

The jet pump suction, recirculation pump suction, and jet pump exit plane uncovery comparisons for Test 6426 are shown in Figures 17 - 19. The jet pump suction was calculated to uncover at 8.4 seconds compared to 8.5 seconds measured in the experiment. The recirculation pump suction line uncovered at 8.8 seconds both in the void fraction calculation and the data. The jet pump exit plane was calculated to uncover at 33 seconds compared to 34 seconds in Test 6426. These calculations were quite good, and they were better than the calculated results in Test 6425, based on the void fraction comparisons.

4.1.2 ECC Injection Comparisons

For Test 6425, significant departures from the data were calculated in the timings of the LPCS and LPCI injection. Figures 20, 21, and 22 display the ECC injection comparisons for the HPCS, LPCS and LPCI systems. TRAC-BD1 calculated the onset of injection at 25.5, 52.0, and 56.1 seconds,

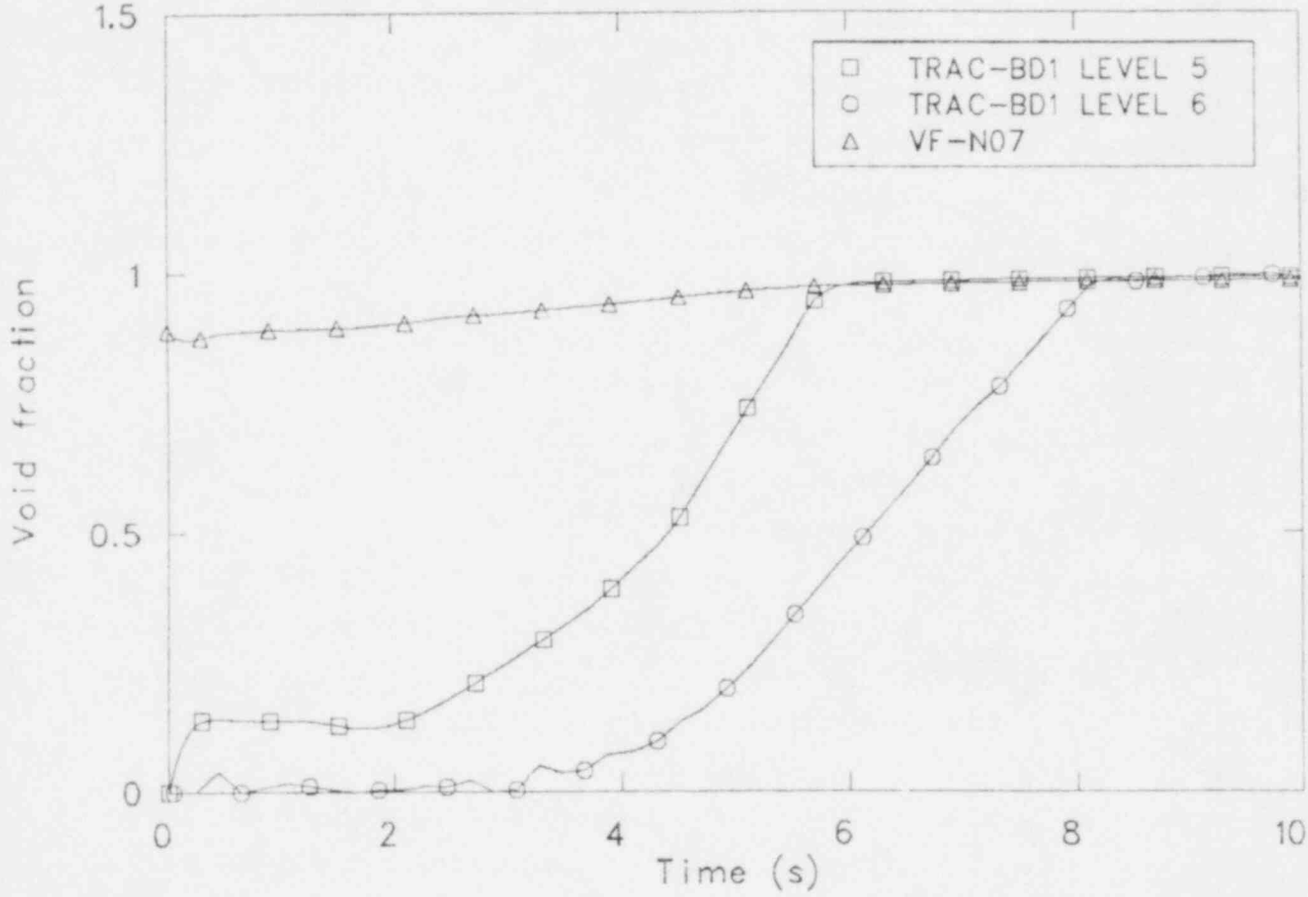

Figure 14. Jet pump suction uncovery comparison as determined from the downcomer void fractions for TLTA Test 6425.

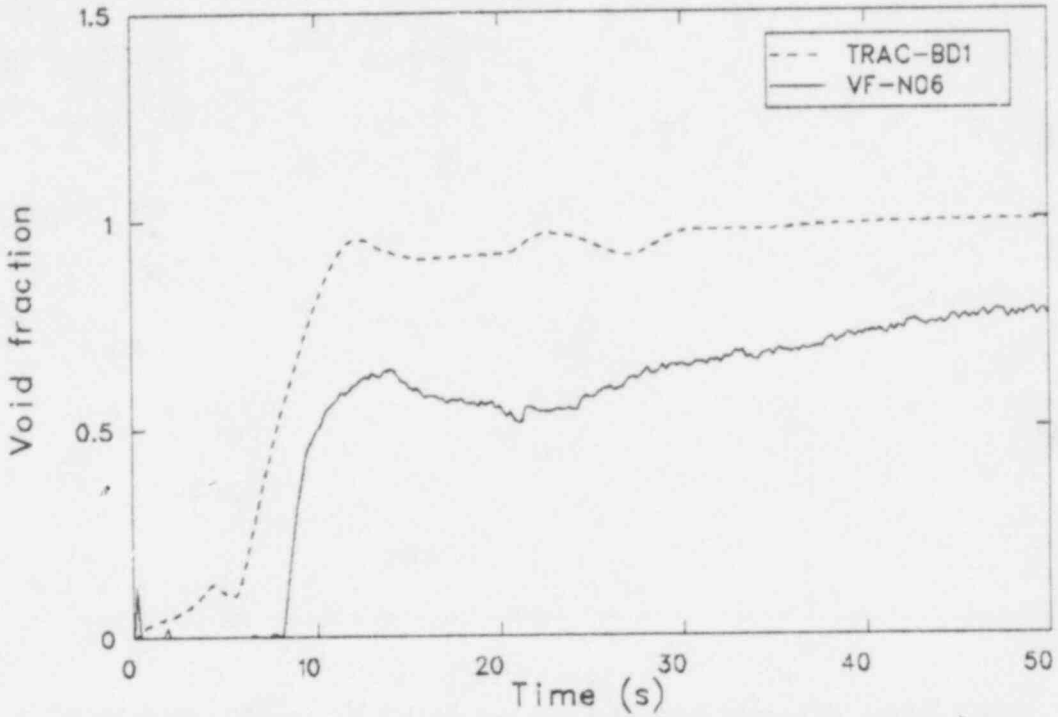

Figure 15. Recirculation pump suction line uncovery comparison as determined from the downcomer void fraction

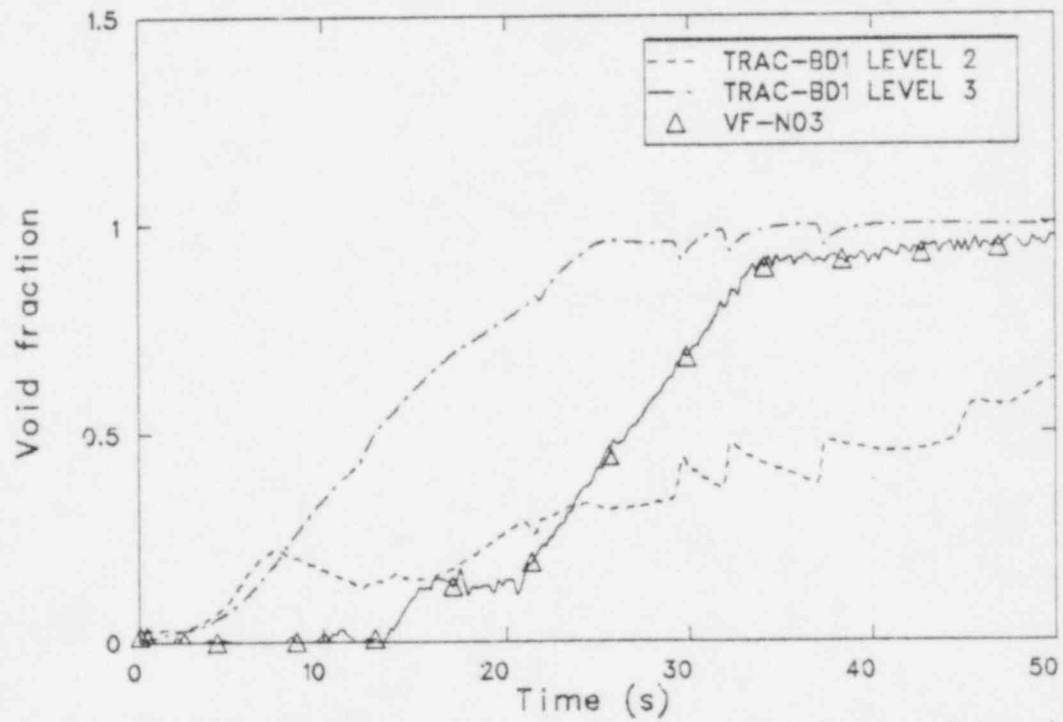

Figure 16. Jet pump exit plane uncovery comparison as determined from lower plenum void fractions for TLTA Test 6425.

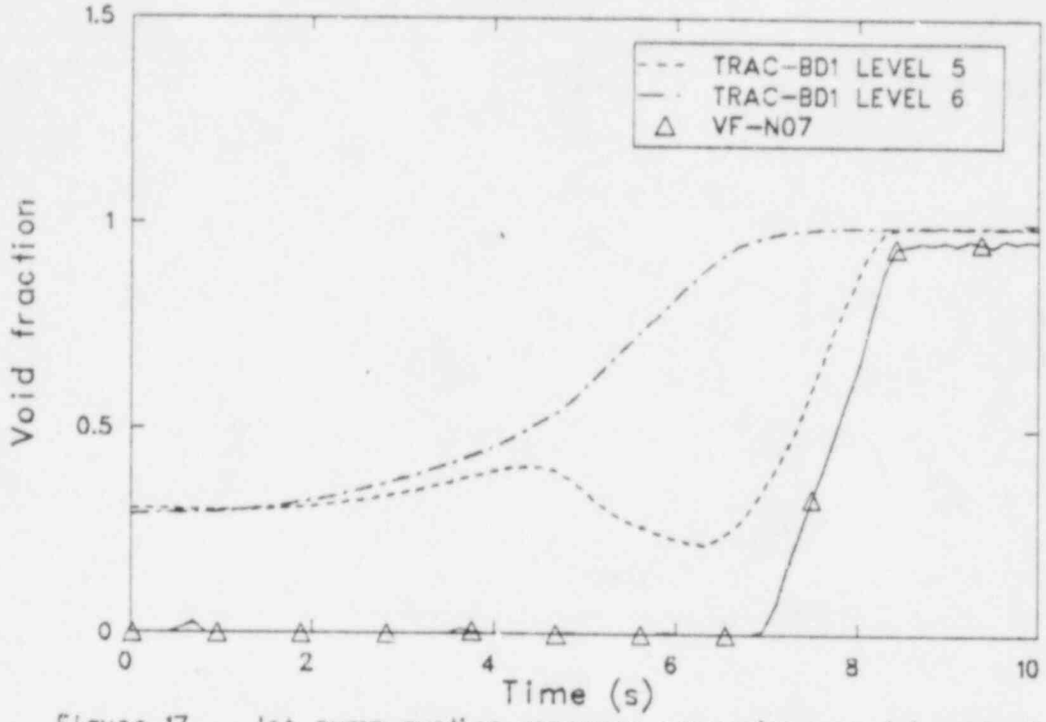

Figure 17. Jet pump suction uncovery comparison as determined from the downcomer void fraction for TLTA Test 6426.

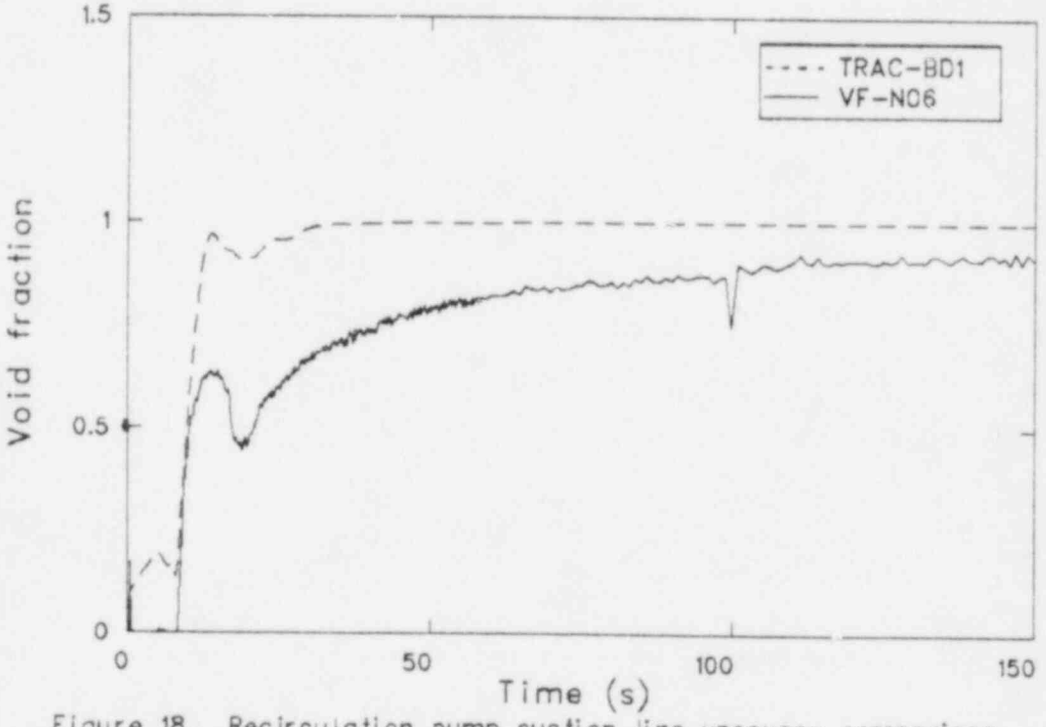

Figure 18. Recirculation pump suction line uncovery comparison as determined from the downcomer void fraction for TLTA Test 6426.

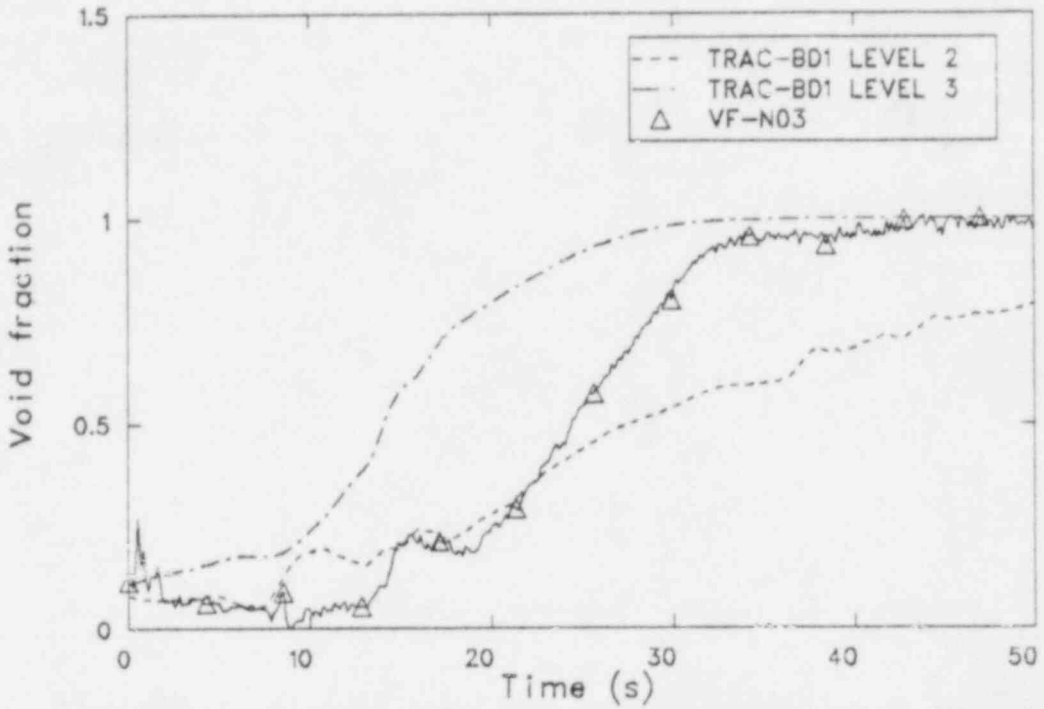

Figure 19. Jet pump exit plane uncovery comparison as determined from lower plenum void fractions for TLTA Test 6426.

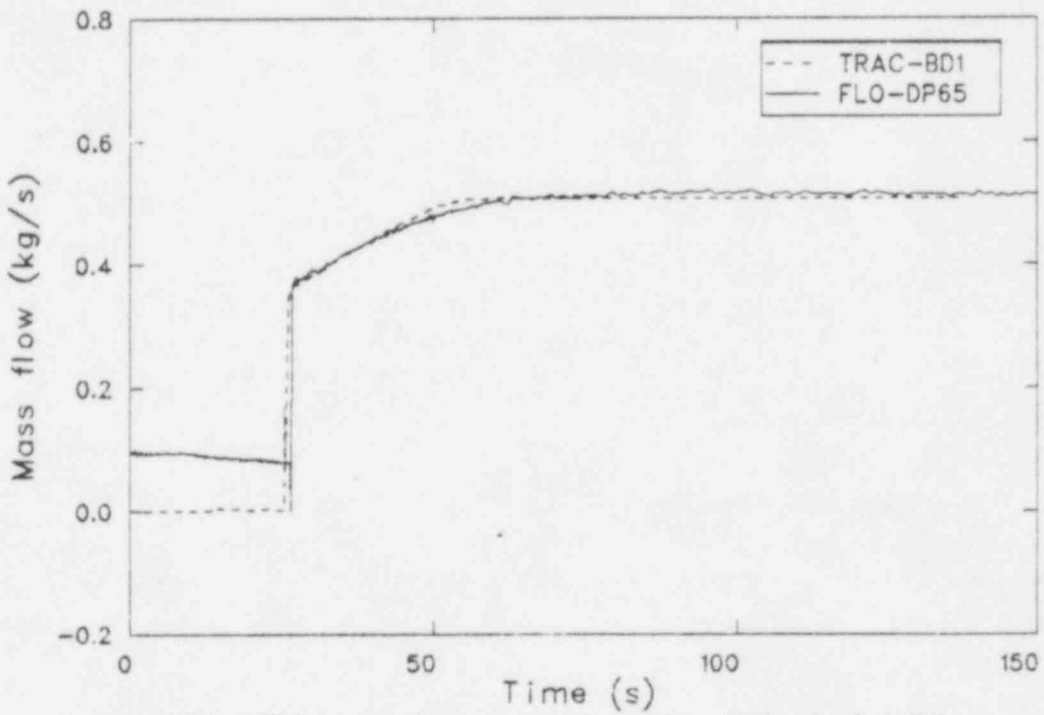

Figure 20. HPCS mass flow comparison for TLTA Test 6425.

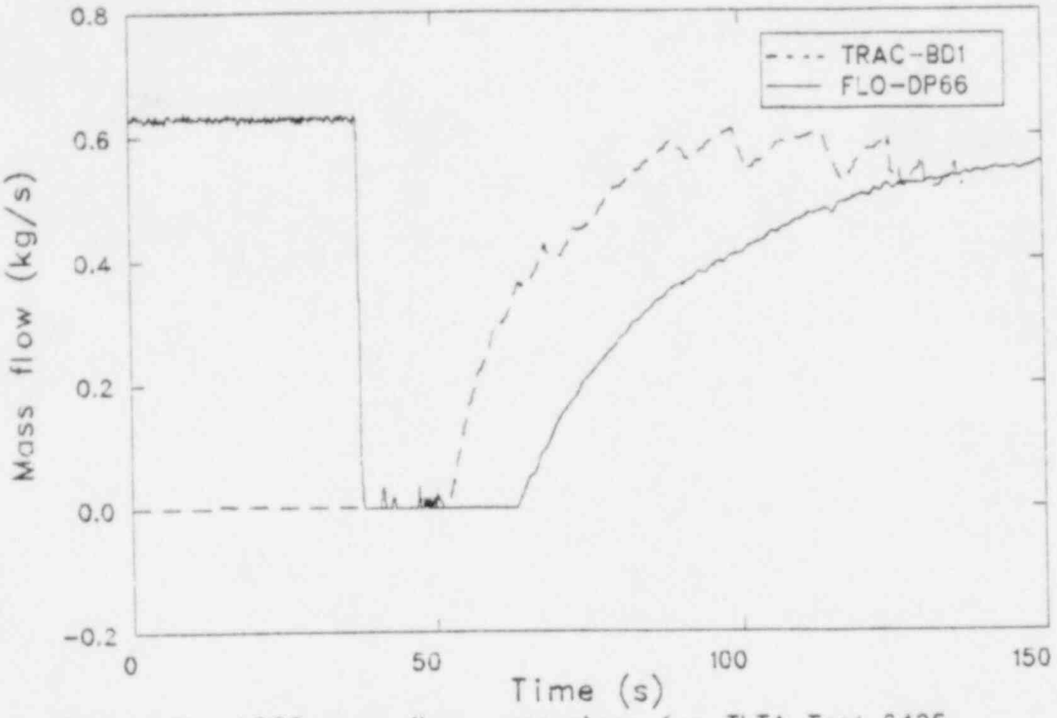

Figure 21. LPCS mass flow comparison for TLTA Test 6425.

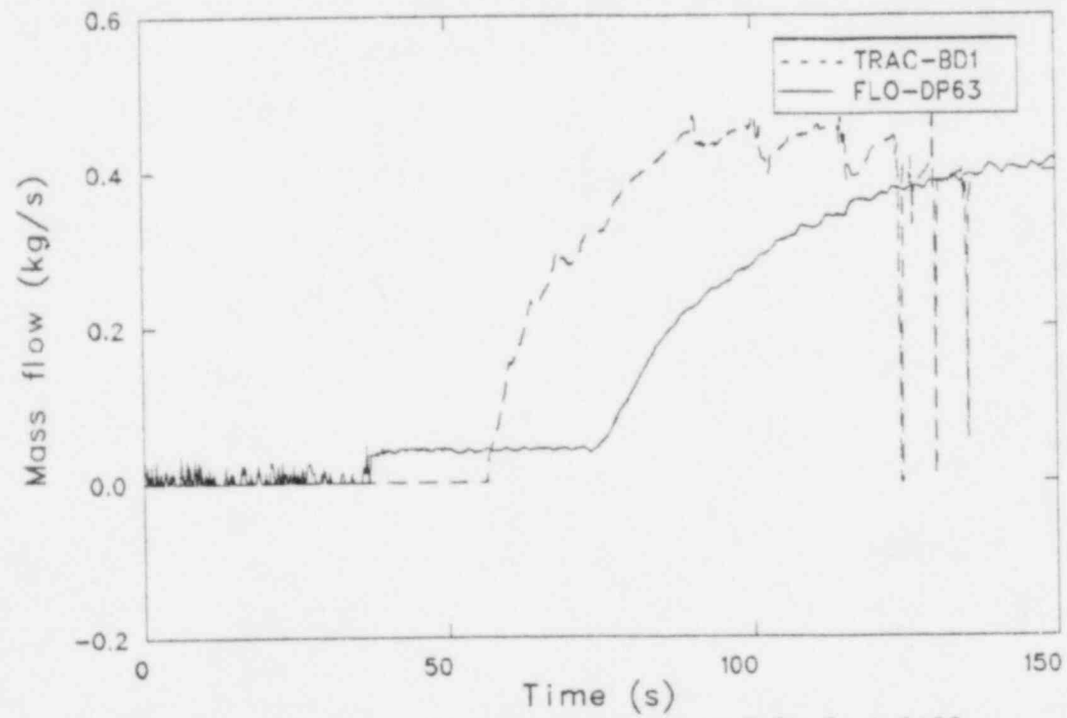

Figure 22. LPCI mass flow comparison for TLTA Test 6425.

respectively for the three systems, compared to 26.6, 63.2, and 75 seconds measured in Test 6425.

Since pressure versus velocity fills were used to model the TLTA ECC systems in the TRAC-BD1 calculation, the goodness of the injection comparison depended on the accuracy of the vessel depressurization calculation and the shape of the various ECCS flow curves. The flatter HPCS curve and the earlier onset of HPCS injection resulted in excellent agreement with the calculation, as shown in Figure 20. The LPCS and LPCI injection pumps were more responsive to vessel pressure changes than the HPCS pump. Thus, because the calculated pressure in the vessel was less than the data, the LPCS and LPCI systems were activated too early by TRAC-BD1. The vessel depressurization is discussed further in the Section 4.4.

4.1.3 Vessel Differential Pressures

In this section, comparisons are made between the calculated and measured differential pressures. This method of comparison was favored over a mass inventory comparison because the differential pressures were direct measurements rather than derived data.

Figure 23 shows the differential pressure in the downcomer for Test 6425. There was a 0.49 meter elevation difference between the centers of vessel Levels 4 and 5 as compared to the 0.31 meter measurement height of DP6. (DP7 was inactive in this test.) The curves on Figure 23 were not adjusted for the elevation difference because the calculated mixture density history was not available. Qualitatively, water in the downcomer accounted for the shift between the curves prior to recirculation pump suction uncovery; the shift incurred as the void fractions approached unity (beyond 10 seconds) was negligible.

Figure 24 is an expansion of the differential pressure scale of Figure 23 and better shows the emptying and refill of the downcomer in Test 6425. TRAC-BD1 calculated that the downcomer depressurized too rapidly and that it did not refill. TRAC-BD1 significantly undercalculated the downcomer differential pressure, a result of the overcalculation of the

two-phase break flows, further discussed in Section 4.3. TRAC-BD1 calculated 85 seconds to minimum downcomer differential pressure. In the experiment, the minimum was reached at 50 seconds, and the downcomer level remained near its minimum until 78 seconds.

The downcomer differential pressure comparison for TLTA Test 6426 is shown in Figure 25. With DP7 available in Test 6426, the instrument tap height was 0.58 meter compared to 0.49 meter for the TRAC nodal elevation difference. As expected, the calculated differential pressure was less than the data for the subcooled blowdown. The undercalculation was not fully accounted for by the nodal elevation shift. The same was true for the remainder of the test, and TRAC-BD1 undercalculated the downcomer differential pressure. Again, the undercalculation in downcomer ΔP was a consequence of the overcalculation of break flows during the two-phase blowdown. TRAC calculated the time to minimum ΔP at 77 seconds. In the experiment, the downcomer level was still decreasing at the end of the 300 second transient. The downcomer differential pressure comparisons could be expected to improve with finer noding of the vessel.

Figure 26 compares the measured and calculated pressure drops across the lower plenum for Test 6425. The problem of the noding not corresponding to the instrumentation was again observed. Measurement column height for DP cells 1-4 was 1.14 meters, compared to a 0.63 meter elevation difference between TRAC-BD1 vessel Levels 1 and 3. As a result, measured values were higher than calculated pressure drops, as shown by curve 2 of Figure 26. Curve 3 was a comparison of DP Cells 1-3 with the TRAC calculation, a measurement height of 0.87 meter compared to the 0.63 meter cell height. This resulted in a somewhat better comparison. The measurements indicated that the lower plenum level fell until it reached the jet pump exit plane at 33 seconds and that it remained constant thereafter. TRAC-BD1 calculated a gradual level decrease until 90 seconds, a nearly constant level until 117 seconds, and a gradual refill until the end of the calculation.

The results of the differential pressure comparision were also reflected in the lower plenum void fraction calculation, which was amplified compared to the data due to the liquid-vapor cellular

homogenization within the code. This effect is shown by the void fraction comparison in Figure 27. Experimentally, a relatively constant liquid level was maintained from 40 to 105 seconds, followed by a 20 second refill and a drop in level as depressurization continued. The lower plenum voided continually in the TRAC-BD1 calculation, the level apparently reaching a minimum at 80 to 90 seconds as deduced from the time to maximum void fraction at the two bottom lower plenum nodes. Caused by too rapid a blowdown, the high void accounted for the undercalculation of the lower plenum pressure drop. However, refill was well calculated, occurring at 105 seconds based on the downcomer void fraction.

The lower plenum differential pressures for Test 6426 are shown in Figure 28. The apparent undercalculation during the subcooled blowdown was a consequence of the noding heights. However, the elevation differences were not sufficient to explain the undercalculation for the duration of the assessment. The undercalculation beyond 9 seconds was quite pronounced. There was also an abrupt reduction in the calculated ΔP at 119 seconds which was not explainable.

Figure 29 shows the lower plenum void fraction comparison for the NO ECC test. The effects of the more rapid calculated vessel depressurization were equally pronounced for this test. TRAC-BD1 Level 2 reached maximum void after 71 seconds. The calculated lower plenum level dropped to 0.03 meter in the vessel at the end of the transient, compared to approximately 0.25 meter in the experiment, both based on the equivalent collapsed liquid column height.

Figures 30 and 31 show pressure drop comparisons in the heated bundle and the bundle bypass tables, respectively, for Test 6425. Both comparisons showed good quantitative agreement with the data. The prominent spikes beyond 100 seconds were due to numerical stability problems in the calculation and did not represent actual physical phenomena. These calculated flow oscillations in the core and the bypass correlated to oscillations in the core heat transfer between the film condensation and the nucleate boiling modes. The heat transfer oscillations were believed to have been a real representation of actual

phenomena. The flow oscillations were not real, and they affected the subsequent transient calculations in Test 6425, contributing to the vessel pressure oscillations.

The core differential pressure measurements for Test 6426, shown in Figure 32, correlated well with the suction side break mass flow. The differential pressure excursion at 15 seconds indicated upward expulsion of fluid out the top of the core. A flow surge out the suction side break followed which lagged the core flow surge by 4 seconds. TRAC-BD1 captured the core flow phenomena qualitatively during the first 20 seconds of blowdown. The core pressure drop calculation agreed closely with the experiment during the two-phase blowdown but undercalculated this parameter during the single-phase vapor flow period beyond 55 seconds. The core bypass pressure drop calculation, shown in Figure 33, was also in good agreement with the data. The results showed the same qualitative behavior as the core pressure drop calculation, as expected for these parallel flow paths.

The upper plenum differential pressure comparisons are shown in Figures 34 and 35, for Tests 6425 and 6426 respectively. The 6425 calculation agreed well with the test data for the subcooled blowdown. Beyond 13 seconds, TRAC-BD1 undercalculated the amount of liquid held up by the upper tie plate. The instrument tap height was 1.35 meters compared to a node height of 1.12 meters for this comparison, taken between the Chan Cell 8 and the Vessel Level 10. The 0.23 meter elevation difference did not account for the disparity between measured and calculated results. The time to minimum ΔP in the upper plenum occurred at 45 seconds in the calculation as compared to 125 seconds in the experiment. The increase in the calculated pressure drop beyond 60 seconds was due to the LPCS injection into the mixing plenum. The calculated upper plenum differential pressure increased at the onset of HPCS injection at 25 seconds, evident in the first TRAC curve of Figure 34. Refill of the mixing plenum began at 27 seconds in the TRAC-BD1 calculation. The subcooled HPCS liquid was boiled and convected out the top of the upper plenum, because it was not held above the upper tie plate in as large a quantity as measured, nor did it flow downward into the core or the bypass tubes.

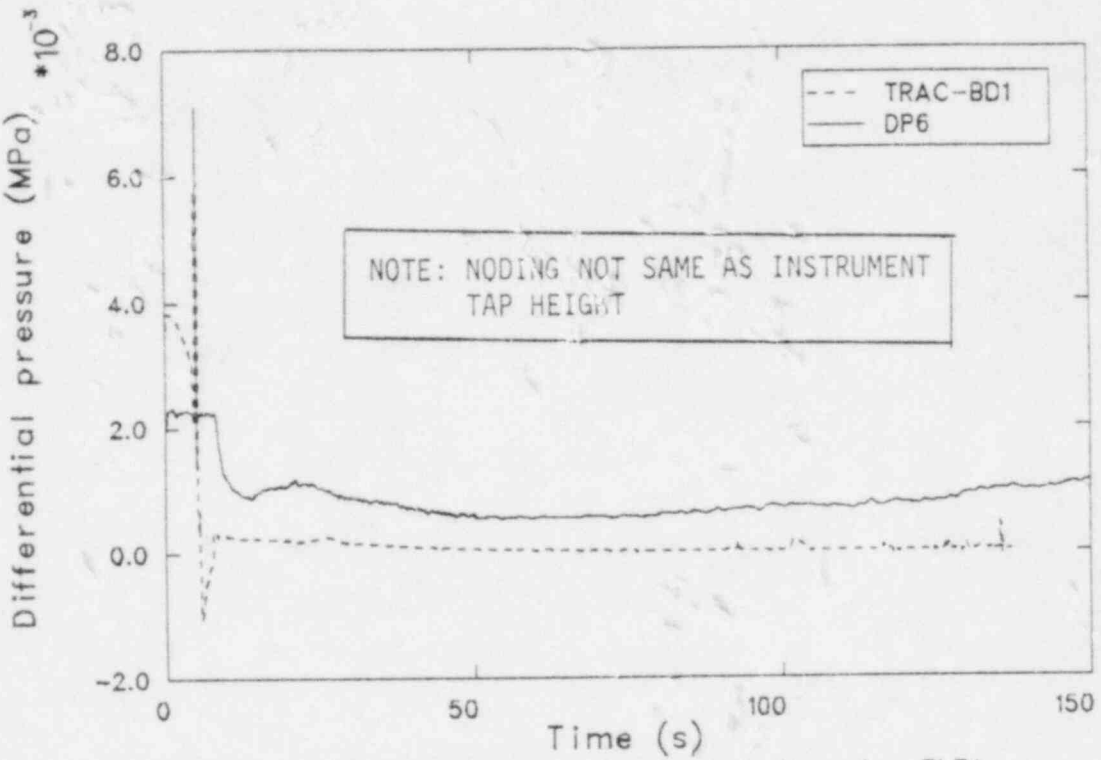

Figure 23. Downcomer pressure drop comparison for TLTA Test 6425.

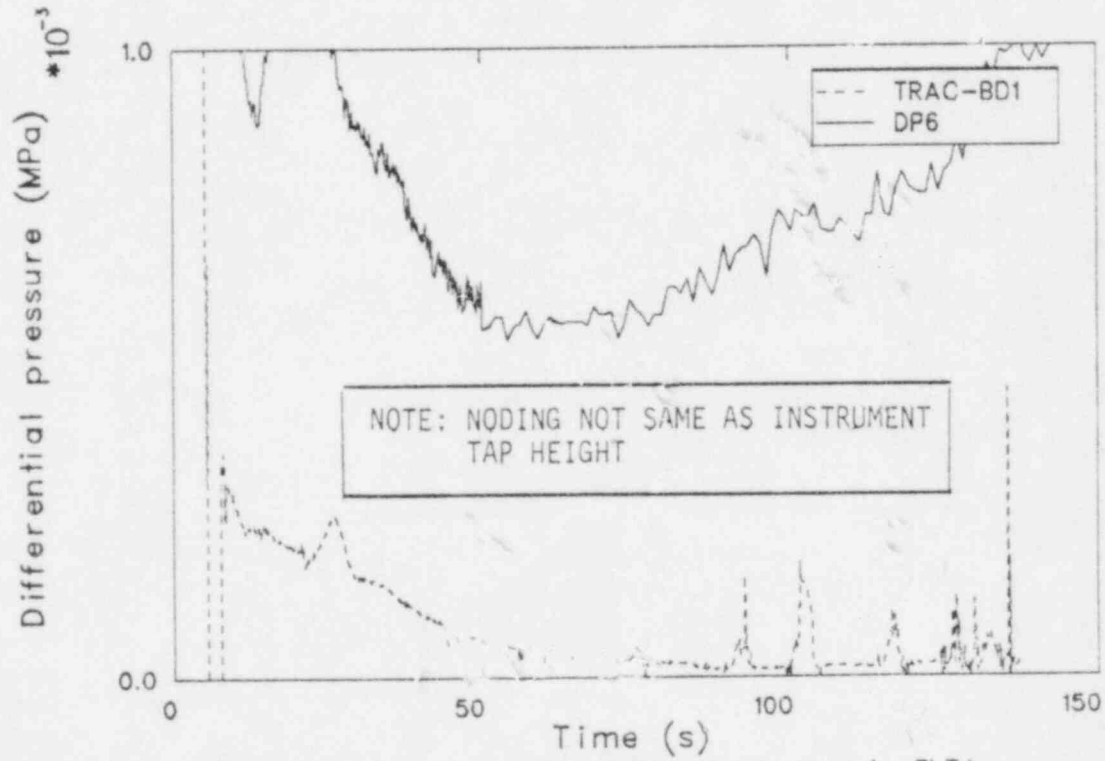

Figure 24. Emptying and refill of the downcomer in TLTA Test 6425.

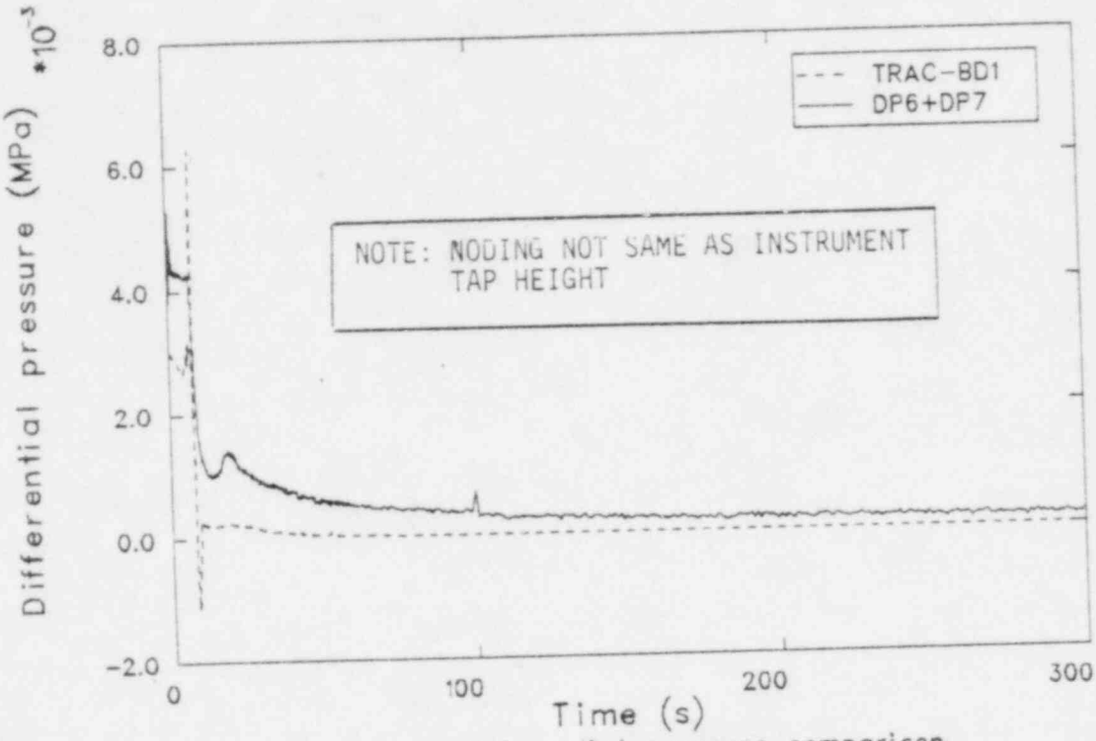

Figure 25. Downcomer differential pressure comparison for TLTA Test 6426.

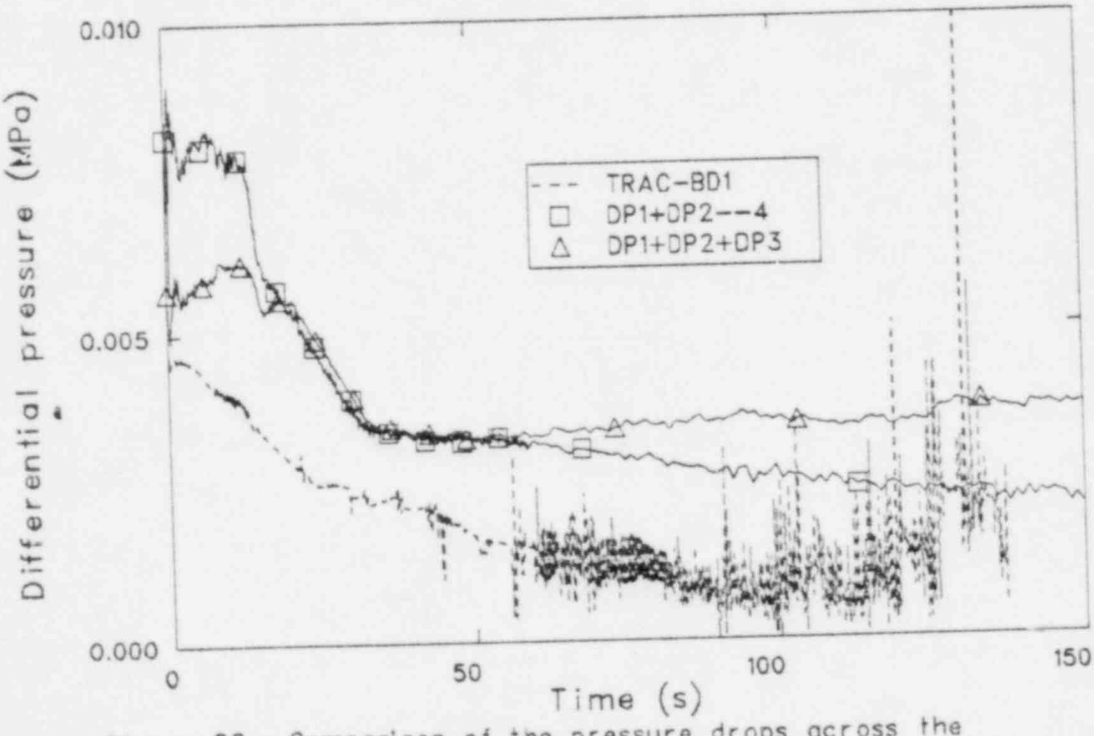

Figure 26. Comparison of the pressure drops across the vessel lower plenum for the TLTA Test 6425.

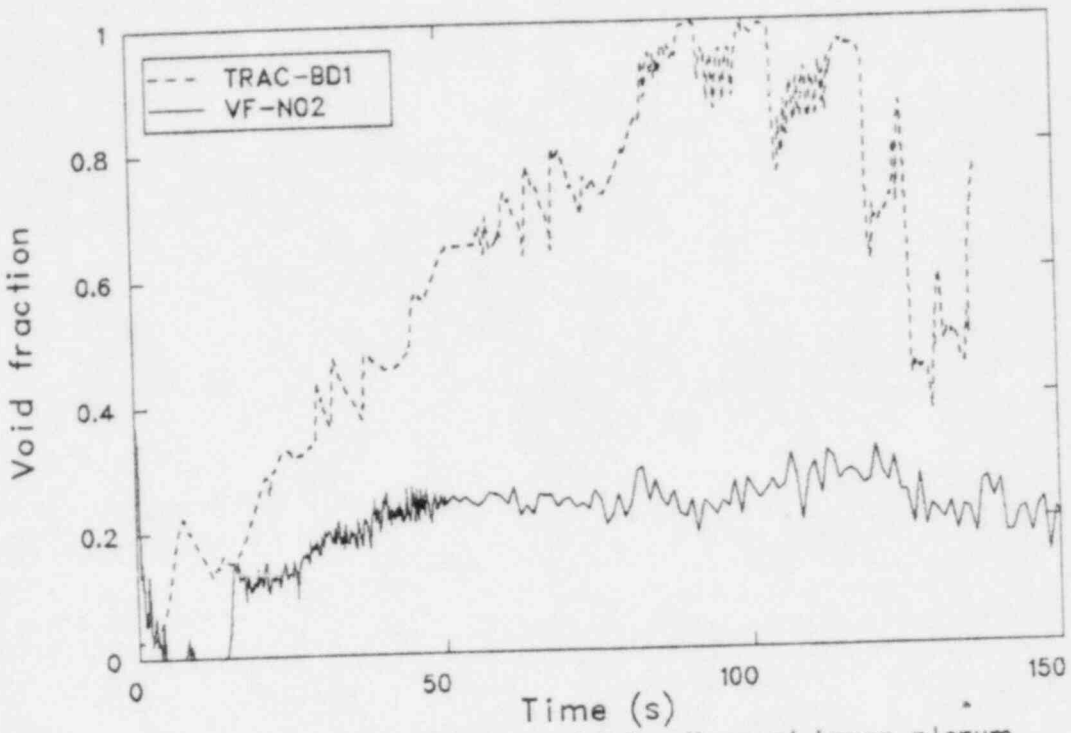

Figure 27. Comparison of the void fractions at lower plenum level 2 for the TLTA Test 6425.

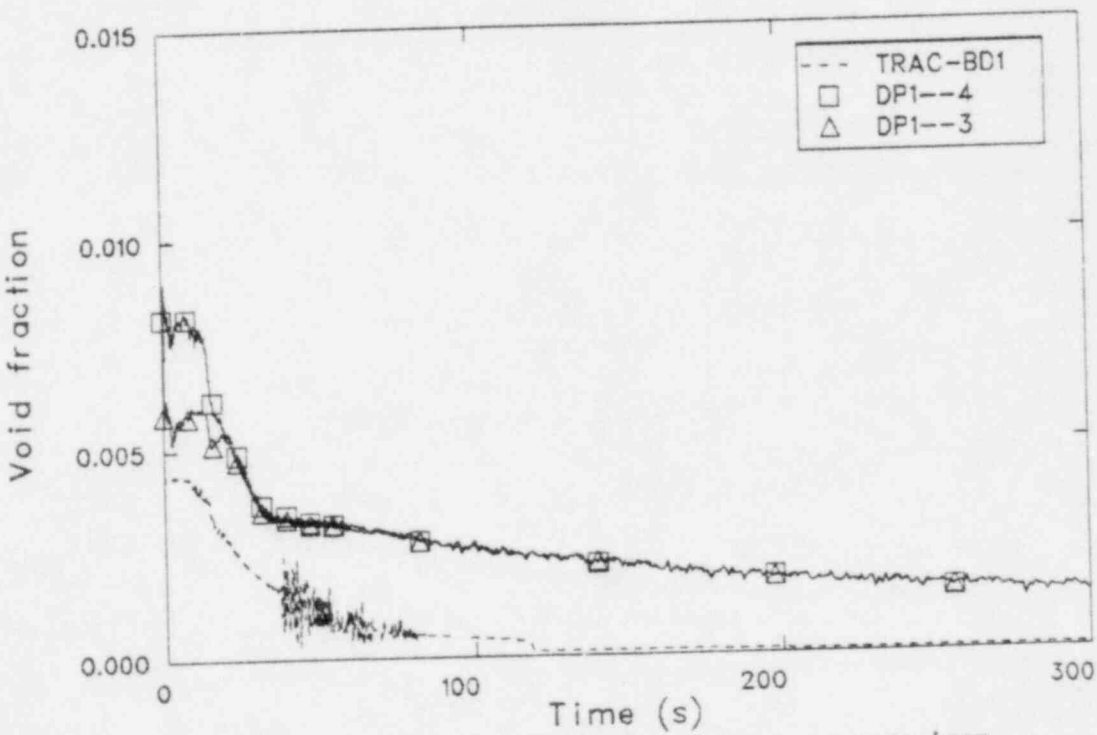

Figure 28. Lower plenum differential pressure comparison for TLTA Test 6426.

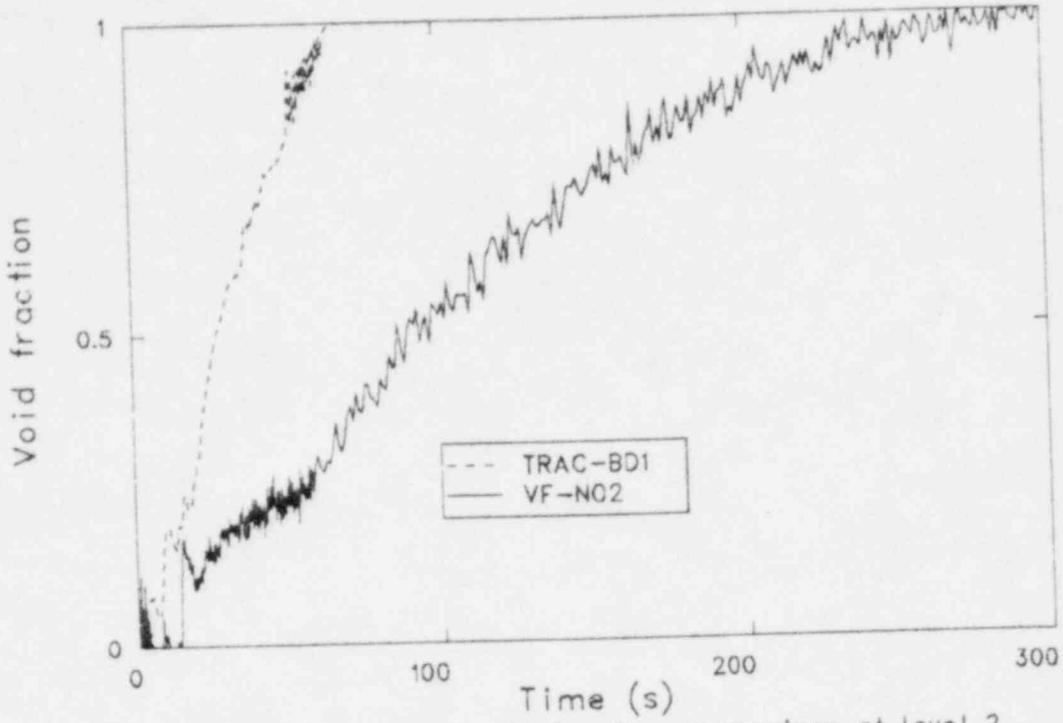

Figure 29. Lower plenum void fraction comparison at level 2 for TLTA Test 6426.

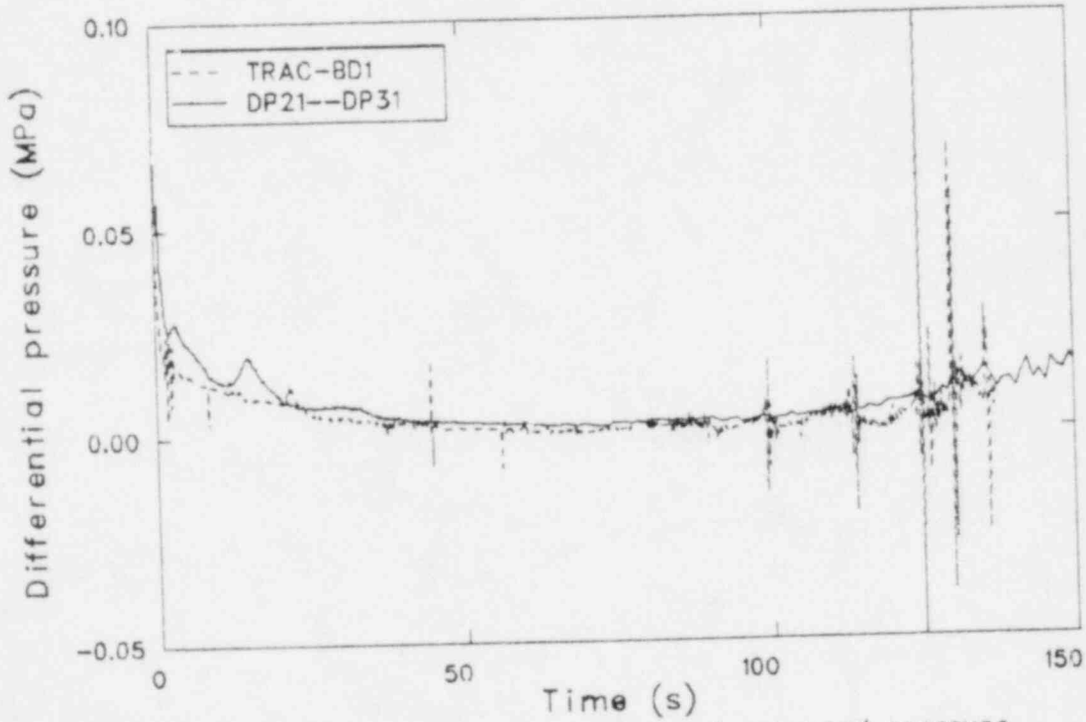

Figure 30. Comparison of calculated and measured pressure drops across the core in TLTA Test 6425.

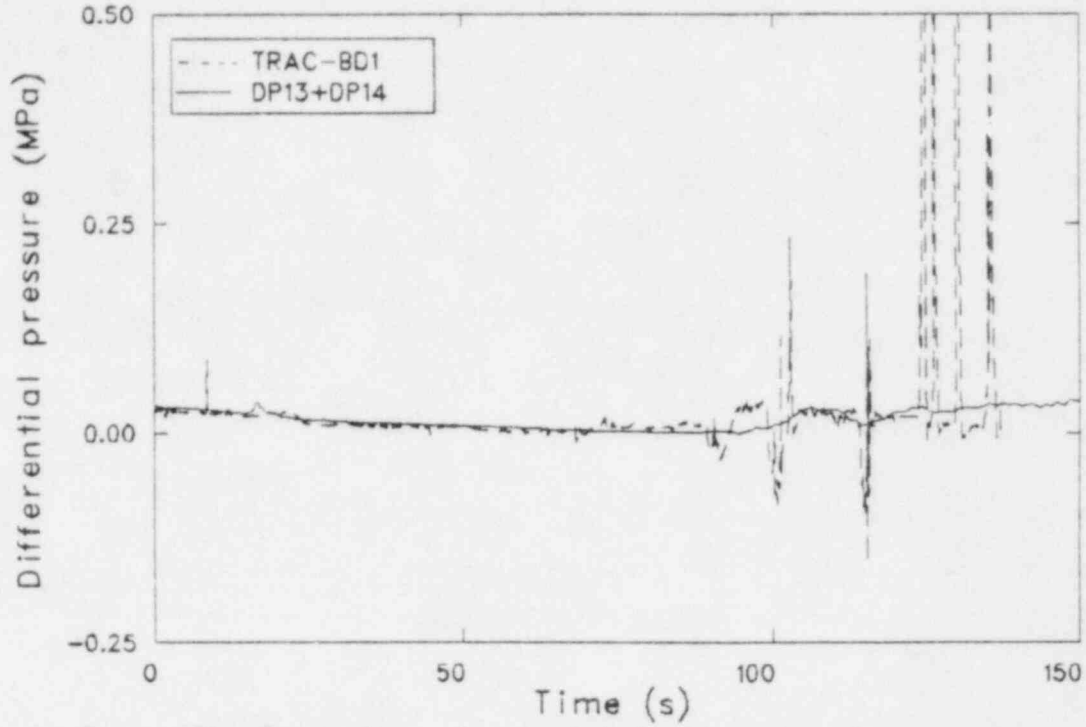

Figure 31. Comparison of calculated and measured pressure drops across the bypass tubes in the TLTA Test 6425.

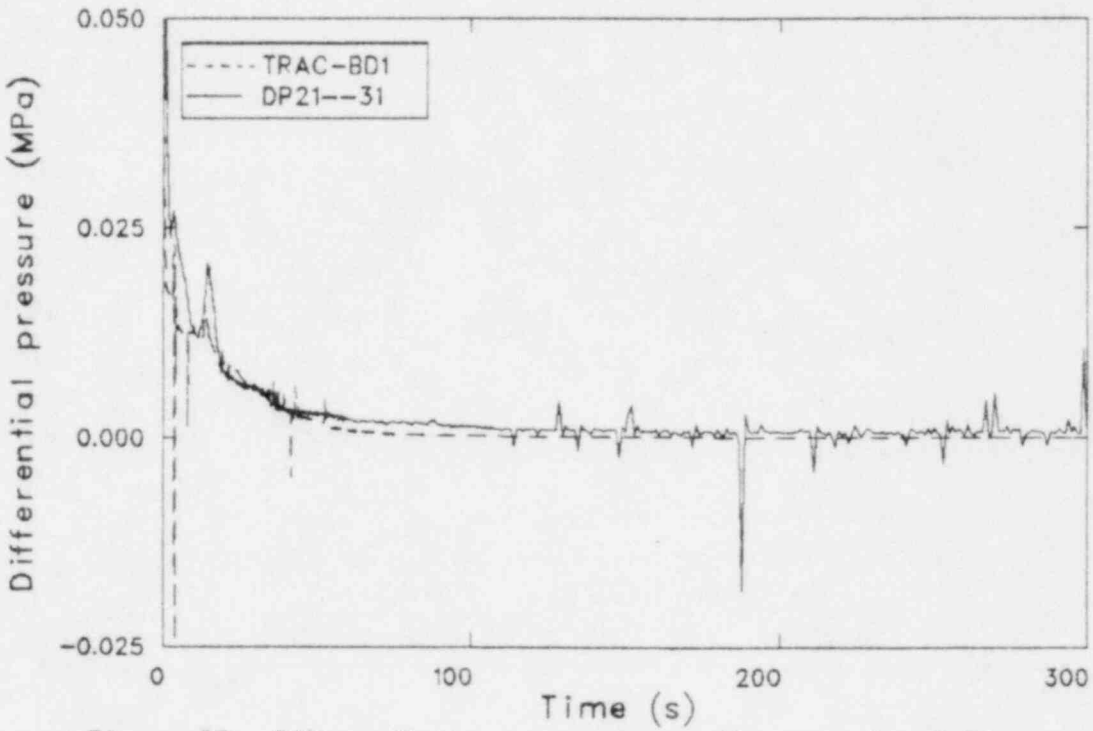

Figure 32. Differential pressure across the core for TLTA Test 6426.

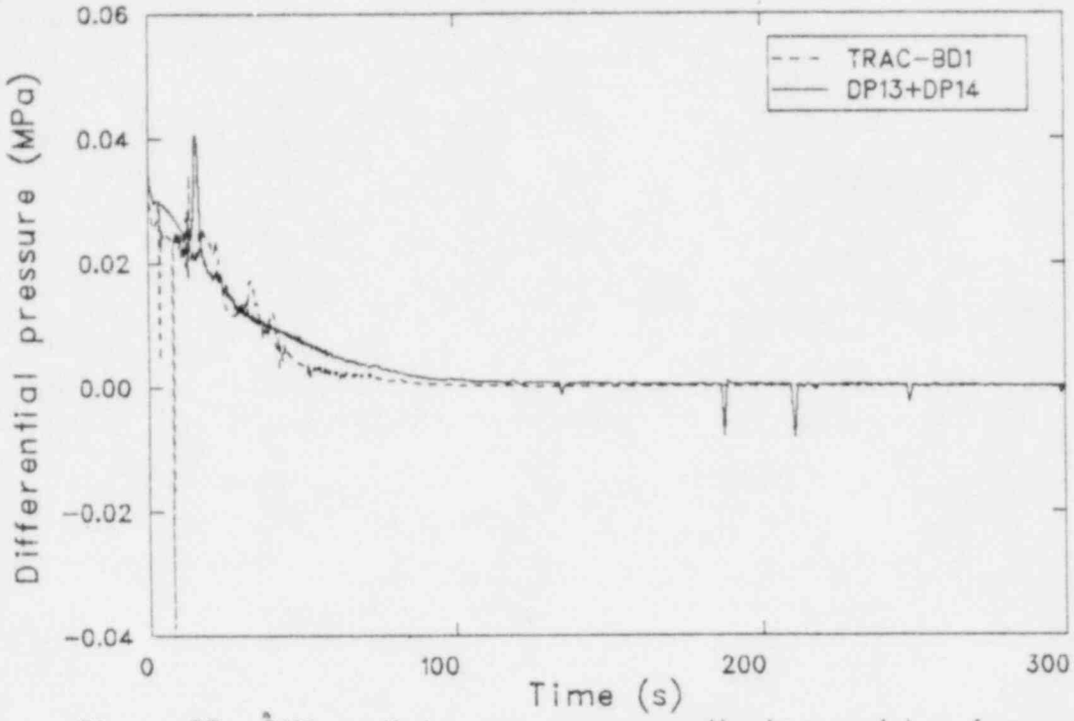

Figure 33. Differential pressure across the bypass tubes for TLTA Test 6425.

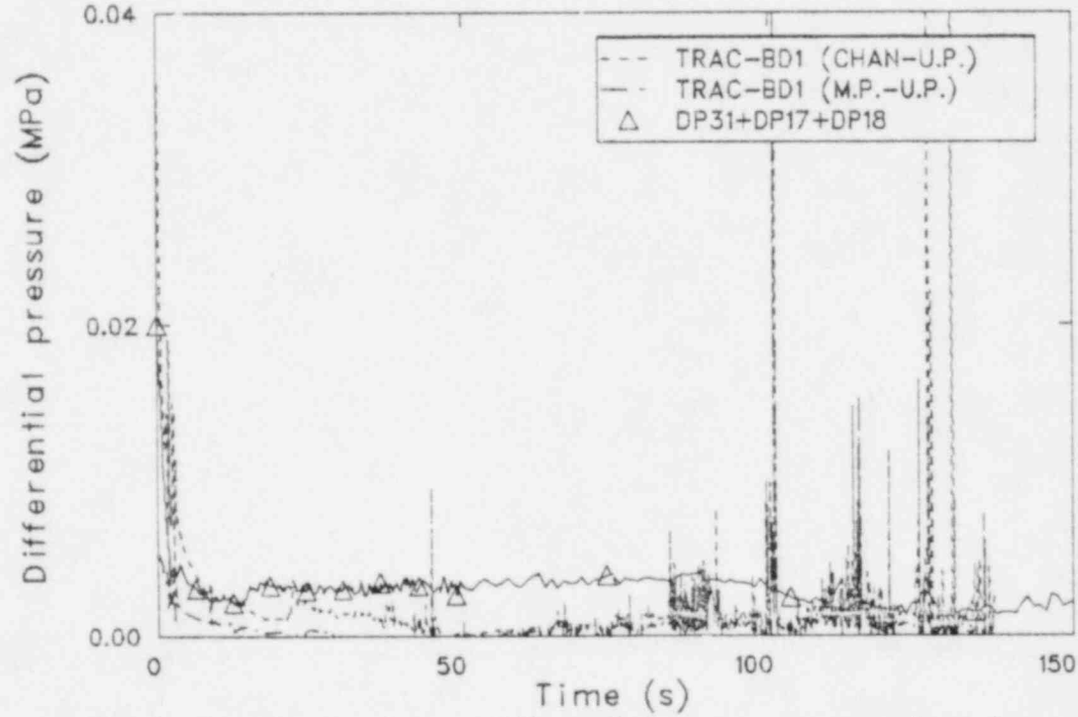

Figure 34. Upper plenum differential pressure comparison for TLTA Test 6425.

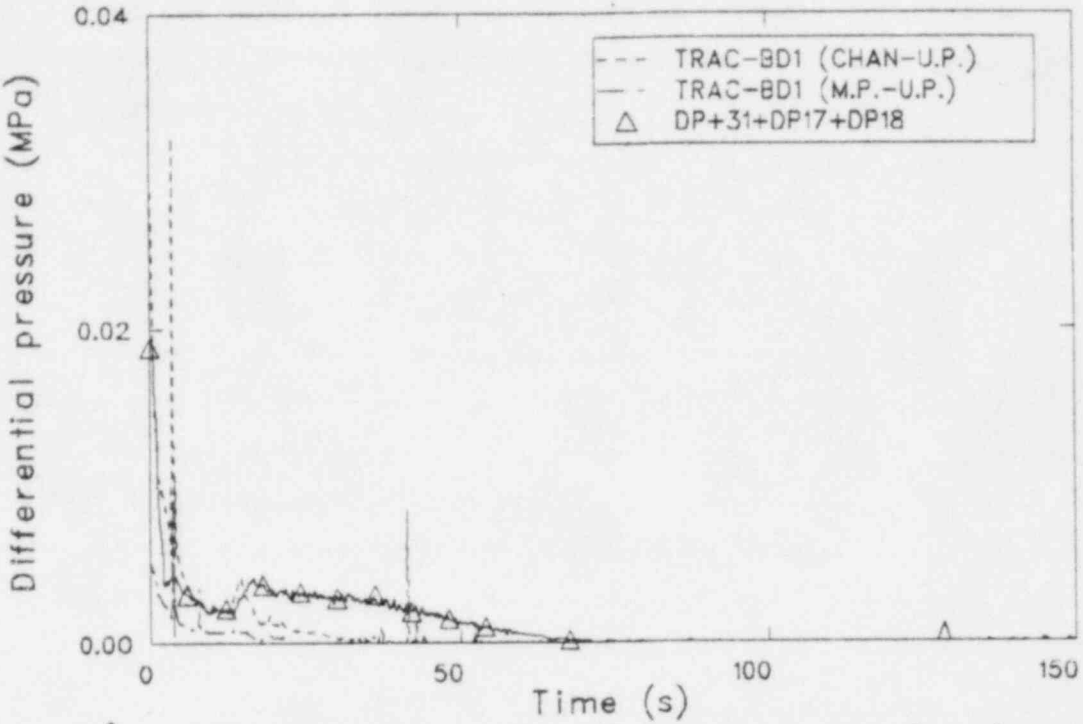

Figure 35. Upper plenum differential pressure comparison for TLTA Test 6426.

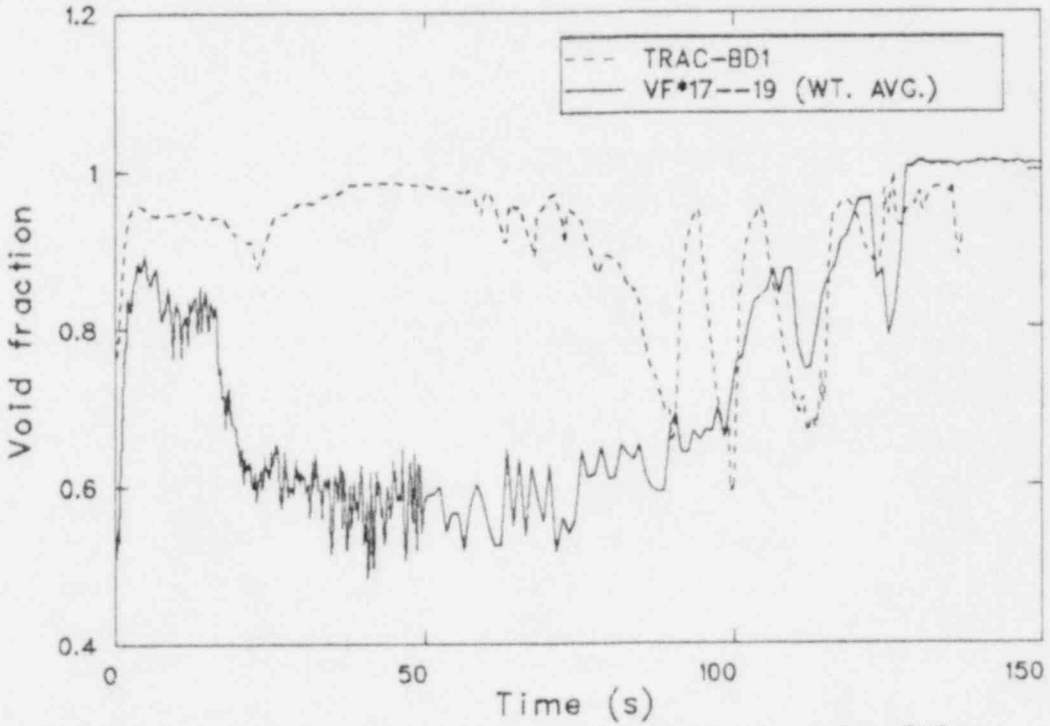

Figure 36. Upper plenum void fraction comparison for TLTA Test 6425.

The 6426 calculation behaved in the same manner as 6425 with respect to liquid holdup and flow out the core. A liquid level was calculated in the upper plenum for the first 45 seconds as compared to 73 seconds in the experiment. TRAC-BD1 calculated less liquid holdup in the upper plenum but a faster fluid removal rate to the separator-dryer.

The upper plenum void fraction comparisons for Tests 6425 and 6426 are shown in Figures 36 and 37. The calculations were compared to a weighted average of the measurements at DP Cells 17, 18 and 19, which better characterized the data in each case. The void fraction comparisons demonstrated that the undercalculation of the differential pressure across the upper plenum was related to differences between the calculated and measured liquid levels. The higher void fractions calculated by TRAC were consequences of the more rapid blowdown compared to the experiment.

4.2 Break Inlet Conditions

Figures 38 and 39 show the break inlet pressures for Tests 6425 and 6426. These are very nearly the same as the steam dome pressures, which will be further discussed in Section 4.4.

The void fraction comparison at the suction side break inlet is shown in Figure 40. Based on the calculation, the subcooled blowdown lasted until 5.7 seconds in Test 6425, at which time the break inlet void fraction increased sharply. The inlet void fraction calculation oscillated above 0.9, not showing as distinct a liquid-vapor transition as did the data. At 31 seconds, the calculated void fraction increased to 0.98, a timing which correlated to the jet pump exit plane uncovery. High void inlet conditions prevailed beyond 38 seconds for the bulk of the calculation. Calculated void departures from unity were caused by small amounts of entrained liquid from the separator-dryer. This was consistent with the higher calculated boiloff rate of HPCS liquid from the mixing plenum.

Figure 41 compares the drive side break inlet void fractions for Test 6425. The differences between the two curves were due to the fact that the instrumentation was in the downcomer whereas the calculation was made in the jet pump throat. Reflood was evident beyond 75 seconds on

Figure 41, reflected by the reduced drive side break inlet void fraction. By comparison, lower plenum reflood commenced at 93 seconds in Figure 27 based on the calculated void fraction at Vessel Level 2.

Figures 42 and 43 show the suction and drive side break inlet void fraction comparisons, respectively, for TLTA Test 6426. The suction side calculation showed good qualitative agreement with the 6425 calculation. Differences during the subcooled blowdown were the result of different downcomer void fractions used to initialize two transients. Similarly, the higher void fraction during subcooled blowdown and the shorter two-phase transition period at the drive side inlet in the Test 6426 calculation compared to Test 6425 were the result of different downcomer void initializations. Lower plenum reflood and the attendant liquid carryover to the drive side break were conspicuously absent in the jet pump exit pipe void fractions for Test 6426 compared to Test 6425, as shown in Figure 44 beyond 55 seconds. This had an important effect on the vessel depressurization and is further discussed in Section 4.4.

Figure 45 compares the temperatures at the break inlet for Test 6425. The calculated temperature followed the saturation curve and reflected the faster vessel depressurization rate calculated by TRAC-BD1. The calculated temperature oscillations seen here were ramifications of the vessel pressure instability. The data indicated that the downcomer thermocouple did not dryout during the experiment, and the TRAC-BD1 calculation was in good qualitative agreement with this measurement for the ECC test.

Figure 46 shows the break inlet temperature comparison for the NO ECC test. The calculation showed good agreement with the data. Dryout of the downcomer thermocouples was observed in this experiment, and TRAC-BD1 calculated this event at 51 seconds compared to 73 seconds in the data. The quantitative comparison between the break inlet temperatures improved as the break flow calculation improved, which will be more apparent upon examination of the break flow plots in the next section.

The break inlet subcooling comparisons for TLTA Test 6425 are shown in Figures 47-48. The suction side subcooling calculations were made in the first cell of Tee 4, immediately upstream of the choking plane. The drive

side break inlet subcooling calculations were made in the throat of the broken loop jet pump at Cell 1 of the primary leg. The subcooling calculations were compared to downcomer measurements at an height equivalent to TRAC-BD1 Level 5 or 6, as appropriate depending on the test.

The suction side break inlet subcooling comparison for Test 6425 is shown in Figure 47. A short term comparison was made because the liquid blowdown was the main interval of interest. Fluid conditions became saturated after 8.3 seconds and remained so for the duration of the calculation. Fluid conditions in the experiment reached saturation after 5.9 seconds. From then on the data indicated that the downcomer was above the saturation temperature. It was more probable that the downcomer thermocouples were irradiated by the vessel wall than it was for the downcomer to contain superheated steam.

The drive side break inlet subcooling comparison for Test 6425 is shown in Figure 48. The TRAC-BD1 calculation indicated that fluid conditions were subcooled for the first 11.6 seconds in the jet pump throat and were saturated thereafter, compared to a transition from subcooled to superheated conditions in the downcomer at 6 seconds in the experiment.

Short term break inlet subcooling comparisons for Test 6426 are shown in Figures 49-50. The suction side break inlet was calculated to have saturated after 10.4 seconds, whereas the drive side break inlet remained subcooled for 12.9 seconds. Data at both Levels 5 and 6 in the downcomer indicated that the fluid was superheated for the entire experiment, as exemplified by Figure 51. The measured superheat was questionable before 65 seconds, because the steady state data also indicated that superheated conditions existed in the downcomer--below the liquid level.

The drive side break inlet subcooling calculation shown in Figure 52 is presented here to enable comparison to the drive side break flow data, Figure 56. The calculated superheat interval from 35 to 56 seconds correlated well to the interval of best mass flow comparison out the drive line. No explanation was found for this behavior.

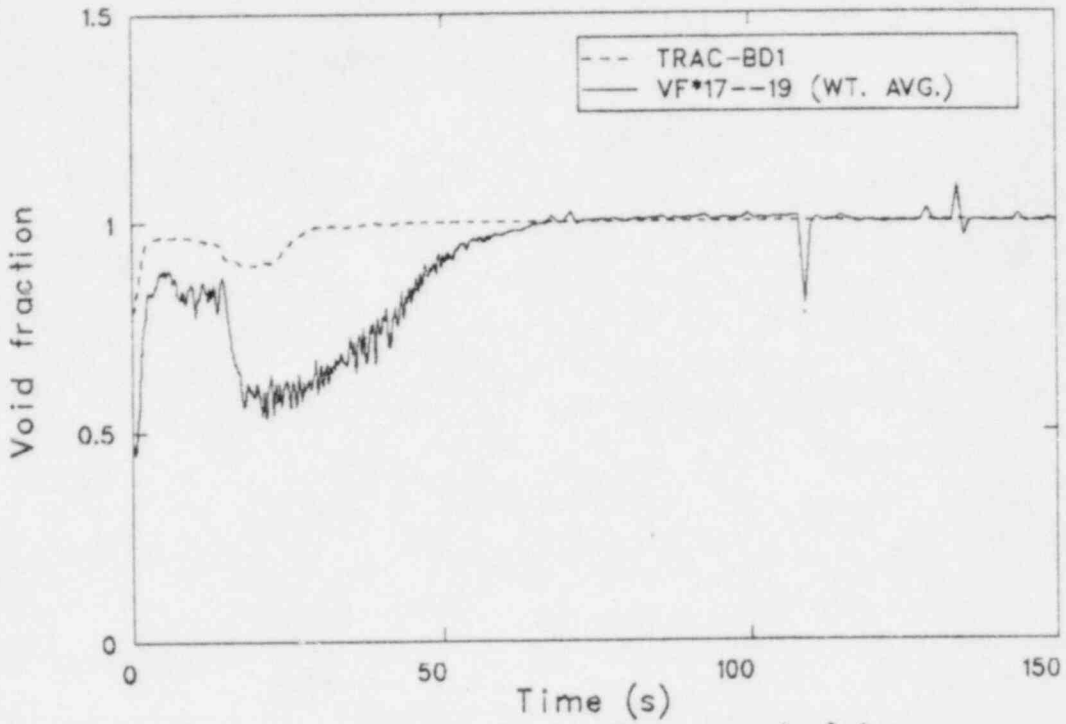

Figure 37. Upper plenum void fraction comparison for TLTA Test 6426.

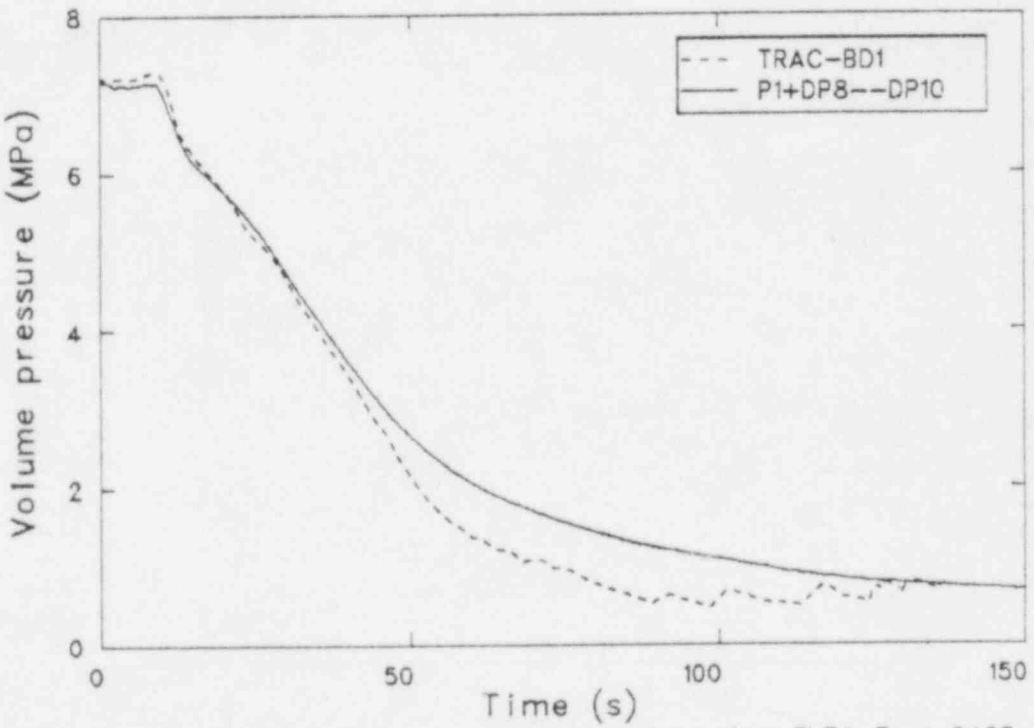

Figure 38. Break inlet pressure comparison for TLTA Test 6425 at the downcomer level 5.

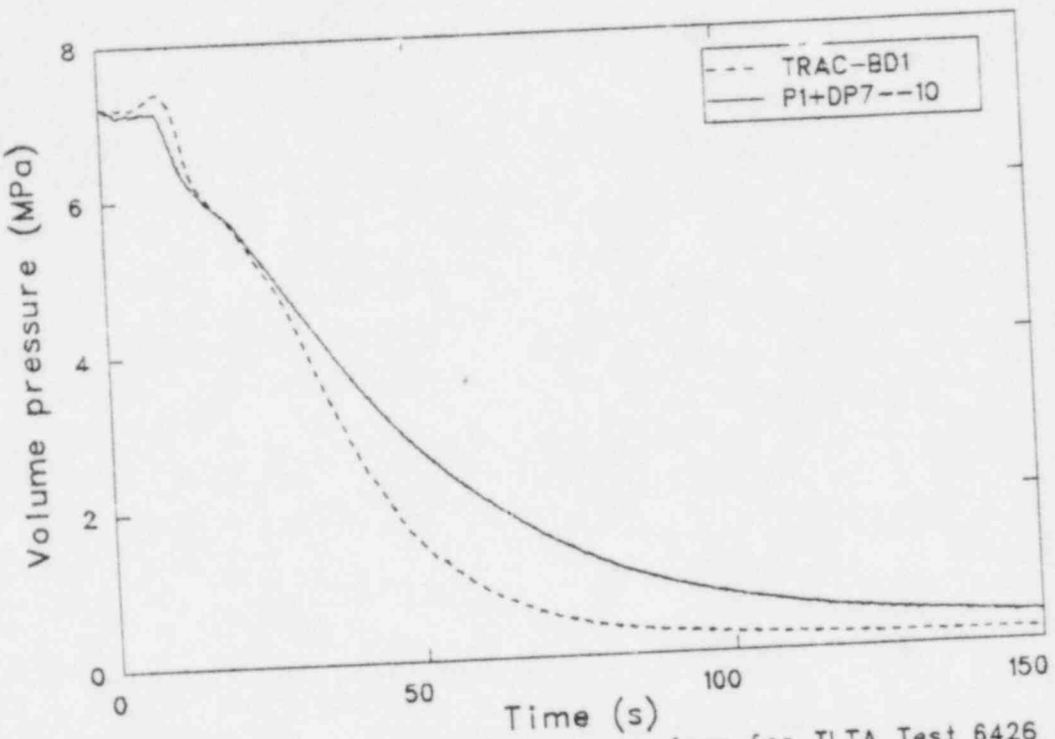

Figure 39. Break inlet pressure comparison for TLTA Test 6426 at downcomer level 5.

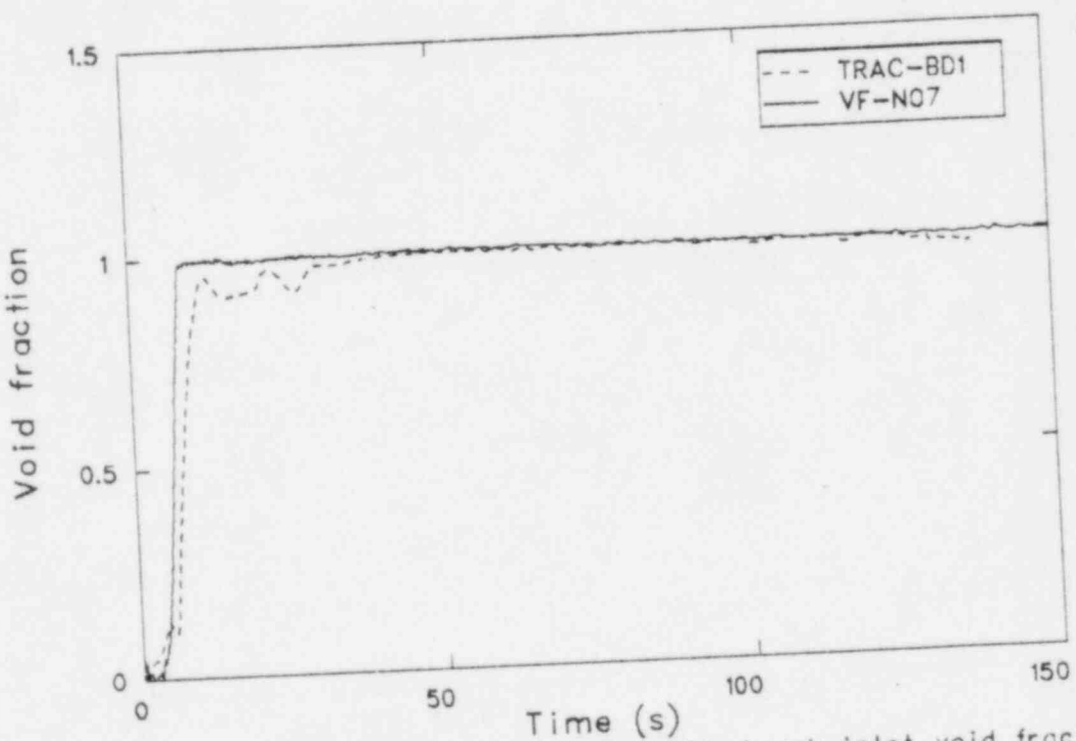

Figure 40. Comparison of the suction side break inlet void fractions for TLTA Test 6425 as calculated in Tee 4,cell 1.

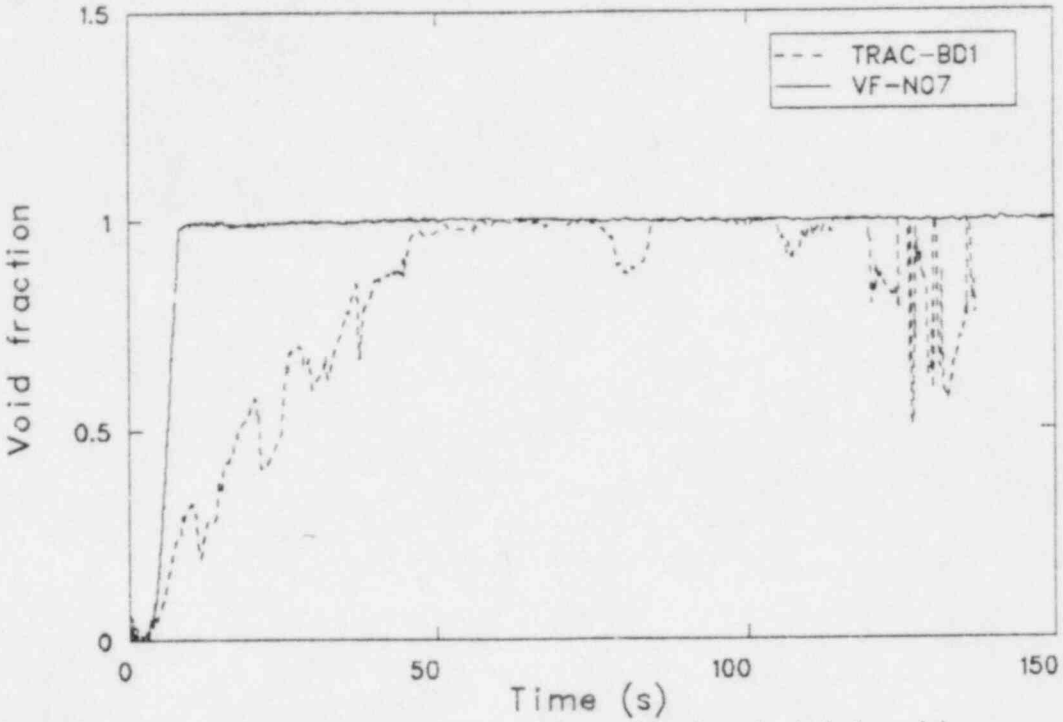

Figure 41. Comparison of the drive side break inlet void fractions for TLTA Test 6425 as calculated in the jet pump throat.

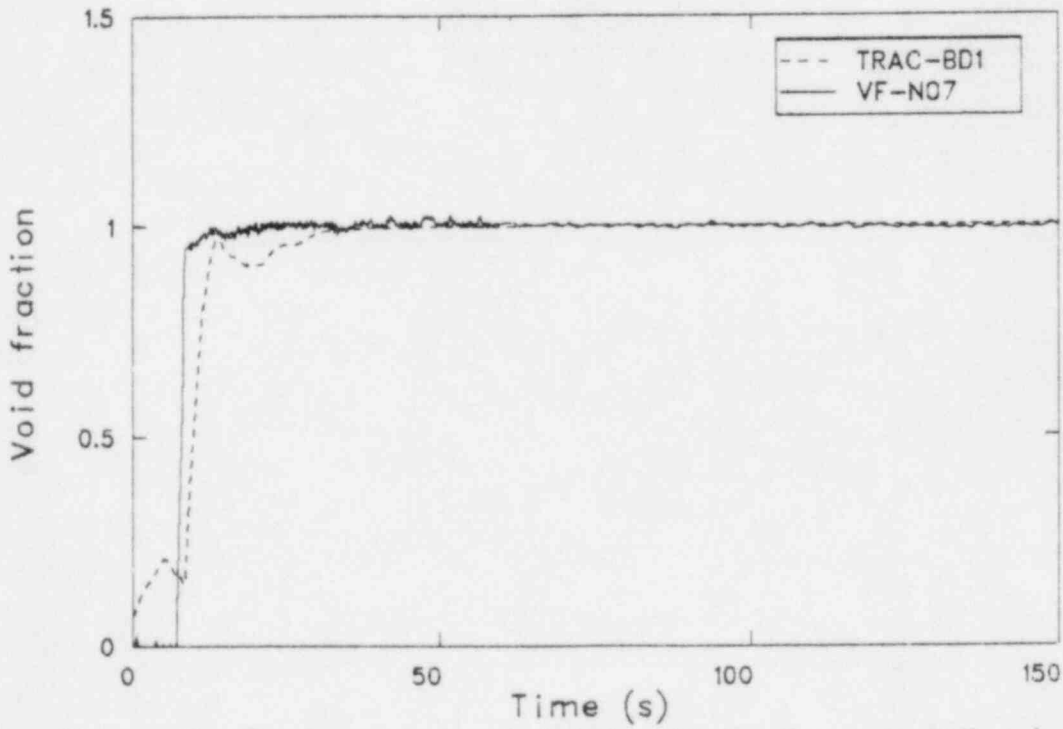

Figure 42. Suction side break inlet void fraction calculation in Tee 4, cell 1 compared to downcomer data for TLTA Test 6426.

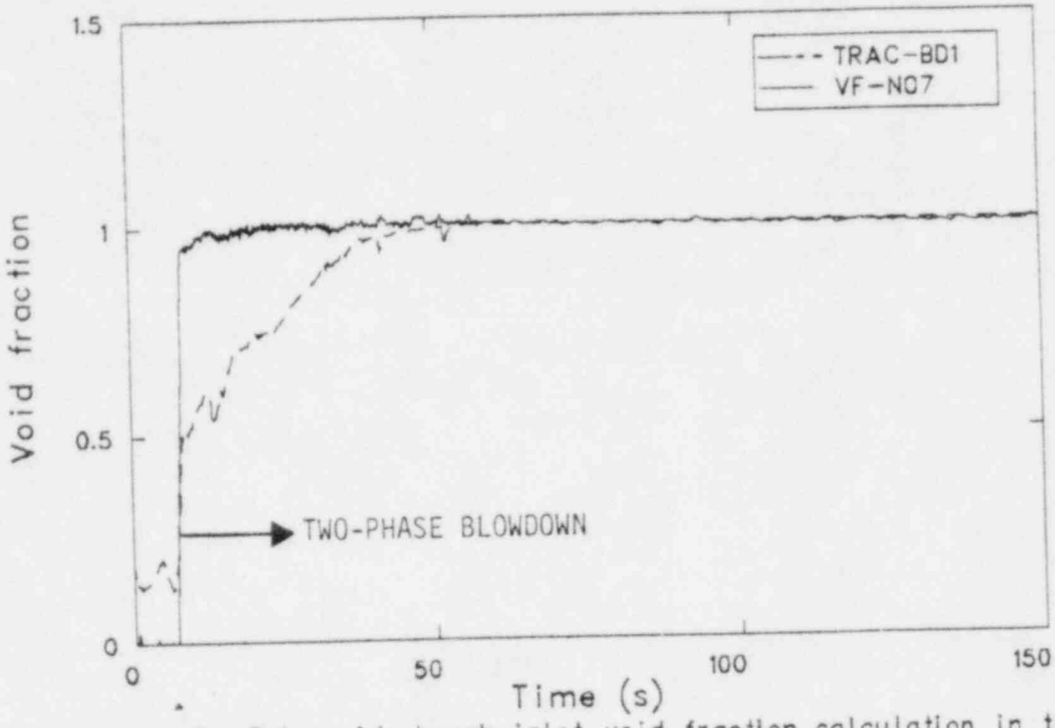

Figure 43. Drive side break inlet void fraction calculation in the jet pump throat compared to downcomer data for TLTA Test 6426.

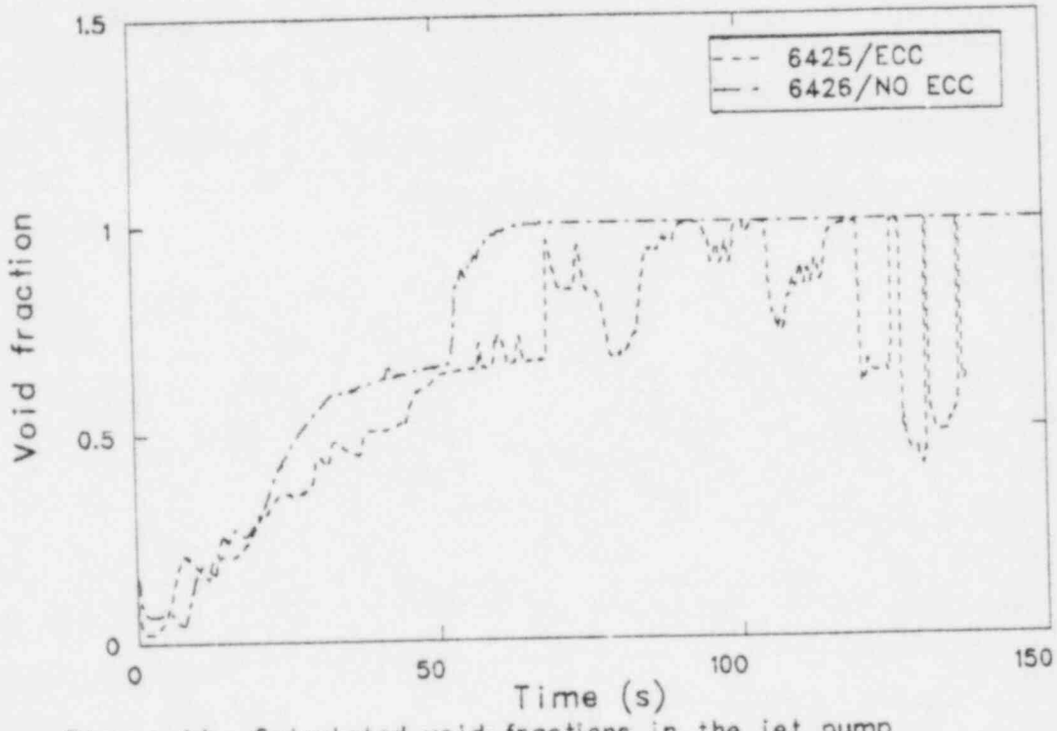

Figure 44. Calculated void fractions in the jet pump exit pipe for TLTA Test 6425/6426.

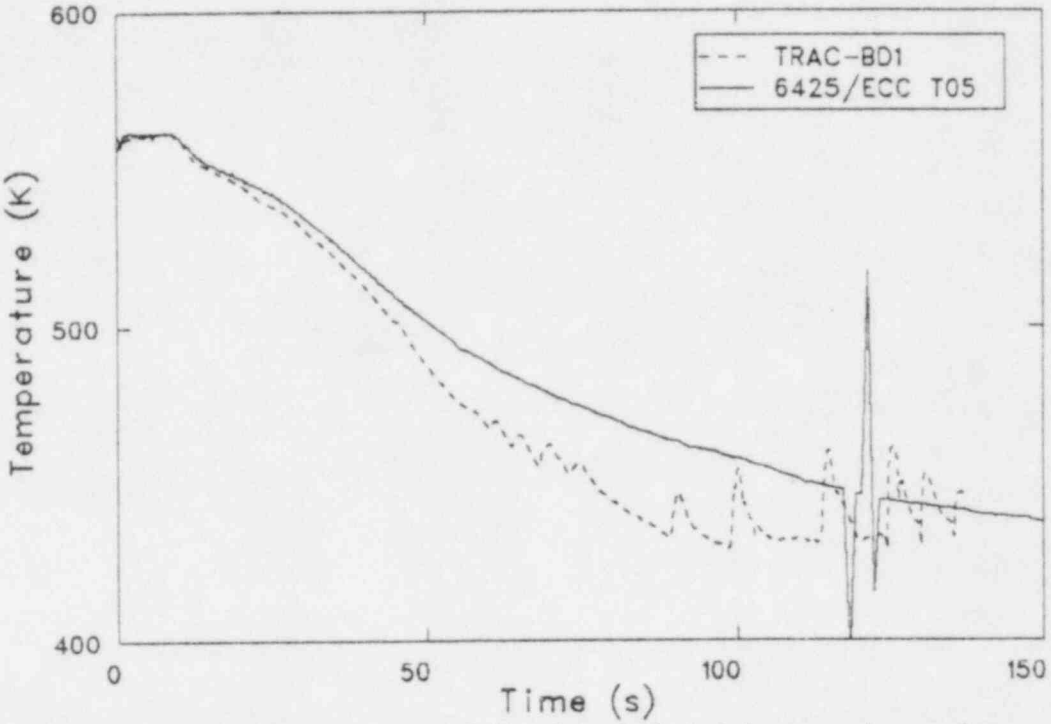

Figure 45. A comparison of the break inlet temperatures for TLTA Test 6425 at downcomer level 5.

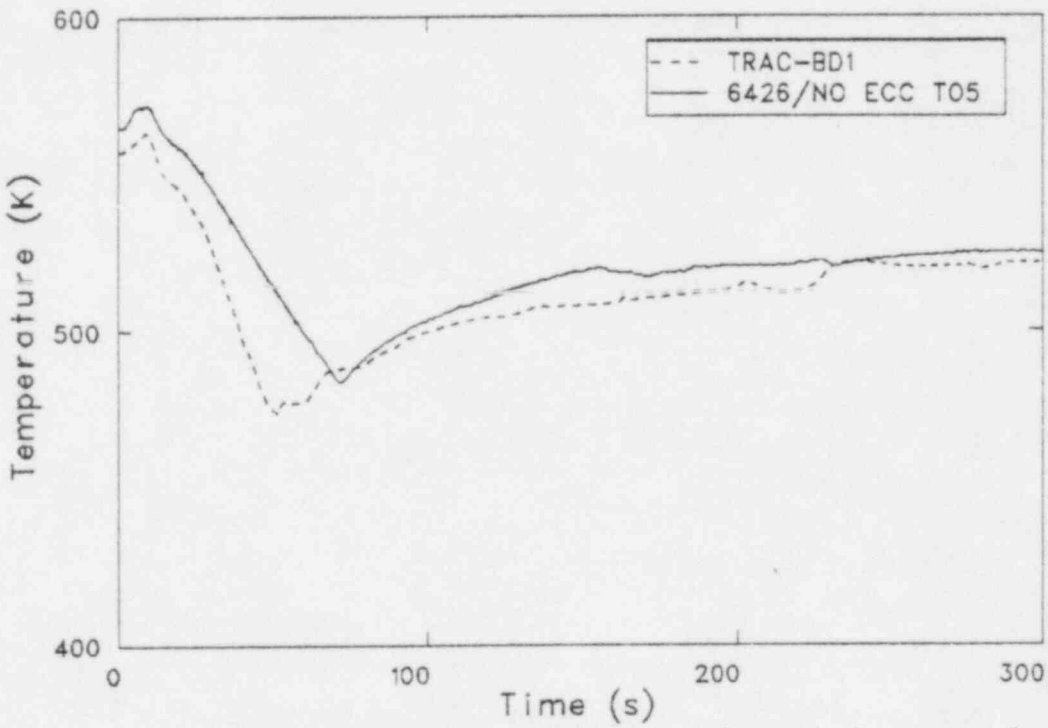

Figure 46. Break inlet temperature comparison at downcomer level 5 for TLTA Test 6426.

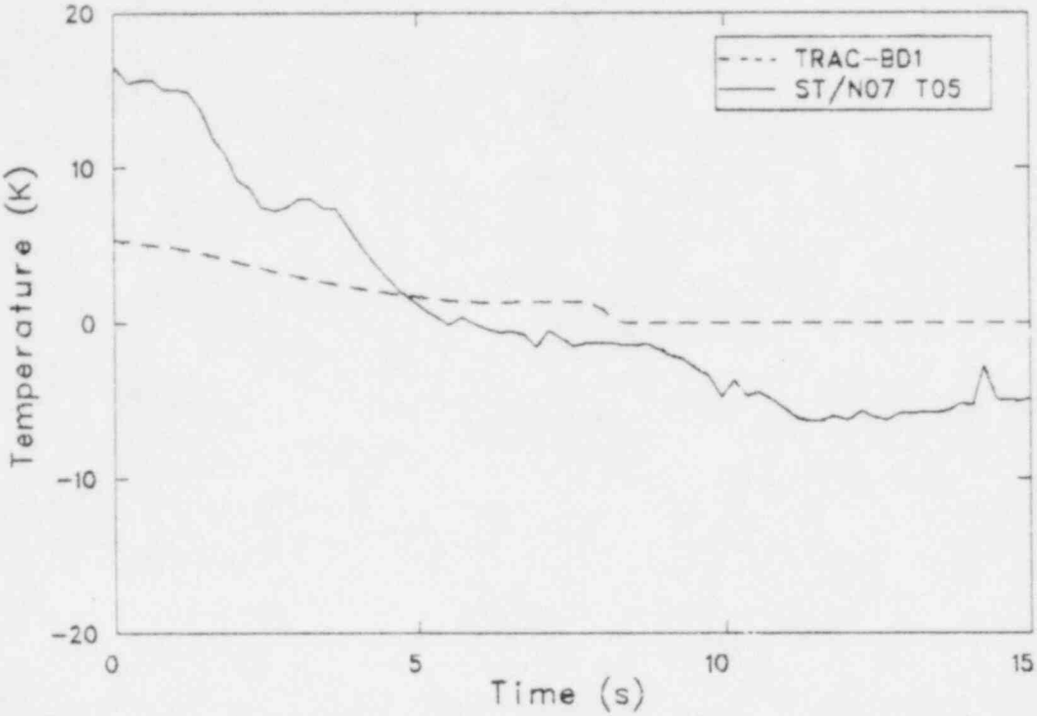

Figure 47. Calculated suction side breck inlet subcooling at Tee 4, cell 1 compared to measured subcooling at downcomer level 5 for TLTA Test 6425.

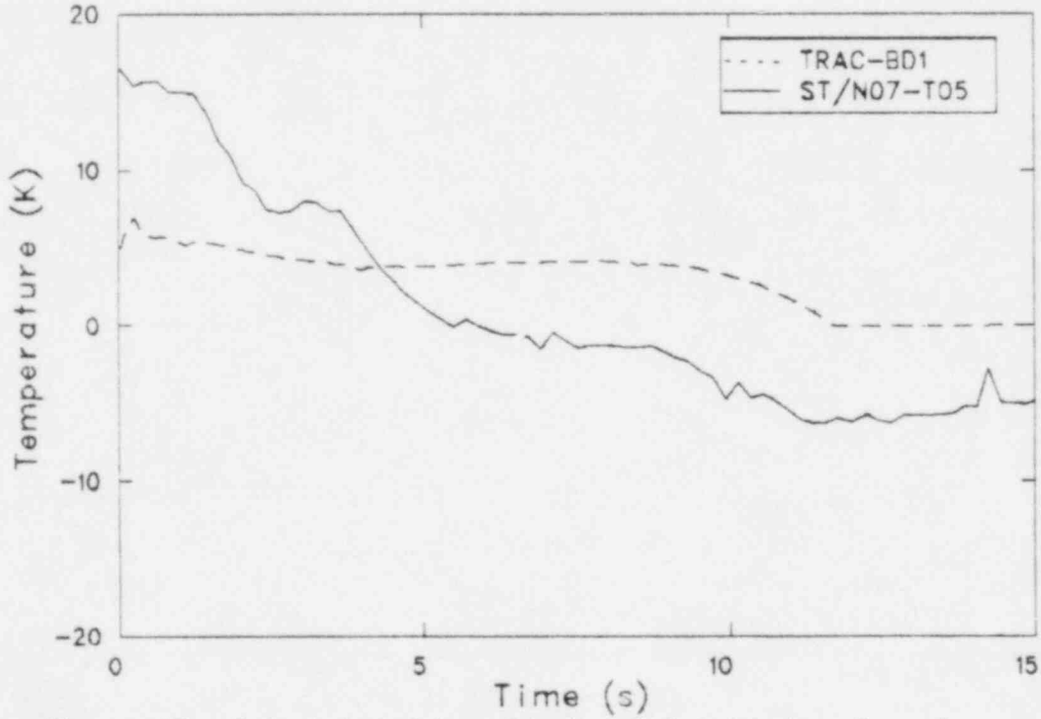

Figure 48. Calculated drive side break inlet subcooling at jet Pump 8, cell 1 compared to measured subcooling at downcomer level 5 for TLTA Test 6425.

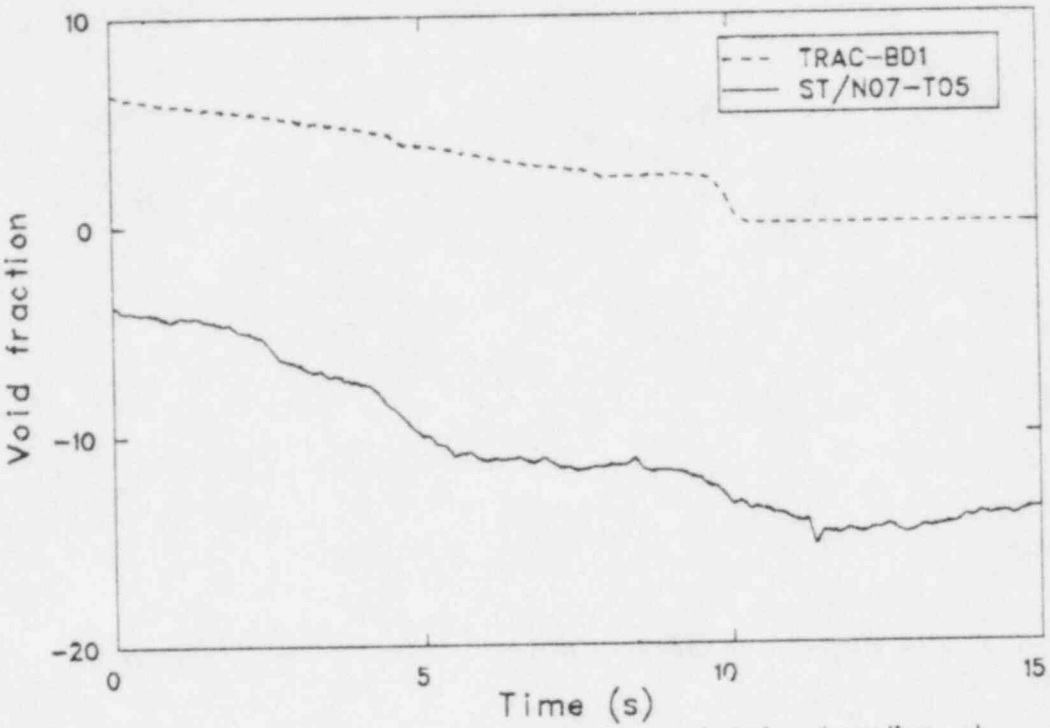

Figure 49. Calculated suction side break inlet subcooling at Tee 4, CELL 1 compared to the data at downcomer level 5 for TLTA Test 6426.

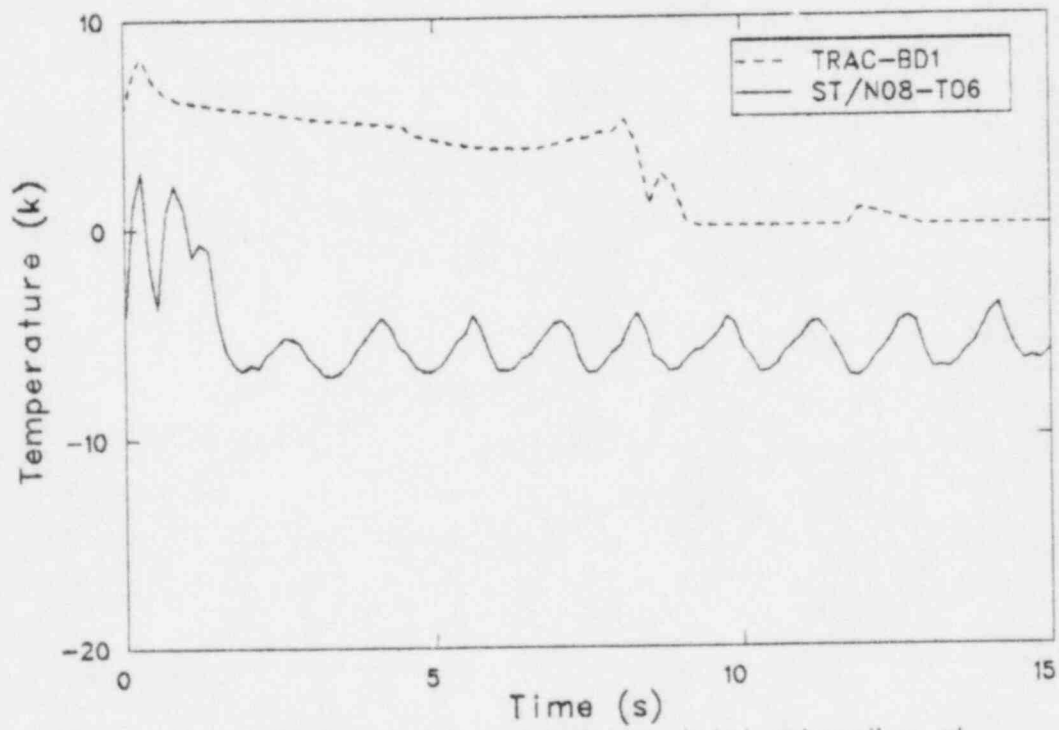

Figure 50. Calculated drive side break inlet subcooling at Jet Pump 8, cell 1 compared to the data at downcomer level 6 for TLTA Test 6426.

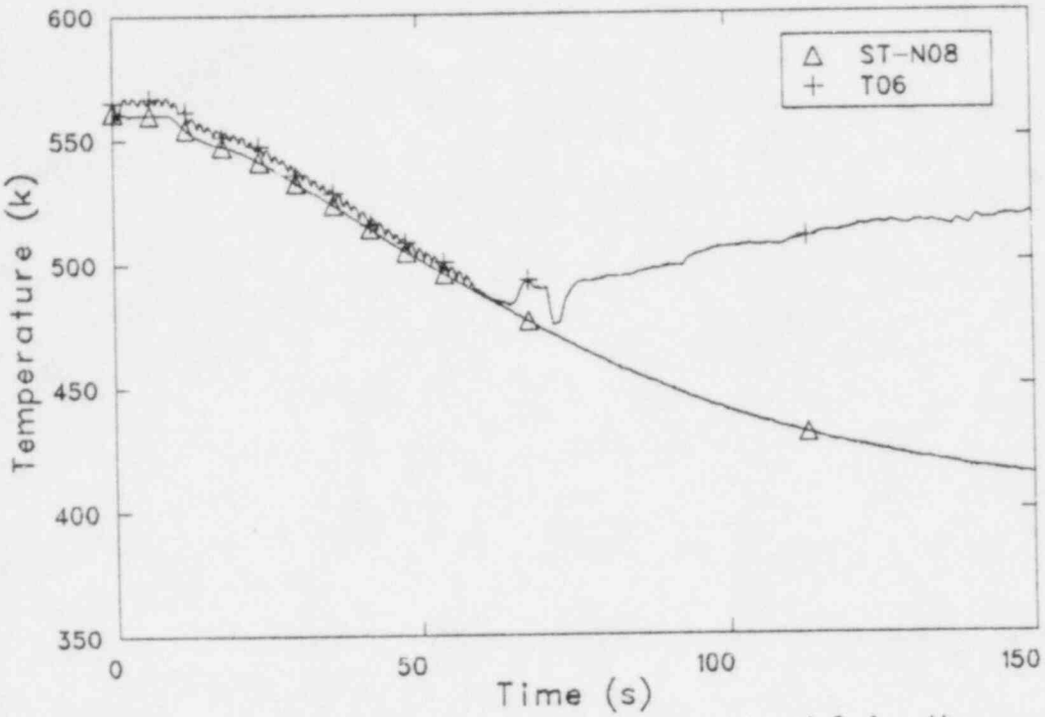

Figure 51. Apparent superheat at downcomer level 6 for the TLTA Test 6426 transient. Data are questionable.

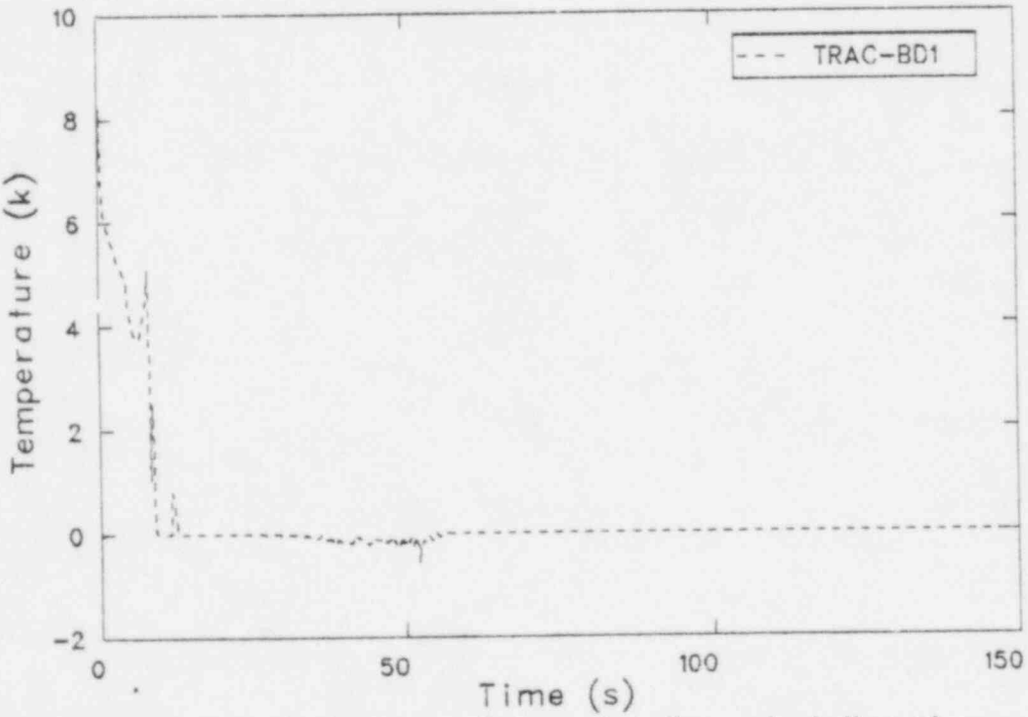

Figure 52. Drive side break inlet subcooling calculation at the broken loop jet pump throat for TLTA Test 6426.

4.3 Break Flow Comparisons

Break flow comparisons are made on the basis of mass flows in this section. Due to the problems discussed in Section 3.1.1, erroneous calculations of the pressure downstream of the choking planes precluded valid volumetric flow comparisons.

The suction side break flow comparisons are shown in Figures 53 and 54. The results for Test 6425 showed an undercalculation of the subcooled break flow by an average of ten percent. There was a one second period at the onset of the transient when TRAC-BD1 calculated a large flow spike which fell well outside the data. This was caused by exit plane Break 24. Removal of blowdown Valve 22 from the model at the start of the transient subjected the system to a full pipe diameter break instantaneously, which was not an accurate simulation of the TLTA blowdown valve operation.

The subcooled flow period ended at 6.3 seconds in the 6425 calculation compared to 9.3 seconds in the experiment. These times correlated well to the calculated and measured recirculation pump suction line uncovery points of 7.4 and 9.4 seconds, respectively, which had been determined in Section 4.1.1 using the downcomer void fractions. From 6 to 12 seconds, there was a transition period in the calculation between the liquid blowdown and the two phase blowdown. This was due to the time required for downcomer level 5 to empty. The break flow was overcalculated by a maximum of 65 percent during the two phase blowdown. However, this large error decreased as the calculation progressed, and the TRAC-BD1 results were in good agreement with the experiment for the duration of the calculation. In fact, examination of the data error bands presented on Figure 53 indicated that the suction side break flow calculation was within tolerance for almost the entire assessment.

The suction side break mass flow for Test 6426 is shown in Figure 54. TRAC-BD1 undercalculated the subcooled break mass flow by an average of 14 percent. The onset of the two phase blowdown was well calculated. The calculated transition time between the subcooled and the two phase

blowdowns could have been reduced by finer vessel noding. The two-phase flow out the break was again overcalculated by a maximum factor of 1.75 at 16 seconds. This error gradually decreased as the vessel emptied, and the calculation was in good agreement with the data beyond 50 seconds, during the single-phase vapor blowdown.

The drive side break flow for Test 6425 is shown in Figure 55. The calculated flow spike at one second was caused by the lack of a blowdown valve in the model as discussed earlier. The overall mass flow comparison for the drive side was generally not as good as the suction side. Mass flows were again undercalculated for the subcooled blowdown, this time by an average of 40 percent. However, the drive side calculation showed a substantial improvement in the two-phase blowdown compared to the suction side calculation, and it agreed very well with the data from 15 to 57 seconds. The drive side mass flow was significantly undercalculated from 57 to 120 seconds, during a vapor blowdown period. Drive side mass flows increased beyond 120 seconds and were in apparent agreement with the data. However, little confidence was placed in the calculation at these times due to the numerically induced vessel pressure buildup discussed in Section 4.5.

Comparison of Figure 55 with the drive side break inlet void fraction shown in Figure 41 revealed that the accuracy of the drive side break mass flow calculation at high void was directly correlatable with the calculated void fraction in the jet pump throat. From Figure 41, when the inlet void fraction increased beyond 0.98, the accuracy of the drive side break mass flow calculation suffered. When the calculated inlet void fraction dropped below this value, the break mass flow calculation agreed with the TLTA data quite well. This particular correlation was not apparent in the suction side break mass flow calculation, suggesting that the drive side problem was either geometry dependent, or possibly caused by the errors in the steam choking model.

The drive side break mass flow comparison for Test 6426 is shown in Figure 56. The results show the same qualitative agreement with the data as observed in Test 6425. The drive side break flow was again undercalculated as the break inlet void fractions approached unity. As

best as could be ascertained from Figure 43, the break flow error occurred when the inlet void fractions exceeded 0.99.

The drive side break flow calculations for the ECC/NO ECC tests were most accurate when the calculated break inlet void fractions were in agreement with the data, so long as the calculated void fraction did not exceed 0.98 to 0.99. This correlation was also apparent in the Test 6426 suction side break flow calculation, but it was more subtle.

As mentioned in Section 3.1.1, errors were discovered in the TRAC-BD1 steam choking model during these assessment calculations. First, the static donor cell pressure calculated from the momentum solution in subroutine TF1D was passed to subroutine CHOKE where it was used incorrectly as the stagnation pressure. Second, the equation in subroutine CHOKE for the isentropic extrapolation to the pressure at the choking plane was erroneous. It was determined that these errors did not affect the ECC/NO ECC assessments. In order for the erroneous coding to have been reached, the flow would have had to have been choked and the donor cell void fraction unity. These conditions were never reached in the calculations.

With the erroneous choked flow coding eliminated, the question still remained as to the reason for the erroneous break mass flow calculation at high void fraction. The matter was investigated further, and it was found that the differences between the calculated and measured break flows were largest when the flow unchoked. Correlative with the unchoking was the increase in the donor cell void fraction described above. As best as could be ascertained from the printouts, with coarse edit intervals, the donor cell choked void fractions were less than 0.985, whereas the unchoked donor cell void fractions were greater than 0.99. Thus, it appeared that the voids changed as the code logic switched from choked to unchoked flow.

The suction side break mass flow calculation for Test 6425 was more accurate because the flow remained choked for the duration of the calculation. In Test 6426, the suction side flow unchoked between 56-59 seconds and remained subsonic thereafter. On the drive side in Test 6425, the curves in Figure 55 converged at 77-80 seconds,

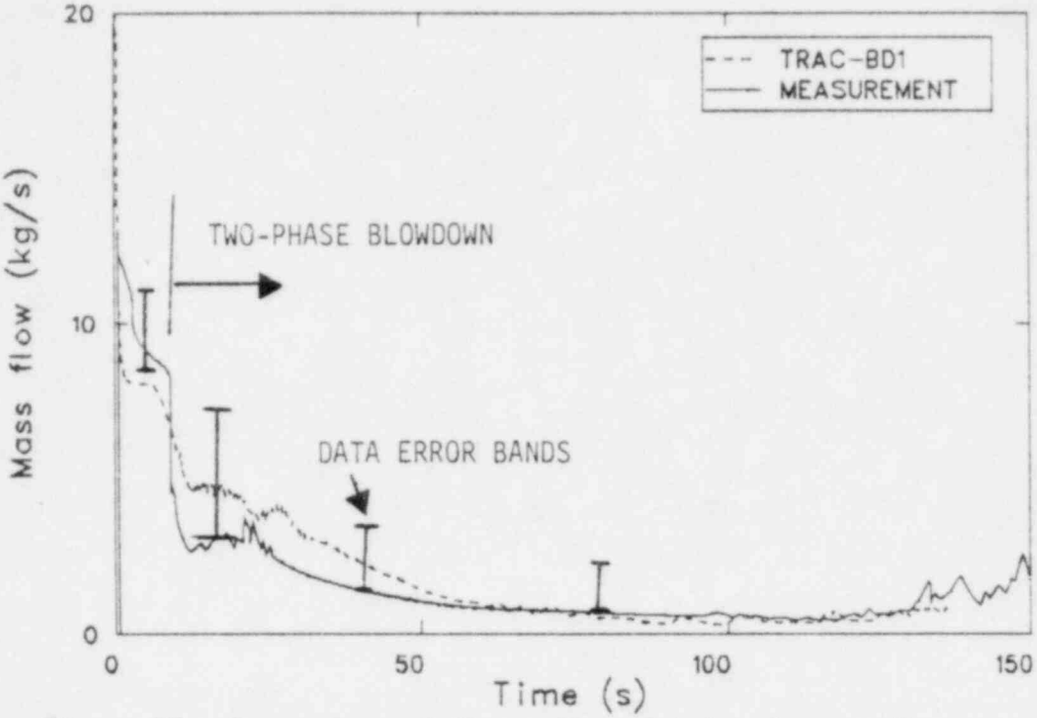

Figure 53. Comparison of the suction side break mass flows for TLTA Test 6425.

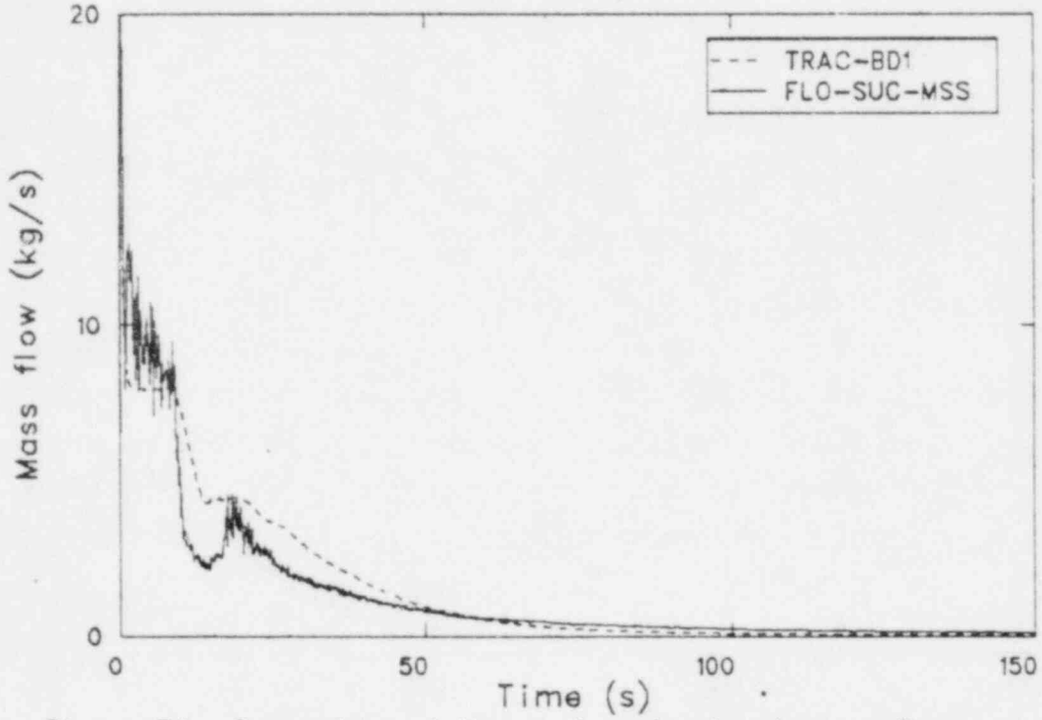

Figure 54. Comparison of the suction side break mass flows for TLTA Test 6426.

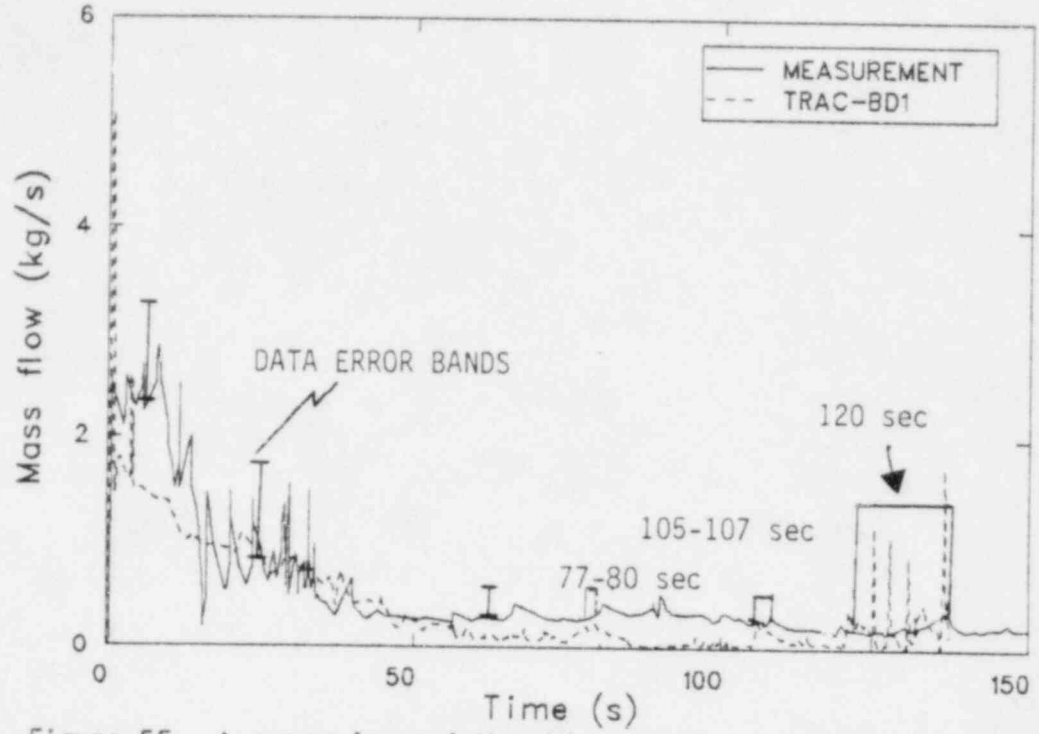

Figure 55. A comparison of the drive side break mass flows for TLTA Test 6425.

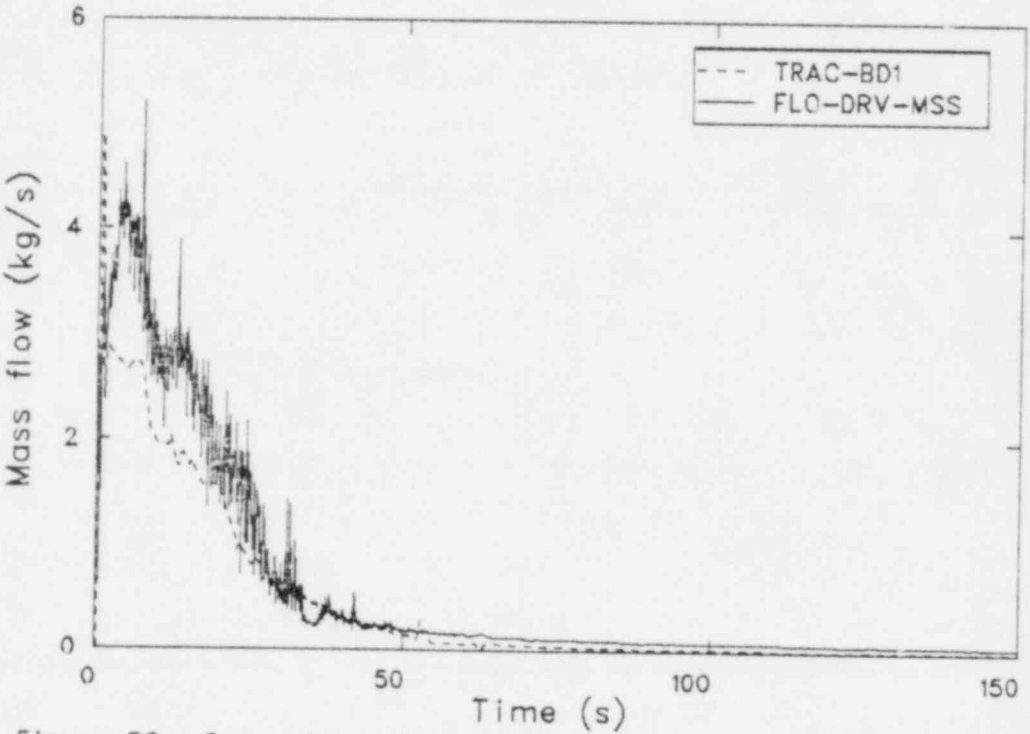

Figure 56. Comparison of the drive side break mass flows for TLTA Test 6426.

105-107 seconds, and beyond 120 seconds. Fair to excellent correlations were noticed between these time periods compared to those periods when TRAC-BD1 calculated choked flow out the drive side blowdown line. On Figure 55, the graphical results diverged at 57 seconds compared to 52 seconds for the transition time from choked to unchoked drive side flow per the printouts. In Test 6426, the curves on Figure 56 diverged at 54 seconds, while the drive side flow unchoked at 52 seconds per hard copy edits.

These correlations, while not perfect, were strong enough not to ignore. They suggested that the TRAC-BD1 choked flow model did a better job of calculating the break mass flows than did solution of the conservation equations in the unchoked flow numerics. However, it was more realistic for the flow to have remained choked in these experiments, and the reason for the TRAC-BD1 departure from acoustic flow at the driveline was not clear.

In summary, the subcooled liquid break flows were undercalculated, the two-phase break flows were overcalculated, and the high void break flows were in good agreement with the data so long as the flow remained choked.

4.4 Depressurization Calculations

The steam dome pressure data for Tests 6425 and 6426 are compared to one another in Figure 57. The vessel showed no depressurization for the first 9 seconds of either experiment, the subcooled blowdown period prior to the recirculation pump suction line uncovery. Note that in Test 6426, the NO ECC case, the vessel depressurized faster beyond 65 seconds than it did for the ECC Test 6425. The calculated results exhibited the same qualitative behavior, as shown in Figure 58, although they separated much earlier, at 25 seconds into the calculation. The comparative depressurization behavior between Tests 6425 and 6426 was due to several things. ECC injection cooled the system and removed energy from the rod bundle. Vaporization of the incoming ECC liquid produced pressure response opposite in direction to that induced by steam condensation and sensible cooling of the internals. Additionally, ECC injection increased the break mass flow during the later stages of Test 6425. It was not immediately

obvious which of the condensation, vaporization, or cooling effects would predominate, or how the break flow would interact. The condensation phenomena were thought to be the least important due to the small interfacial heat transfer areas in the ECC injection systems. The vaporization and break flow effects both tended to maintain the vessel pressure at a higher level in the ECC test compared to the NO ECC test. Vaporization increased the vessel pressure due to the increased steam density. ECC injection increased the liquid flow out the break and caused a vessel pressure maintenance situation similar to that observed during the subcooled blowdown. (The increased liquid break flow after the onset of ECC injection had been exemplified previously in Figure 44.) The relative magnitudes of the vaporization and the break flow effects were not quantified during these calculations but they exceeded the depressurization due to cooling and condensation. The important result was that TRAC-BD1 correctly calculated the qualitative vessel depressurization behavior between the two tests.

Calculated and measured results are compared in Figures 59 and 60 for Tests 6425 and 6426, respectively. In both assessments, TRAC-BD1 undercalculated the pressure in the vessel beyond 25 to 30 seconds. The slope of the calculated depressurization curve agreed better with the data in Test 6425 than in Test 6426, due either to a better initialization of the downcomer void fractions in the former, or the model of the malfunctioning valve in the latter. Recall that the downcomer void fractions were manually reset to zero in the Test 6425 initialization, as discussed in Section 3.1. The separation time between the calculated and measured curves could be adjusted dramatically by a slight vertical shift in the depressurization calculation; the vertical position of the calculated curve depended heavily on the initial downcomer void fractions and the break flows. In Test 6426, initialization was made from the TRAC-BD1 steady state calculated downcomer void fractions. These were greater than zero due to vapor carryunder by the code. The larger initial values of void fraction resulted in a depressurization curve with a steeper slope than the data for the first 60 seconds of the calculation.

Although the undercalculation of the subcooled liquid break flows in the first 10 seconds of the assessment correlated with the overcalculation of the vessel pressure during this period, the void fraction initialization was the more important factor. No correlations could be established between the calculated suction side break mass flows and the slope of the depressurization curves beyond the time of the recirculation pump suction line uncovery. If anything, the integrated mass flow out the suction side break was very slightly higher for Test 6425 in both the calculation and the data. This would have indicated that Test 6425 would have depressurized more rapidly than Test 6426, which was not the case. The drive side results were just as interesting. Both the data and the calculation indicated that the break flow rate was greater in Test 6426 than in Test 6425 for the first 34 seconds of the experiments. The TRAC vessel depressurization results were consistent with this behavior, but the measured steam dome pressures showed no separation during this time period. The conclusion was that either the break flow data or the steam dome pressure data were wrong. At approximately 57 seconds, the break flow behavior reversed, and the measured mass flow out the drive line was greater for Test 6425 then Test 6426. This reversal was reasonable compared to the calculation because it correlated well with the onset of the LPCI injection into the bypass tubes. Reflood of the lower plenum began shortly thereafter, and there was more liquid carryover to the drive side break. The greater liquid flow out the break increased the calculated break mass flow, but the volumetric flow would have been reduced due to lower two phase acoustic velocities. With a lower volumetric break flow rate, it was reasonable for Test 6425 to have depressurized slower than the NO ECC test. The break mass flow data reversal led the vessel depressurization data separation by 5 seconds. Both events led the actual onsets of the LPCS and LPCI injections. This behavior was not readily explainable in the context of the data, but it may have indicated that some of the HPCS fluid flowed from the mixing plenum to the lower plenum earlier than anticipated.

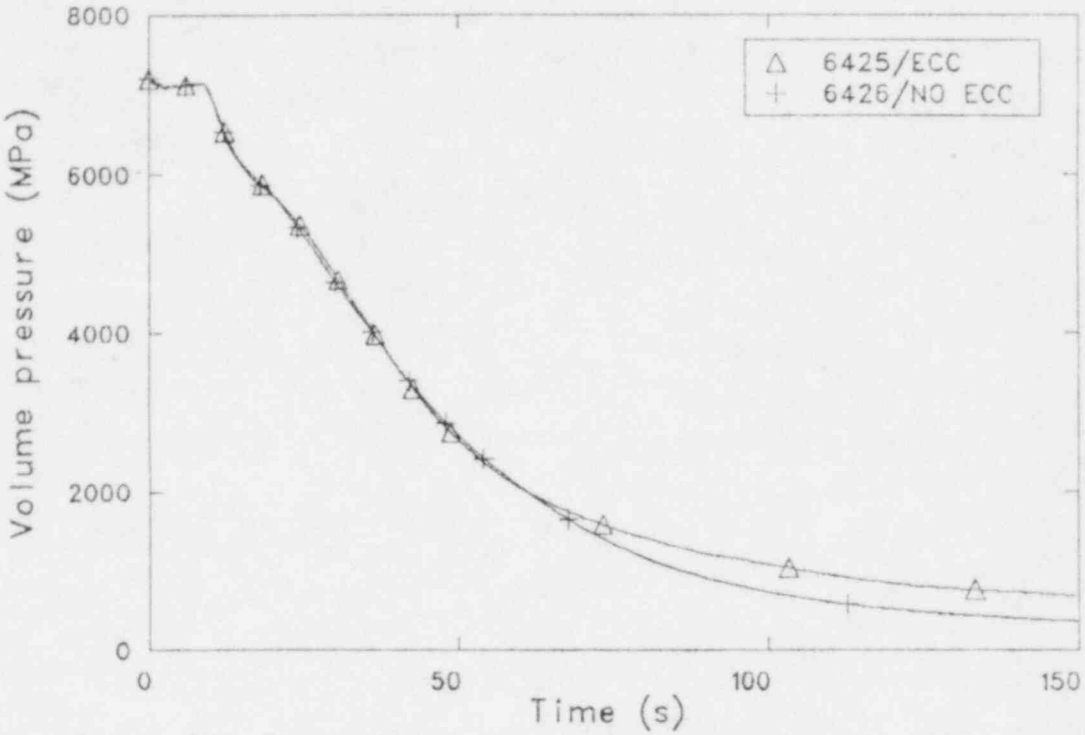

Figure 57. Steam dome pressure data comparison for TLTA Tests 6425 and 6426.

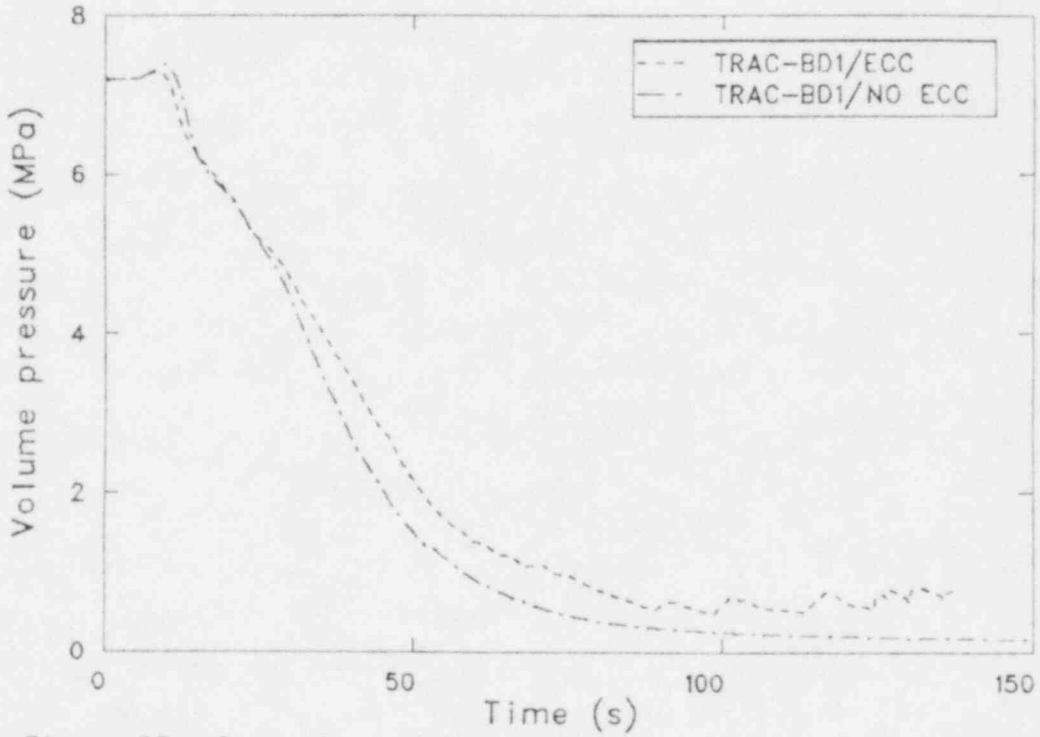

Figure 58. Comparison of the calculated steam dome pressure for TLTA Tests 6425/6426.

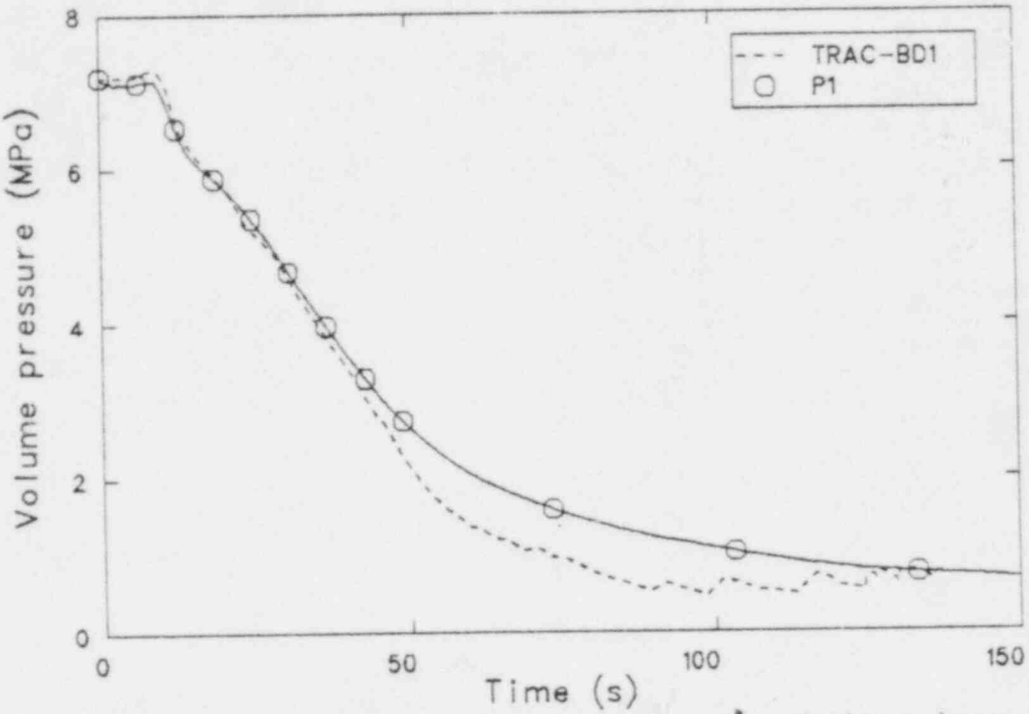

Figure 59. Comparison of calculated and measured steam dome pressures for TLTA Test 6425.

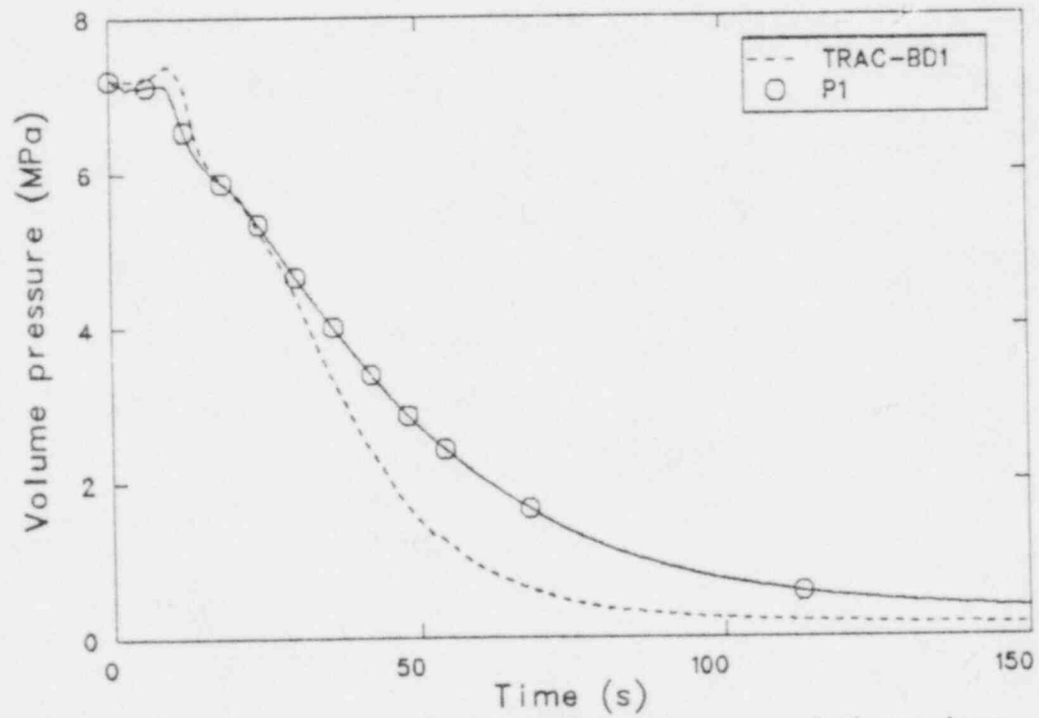

Figure 60. Comparison of calculated and measured steam dome pressures for TLTA Test 6426.

It was probable that volumetric flow comparisons would have been more enlightening for the two-phase blowdown. To have been quantitative regarding the vessel depressurization comparisons, more accurate break flow data were necessary during the subcooled and two-phase blowdown periods. Given these, a better TRAC-BD1 initialization of the downcomer void fractions would be a key factor in correct calculation of the depressurization rate.

The inaccurate vessel pressure calculation affected the onset of the LPCS and LPCI injection, as these systems were activated and controlled by the vessel pressure in Test 6425. The calculated times for LPCS and LPCI injection were 52 and 56 seconds, respectively, compared to 64 and 75 seconds in the experimert. The calculated results for Test 6425 were affected by numerical problems after the ECC systems were activated. The vessel pressure began oscillating near 65 seconds and was a problem for the duration of the calculation. The calculation was not considered reliable beyond 90 seconds, and the pressure increase to apparent agreement with the data was the result of global instability problems related to ECC injection. The manifestations of these problems are discussed in more detail in the next section.

4.5 ECC Problems

Substantial difficulties were encountered with the ECC system modeling in the assessment calculations of TLTA Tests 6425 and 6426. The problem to be modeled was the injection of subcooled liquid into a steam filled pipe. The TLTA system was simple and was modeled in a straightforward way in the TRAC-BD1 calculation, with a pipe component connected between a pressure versus velocity fill and the vessel.

Numerical instabilities were encountered which were related to the timestep size and condensation of steam in the ECC injection pipes. In Test 6426 the difficulties were easily solved by removing the dormant components from the system. In addition to the ECC pipes and fills, the feedwater injection components and the steam line were removed from the model after they became inactive. A total of ten components were deleted from the 6426 model, and the calculation proceeded smoothly thereafter.

The calculation was costing $35-$50 per second of reactor time and running at 1 msec timesteps prior to removing the dormant components. Afterwards, it ran at 10-12 msec and cost $6-$8 per second.

The ECC injection problems were not solved in the TLTA 6425 calculation, and it was terminated at 137 seconds, having been run a sufficiently long time to observe rod quenching. The precursors to trouble while running this calculation were the need for manual timestep control, flow and pressure oscillations in the ECC pipes, and flow instabilities in the guidetube. Convergence problems were also noted elsewhere in the model, globally and in a random fashion. These were believed to be symptomatic of the ECC injection instabilities.

Although a smoothly running calculation was not effected, certain measures improved the results and made it possible to run the calculation through the initial ECC injection periods. It became apparent that TRAC-BD1 would not handle the injection of subcooled liquid into a steam filled pipe, at least at timesteps as low as 1 msec. Two measures worked to circumvent the initial injection problems. First, as long as the void fraction in the ECC pipes was less than 0.65, injection of saturated water into the vessel resulted in a calculation which would run. The injection water temperature was then ramped downward to the desired subcooling. Second, if the ECC pipes were filled with saturated water at the onset of ECC activation, subcooled liquid injection proceeded without pressure oscillations at the ECC pipe-to-vessel interface. These manual procedures also required manual timestep control at less than 2 msec. until ECC injection was established.

Convergence failures in the guidetube tee being a common problem, INEL Code Development personnel examined this component. They noticed that pressure oscillations in the secondary were the precursors to later global instabilities due to liquid holdup at the 0.00432 meter diameter sideleg orifice. A revised noding configuration was recommended, as shown in Figure 61, in which the flow area was opened at the interface between the primary and secondary sides of the tee. The revised noding facilitated running the calculation.

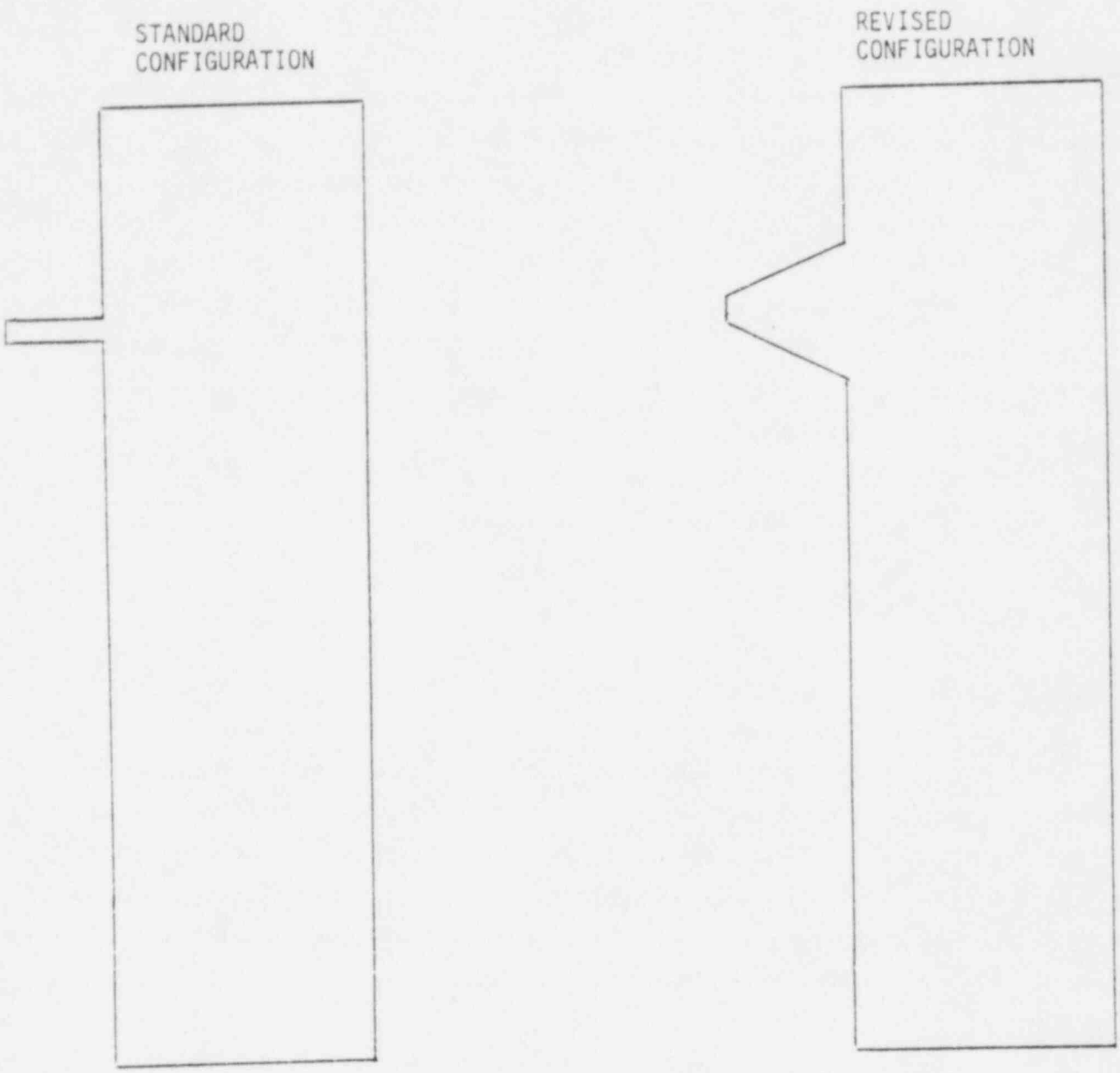

Figure 61. TLTA-5A guidetube models used in the ECC/NO ECC assessment calculations.

Pressure instabilities in the ECC pipes were believed to be condensation related. When the vessel pressure dropped below the ECC injection threshold, high velocity subcooled liquid was injected into the vessel. The condensing steam in the ECC pipe reduced the pressure seen by the injection fill. This caused an increase in the injection rate, the pressure momentarily increased, and the cycle repeated itself.

The LPCI system was typically the most troublesome, so this singly noded pipe was replaced by a pipe with two nodes. The logic here was to halve the vapor-liquid contact area within the cell adjacent to the vessel, thus reducing the interfacial heat transfer by the same factor. This measure helped the stability of the calculation, as it reduced the magnitude of the condensation induced pressure reduction.

A second alternative, not tried in this calculation, would have been to lower the ECC injection velocity. The ECC pipes could be opened up to the dimensions of the exterior TLTA piping, instead of using the dimensions of the piping internal to the vessel, as was done for this assessment calculation. A third alternative would have been to input velocity-time fill tables, adjusted based on the calculated ECC activation time and the vessel pressure. This method might have resulted in a loss of accuracy in the ECC injection rates, but it might have alleviated the oscillations as the ECC pressure-velocity fills responded to vessel pressure changes. It would also have allowed the use of a TRAC-BD1 Type 6 FILL, which would have enabled better user control of important variables such as the ECC injection temperature and void fraction. A fourth alternative would be to use extremely small time steps for the first few seconds of ECC injection. Increments as small as 10^{-5} second would have been necessary in the author's experience.

As stated, global pressure instabilities prevailed after 60 seconds in the 6425 calculation and were more severe beyond 90 seconds. Since the specific causes of these were not isolated, the above discussion has been offered only as a guideline to successful ECC modeling. The recommendations made in this section are by no means firm.

Changes to the latest versions of TRAC-BD1 included improvements in the void diffusion model and in the vessel numerics. These promised improved ECC injection and a more stable calculation of the lower plenum reflood. Error corrections and modeling improvements offered potential for a decreased condensation rate. Two combined effects in this calculation resulted in an overcalculation of the condensation rate. First, the lack of heat transfer from the channel wall to the surrounding fluid (due to a coding error) prevented the ECC fluid from heating up. Second, not modeling the heat transfer across the thin-walled bypass tubes insulated the LPCS and LPCI fluids as they entered the system. The result was too great a subcooling of the ECC liquid inside the vessel. Correction of these problems could be expected to improve the calculational stability.

4.6 Rod Temperature Comparisons

In this section rod surface temperature comparisons are made at several levels in the heated bundle. The peak cladding temperature (PCT) comparisons and the times to PCT, initial rod dryout and core quench are first discussed. Pointwise temperature comparisons for Test 6426 are next presented. Thereafter, the data are averaged whenever possible and the averaged curves compared to the TRAC-BD1 calculational averages. To assess the worth of this comparison, the raw data temperature curves have also been presented in several instances. The core void fraction comparisons are also shown in this section and are discussed with the rod temperatures.

The TRAC-BD1 computational rod grouping is shown in Figure 62. Five rod groups were used in this calculation with geometrical subdivisions among the rods. The geometrical grouping was believed to be a good method for the assessment of the radiation calculation but not as good for modeling differences in peaking factor. In fact, the radial peaking factor profile was taken as 1.0 for each of the TRAC-BD1 powered rod groups. The actual average peaking factors for the TLTA rod groups are listed in Table 7 compared to the TRAC-BD1 power levels. The differences were slight but may well have been important, as TRAC-BD1 generally undercalculated the rod temperatures.

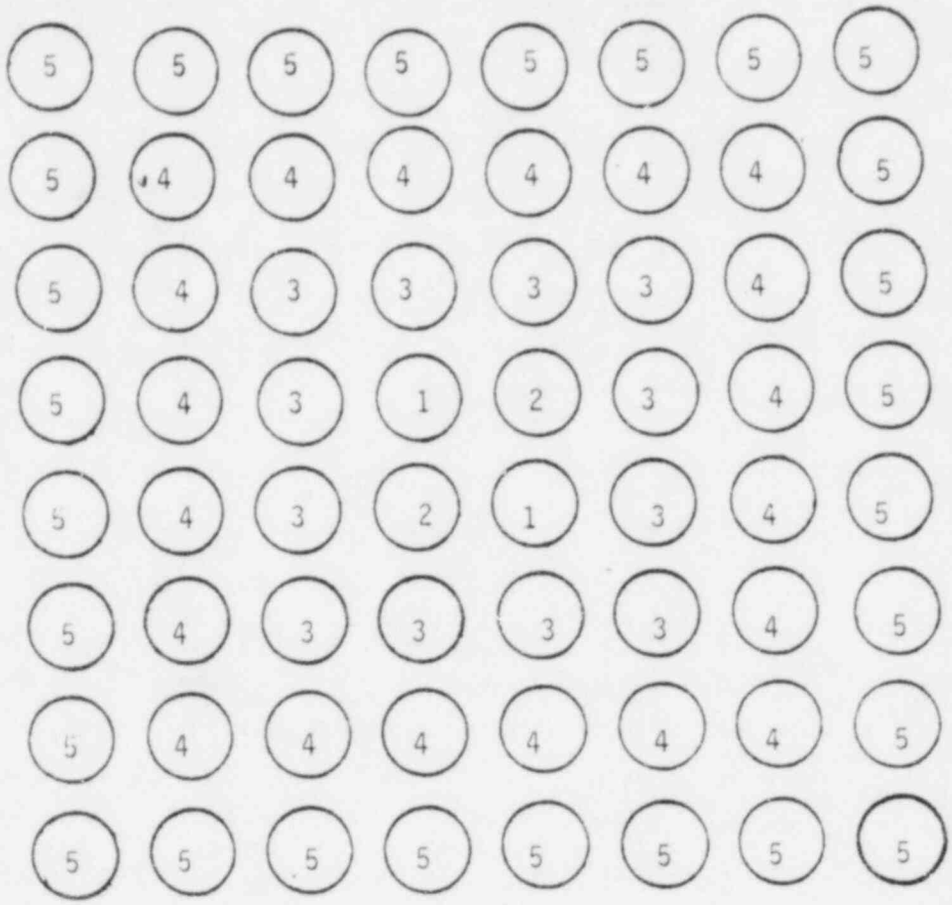

Figure 62. TRAC-BD1 computational rod grouping for the TLTA ECC/NO ECC calculations.

TABLE 7. TLTA-5A ROD PEAKING FACTORS AVERAGED IN CORRESPONDENCE WITH THE TRAC-BD1 ROD GROUPS

TRAC-BD1 Group	TRAC-BD1 Radial P.F.	TLTA-5A Radial P.F.
1	0.0	0.0
2	1.0	1.0205
3	1.0	0.9593
4	1.0	1.0180
5	1.0	1.0014

Differences in the calculated temperatures among the TRAC-BD1 rod groups proved to be negligible. As such, the temperature comparisons were made with TRAC-BD1 rod group 4 without loss of generality. The thermocouple elevations in the rod temperature comparisons which follow were referenced to the bottom of the heated length (BHL) in the electrically powered bundle. Cell 2 in the TRAC-BD1 model, the lowermost heated cell, was also referenced to the BHL for comparative purposes, even though the its bottom cell face did not coincide exactly with the BHL.

Peak cladding temperature (PCT) comparisons for the two tests are shown in Figures 63 and 64. In Test 6425, TRAC-BD1 calculated a PCT of 612 K after 112 seconds compared to a measured value of 645 K after 75 seconds. Although the calculated timing of this event was substantially in error, inspection of Figure 63 revealed that the temperature calculation was within three percent of the data for the majority of the thermocouples at the 2.01-meter elevation. Rod dryout occurred as early as 23 seconds at this elevation, although 35 seconds was more the norm. TRAC-BD1 calculated 46 seconds to rod dryout. The time to core quench was also significantly overcalculated by TRAC-BD1 and occurred after 124 seconds compared to 93 seconds in the experiment at this peak temperature level.

The peak cladding temperature was 1077 K in Test 6426, reached after 295 seconds as shown in Figure 64. TRAC-BD1 calculated a PCT of 923 K after 294 seconds. TRAC-BD1 calculated 42 seconds to initial rod dryout

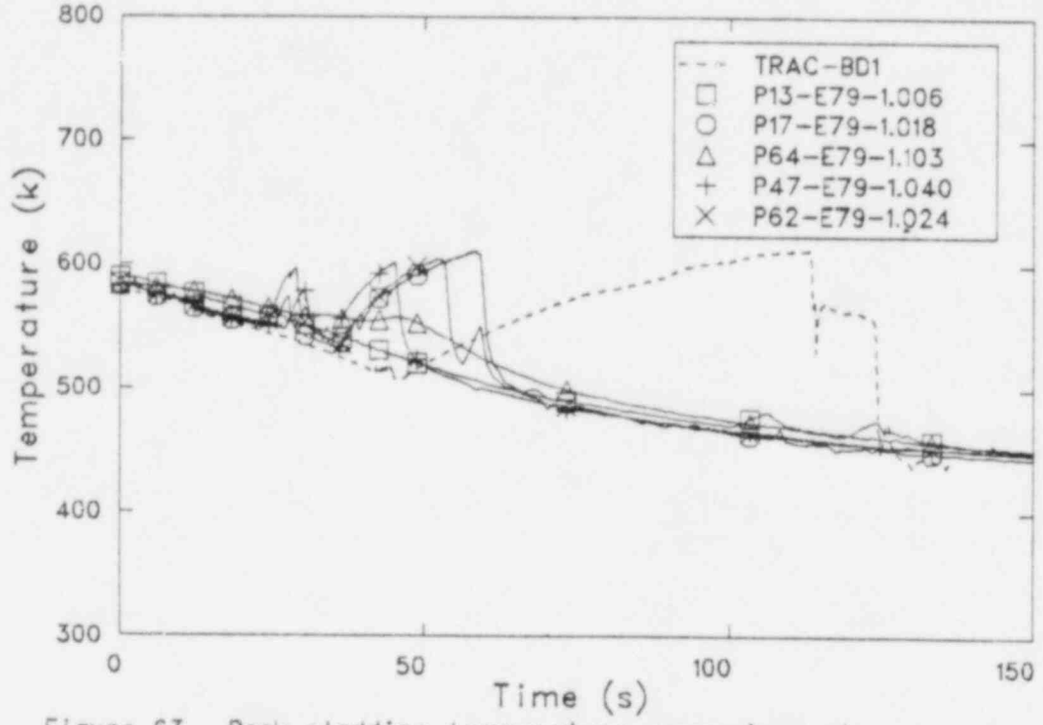

Figure 63. Peak cladding temperature comparison at the 2.01-meter elevation for TLTA Test 6425.

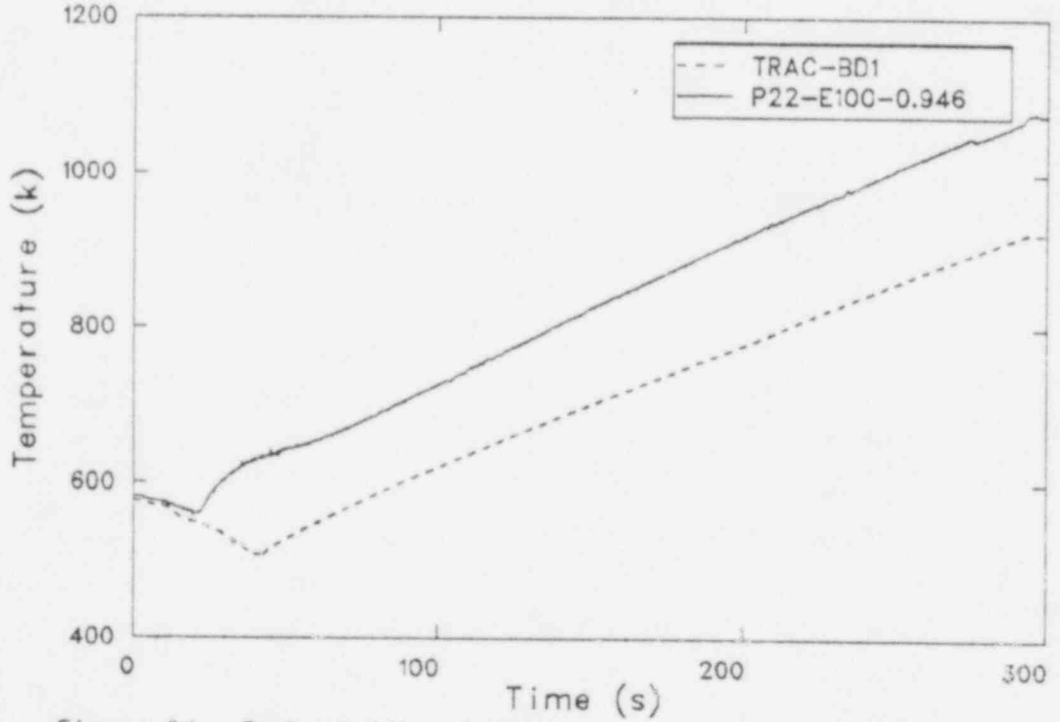

Figure 64. Peak cladding temperature comparison at the 2.54-meter elevation for TLTA Test 6426.

compared to 22 seconds in the experiment. The core was not quenched in this experiment because no ECC was injected. However, the slope of the rod temperature data curve did change sign after 294 seconds, and this was well calculated by TRAC-BD1. This abrupt change in slope corresponded to a bundle power reduction near the end of the experiment.

A pointwise rod surface temperature comparison is made in Table 8 for TLTA Test 6426. In this comparison, several things were observed. TRAC-BD1 consistently undercalculated the peak rod surface temperature by an average of 9.1 percent. The time to peak cladding temperature was well calculated, and the maximum error was 3.3 percent. TRAC-BD1 generally calculated the initial rod dryout time later than the data by a significant factor. However, the reverse was sometimes true and was independent of axial bundle geometry. Single pointwise comparisons were not reliable for assessment of the initial rod dryout (IRD) calculation, but TRAC-BD1 calculated an average of 46 seconds to IRD compared to 39 seconds for the data when the pointwise measurements were averaged. Group by group comparisons with the average of the data were considered a good way to assess the TRAC-BD1 rod temperature calculation. However, very often single thermocouples were the only data available within the TRAC-BD1 rod groups in the 6426 assessment. This resulted in the pointwise comparisons made above and averages across the axial levels of the core.

The void fraction and temperature comparisons for Test 6425 are shown in Figures 65-72. The core void fraction and temperature comparisons at the lowermost heated level are presented in Figures 65-66. TRAC-BD1 calculated a smaller void fraction and a reduced rod temperature compared to the data at the 0.25 meter elevation. TRAC-BD1 calculated a slight initial heatup at 45 seconds but did not calculate the ensuing heatup and quench periods shown by the averaged data curve. The temperature data indicated that the rods experienced dryout from 43 to 100 seconds, corroborated by the measured void fraction. The calculated temperatures fell below data beyond 45 seconds due to the undercalculation of the void fraction at this level.

Comparisons at the 1.80 meter elevation are presented in Figures 67-68. TRAC-BD1 showed an apparently poor comparison to the data

TABLE 8. POINTWISE ROD SURFACE TEMPERATURE COMPARISONS FOR TLTA TEST 6426

TRAC-BD1 Group, Level[a]	Test 6426 Elevation[b] (meters)	TRAC-BD1 PCT[c] (K)	Test 6426 PCT (K)	Time to: TRAC-PCT (s)	6426-PCT (s)	TRAC-IRD[d] (s)	6426-IRD (s)
2, 1	0.48	632	637	293	293	57	38
5, 2	0.89	770	798	294	293	53	38
5, 3	1.27	859	867	295	294	53	35
4, 3	1.60	893	968	294	295	53	36
3, 4	1.80	948	1012	294	293	44	22
5, 4	2.01	897	1022	294	294	45	22
4, 4	2.11	939	998	293	303	44	64
3, 5	2.54	923	1077	294	295	42	22
4, 5	2.72	919	1041	294	295	41	55
4, 6	3.05	839	1039	295	294	38	24
4, 6	3.30	839	920	295	295	38	51
4, 7	3.56	696	846	295	289	41	59

a. Graphics level 1 = channel level 2, etc.

b. Elevation is referenced to bottom of heated length, 1.31 m above vessel base.

c. Peak cladding temperature.

d. Initial rod dryout.

as was evidenced by the average data curves shown in Figure 67. However, a comparison of the TRAC-BD1 calculation with the individual thermocouples was more revealing. The results shown in Figure 68 indicated that TRAC-BD1 compared well with the maximum measured temperatures for the majority of the rods at this level. The final quench time was also well calculated. Intermediate quench times were not well calculated, and TRAC-BD1 calculated a delayed initial rod dryout time compared to the measurements. The average temperature data curve had two disadvantages in this instance. First, the complex radial temperature changes across the bundle were lost in the average curve. Second, considerable quantitative calculations were necessary to construct the average data curves and their standard deviations for what was a qualitative assessment parameter. Thus, the raw data comparison was favored in this instance. A comparison of the minimum and maximum of the rod temperature data also would be viable. This approach would bound the calculation without loss of the physical detail. It is recommended that the use of the average data comparison be considered situation dependent and done as warranted depending on the calculation.

The calculated dryout and quench times correlated well to the calculated void fraction at this level, as shown in Figure 69. The void fraction data were difficult to interpret due to the location of grid spacers in the bundle and were not believed to be typical of the fluid conditions at the 1.80 meter elevation. The effects of the spacers are shown in Figure 70. Rod temperature measurements at the 2.11 meter elevation were totally different than those at 1.80 meters due to localized liquid holdup in the bundle. The grid spacers posed a very complex, detailed geometry which would not be easily modeled. The localized temperature phenomena were well measured through extensive instrumentation, but the void fraction data were generally less reliable locally. There was not an homogeneous fluid column due to the grid spacers.

The TRAC-BD1 results compared favorably to the averaged temperature data at the uppermost heated cell in the core, as shown in Figure 71. The temperature departures beyond 45 seconds were small and were often related to very subtle reductions in the calculated void fraction to values slightly less than one, as shown in Figure 72. When this occurred, the code entered the nucleate boiling mode, overcalculated the heat transfer

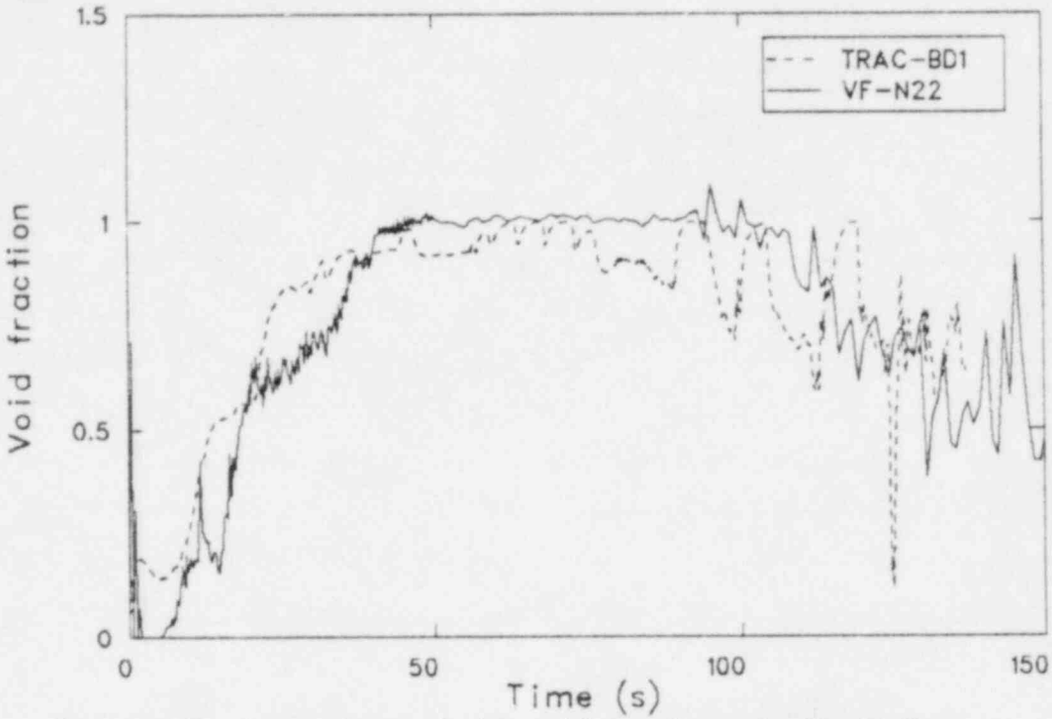

Figure 65. Comparison of the void fractions in the bottom heated cell of the core for TLTA Test 6425.

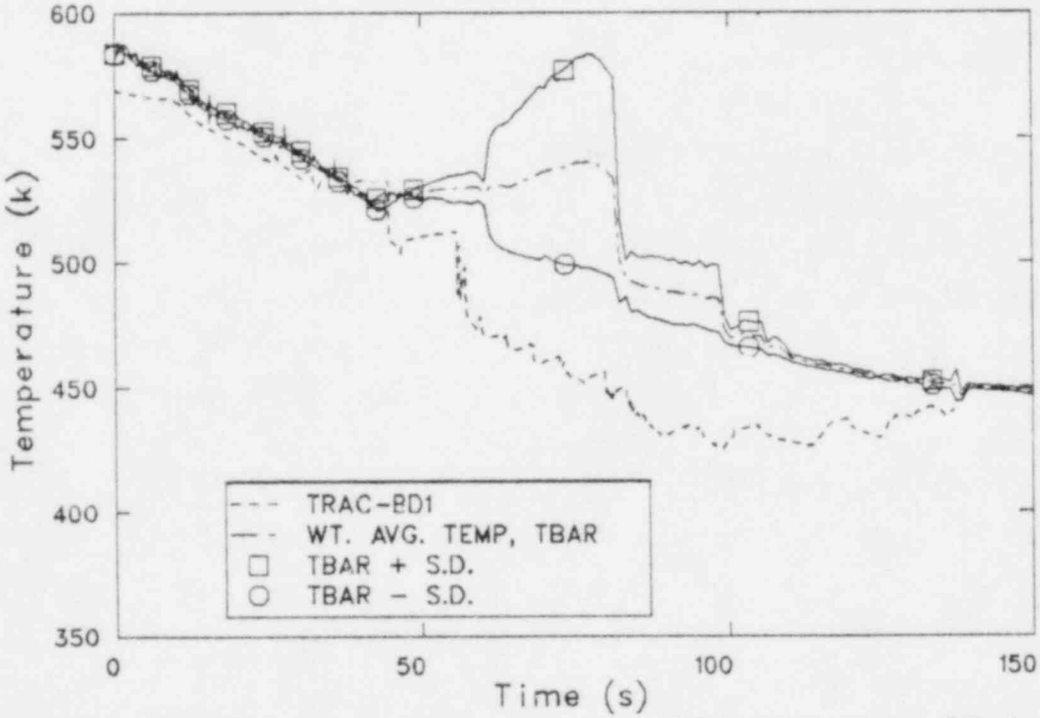

Figure 66. Rod temperature comparison 0.25 meter above BHL in TLTA Test 6425.

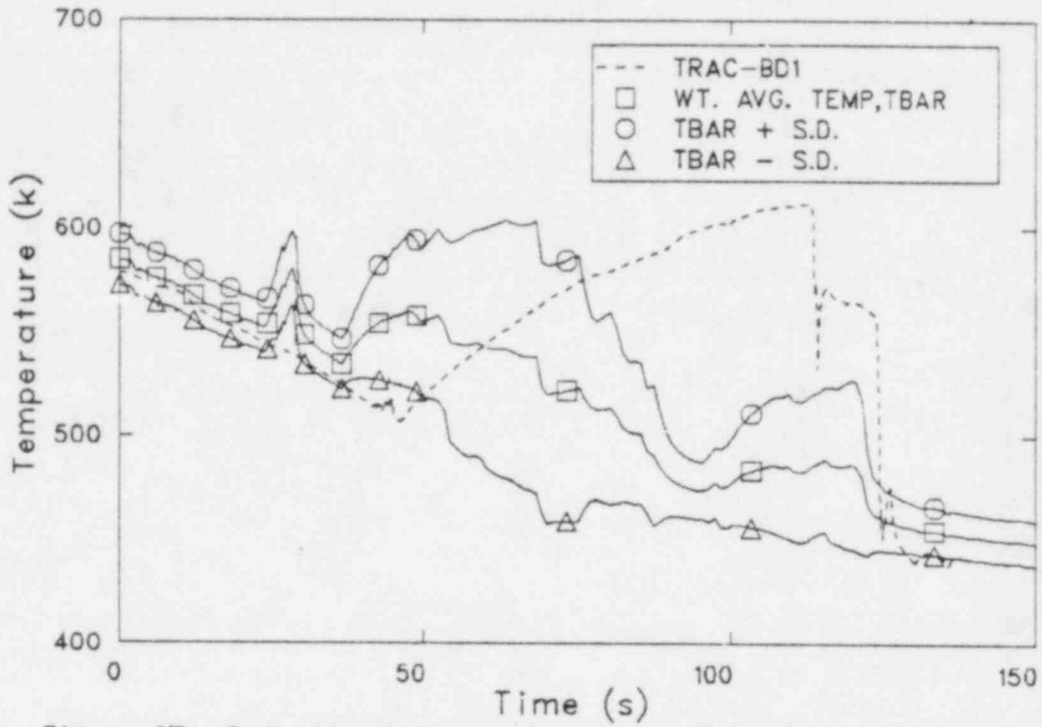

Figure 67. Rod temperature comparison 1.80 meters above BHL for TLTA Test 6425.

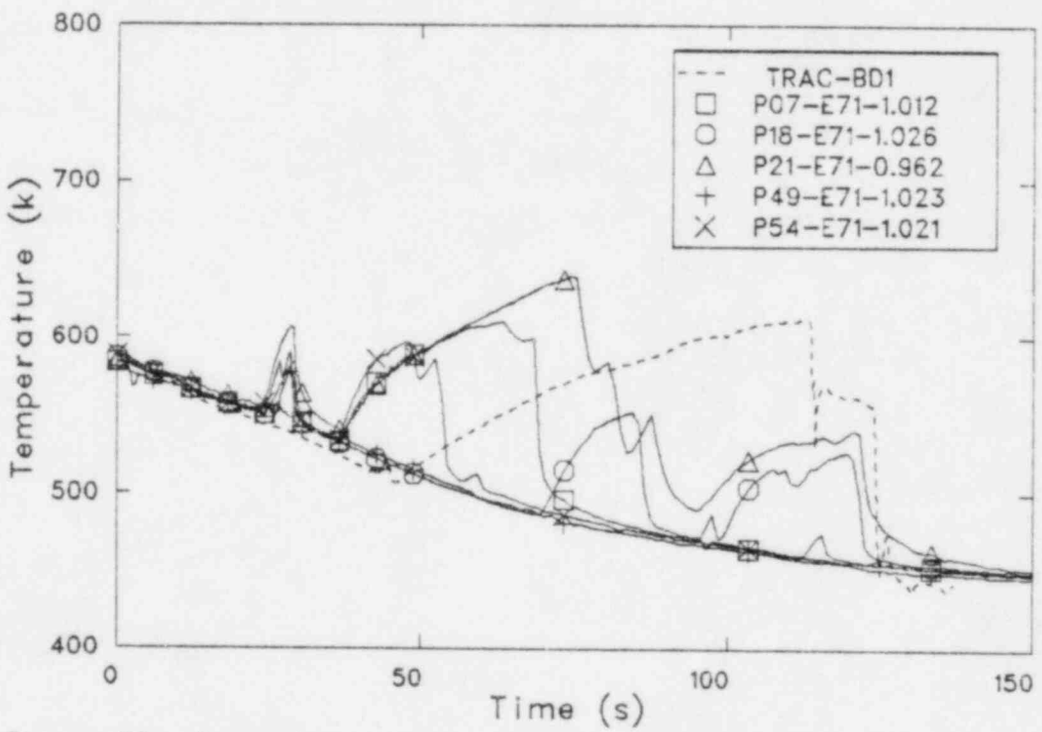

Figure 68. Comparison of calculated rod temperature with the raw data at the 1.80 meter elevation for TLTA Test 6425.

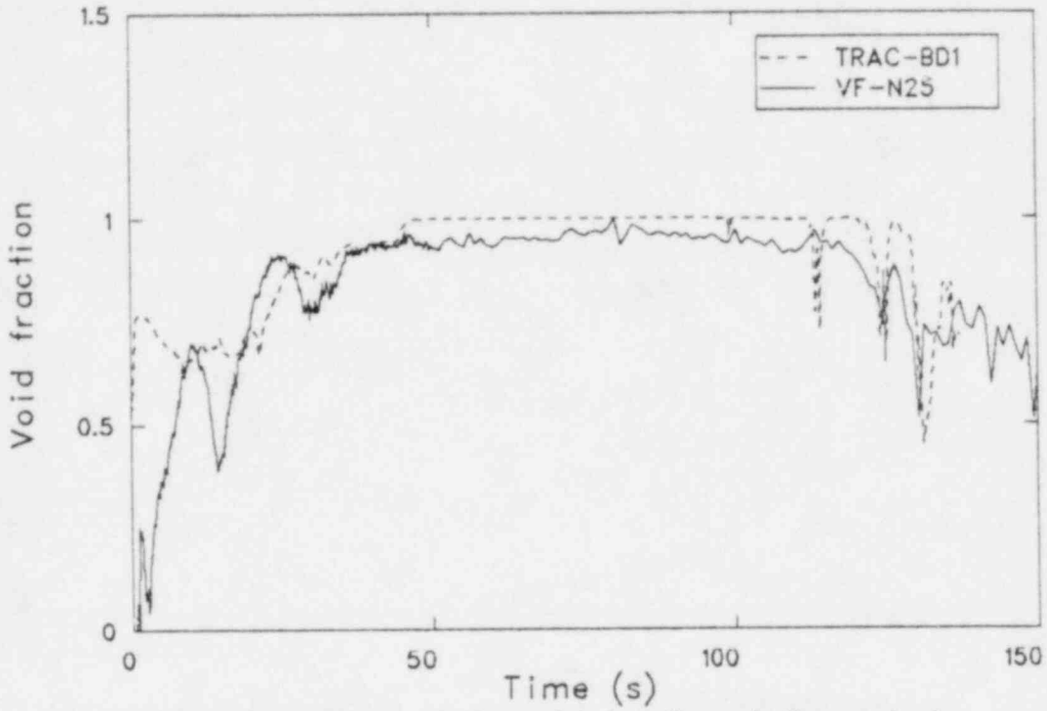

Figure 69. Comparison of the void fraction at the central axial heated level of the core for TLTA Test 6425.

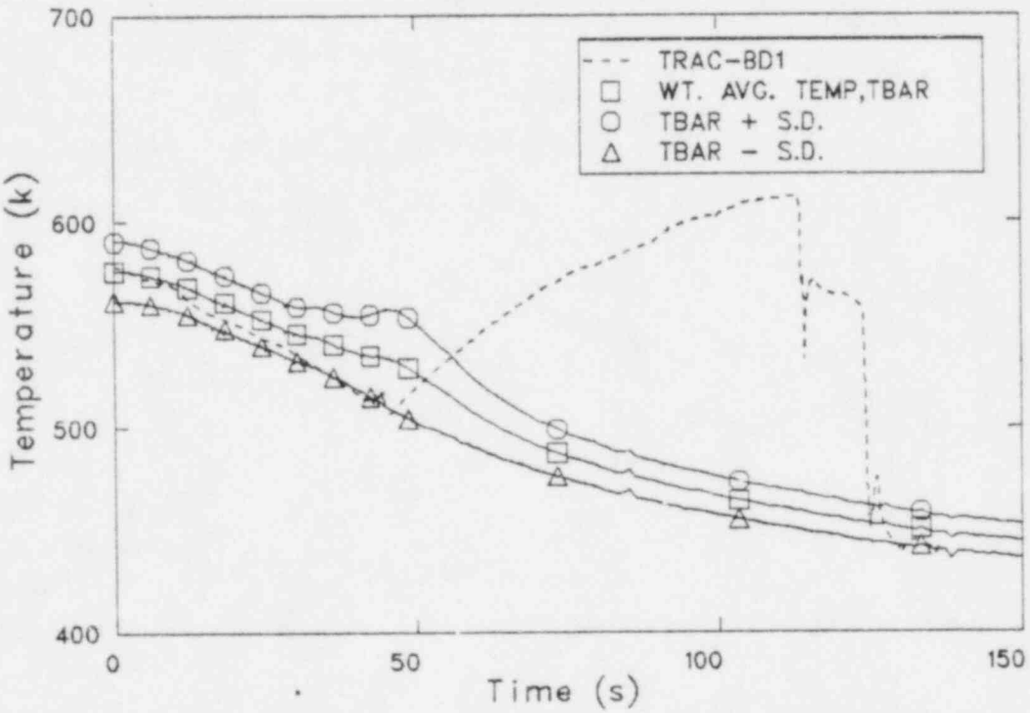

Figure 70. Rod temperature comparison at the 2.11 meter elevation showing the effect of grid spacers for TLTA Test 6425.

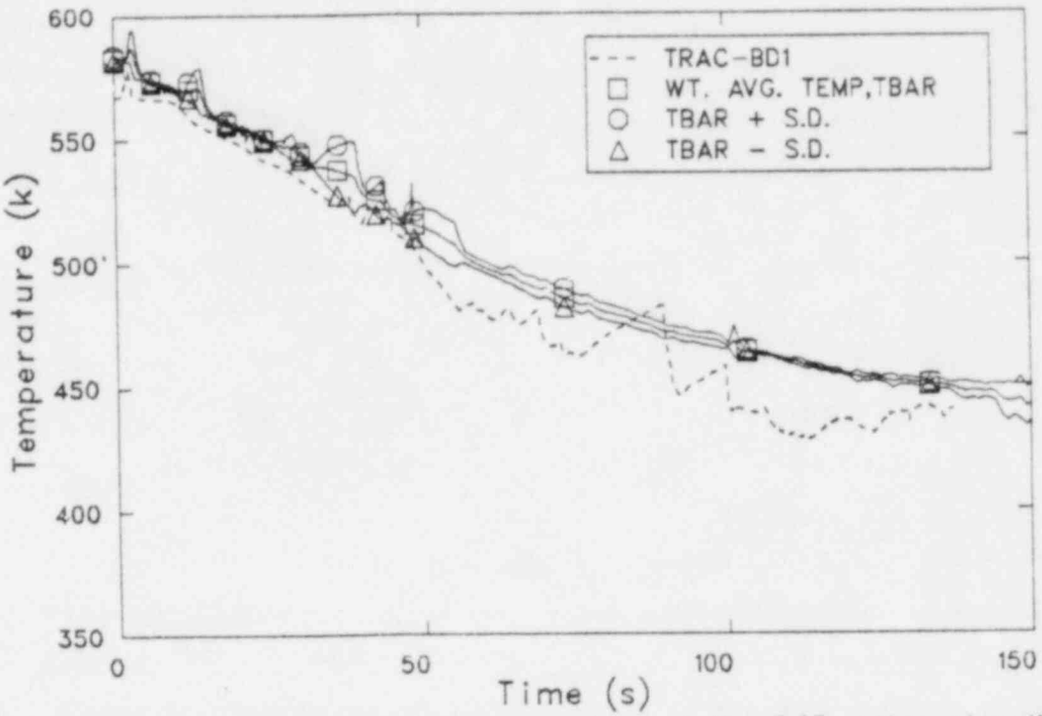

Figure 71. Rod temperature comparison at the 3.63 meter elevation for TLTA Test 6425.

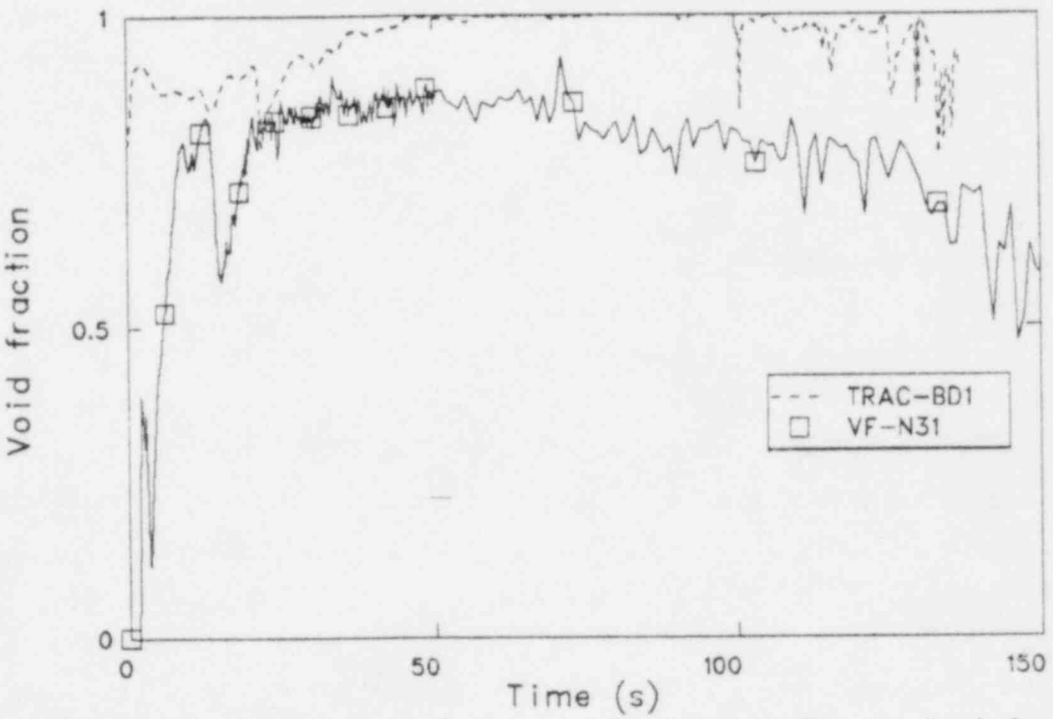

Figure 72. Comparison of the void fractions in the top heated cell of the core for TLTA Test 6425.

rate, and undercalculated the rod temperature. Figure 72 showed that the void fraction was overcalculated in the top of the core. This resulted from the more rapid depressurization calculation, which caused too large a calculated flow rate out the top of the core, entraining the HPCS fluid and minimizing the amount of liquid above the upper tie plate.

The void fractions and rod temperatures for Test 6426 are shown in Figures 73-79. In general, TRAC-BD1 undercalculated the rod temperatures compared to the data for the NO ECC experiment. The undercalculation was most severe at the top heated cell. The temperature comparisons improved in the hotter cells of the bundle.

The temperature comparison at the lowest heated cell is shown in Figure 73. This cell was the lone exception to the general behavior as TRAC-BD1 overcalculated the peak rod temperature by 18 percent. The calculated overheat was explainable in the context of the calculated void fraction at the 0.25 meter level, shown in Figure 74. The calculated initial rod dryout occurred at 58 seconds and correlated well to an abrupt increase in the void fraction. The calculated void fraction remained unity for the duration of the experiment, whereas the data indicated intermittent intervals of surface rewet at this lowermost heated level. The code indicated the rods experienced vapor forced convection at a mass flow rate which was lower than measured beyond 70 seconds, further accounting for the temperature overcalculation.

The rod temperature comparison at the 1.27 meter level is shown in Figure 75. TRAC-BD1 calculated the initial rod dryout at 46 seconds compared to 35 seconds in the experiment. TRAC-BD1 undercalculated the rod temperature at this level by a maximum of 20 percent, but the maximum rod temperature compared within two percent to the average of the data. These possibly were compensating errors. The calculated time to the rod temperature slope turnover agreed well with the test, as expected because the TRAC-BD1 power decay curve was taken from the data. The void fraction at the 1.27 meter level, shown in Figure 76, agreed with the steeper slope of the temperature comparison, as TRAC-BD1 apparently overcalculated the void fraction. The measured value was possibly influenced by the presence of a grid spacer at the 1.53 meter level which could have held the liquid

apparently measured by DP25. However, it was equally probable that the data were in error, as the same measured behavior was observed at DP27 and DP29, which had no spacers between their instrument taps. In any case, the more rapid calculated rod heatup rate was due to the calculated rod dryout past 46 seconds and undercalculation of the heat removal in the vapor forced convection mode.

The comparisons at the 2.29 and the 2.72 meter levels were qualitatively the same as the comparisons at 1.27 meters, both in the temperatures and the void fractions. The quantitative temperature comparisons were not as good, however. TRAC-BD1 undercalculated the maximum rod temperatures compared to the weighted averages of the data by 13 and 30 percent, respectively, at these two elevations. Figure 77, at the 2.29 meter elevation, exemplified this behavior. Note that the slope of the calculated temperature curve was flatter with respect to the data than at the 1.27 meter elevation. Because of this the maximum error occurred at the end of the transient, the reverse of the data at the lower elevation. TRAC-BD1 correctly calculated that the peak rod temperature occurred at the 2.29 meter level, despite the error at this elevation.

The temperature and void fraction comparisons at the uppermost heated level are shown in Figures 78 and 79. TRAC-BD1 calculated that the top level voided after 37 seconds compared to 71 seconds in the experiment. Despite the early voiding calculation, TRAC-BD1 undercalculated the rod surface temperature by a maximum of 30 percent at the end of the transient. This indicated that the calculated heat transfer coefficient was too high for the vapor forced convection mode calculated in the top of the core. The calculated behavior was puzzling in the context of the channel wall heat transfer having been omitted. However, another coding error existed in Version 11 in which the convective heat transfer contribution was added twice. This could have accounted for the undercalculation of the rod temperatures in the vapor forced convection heat transfer mode predicted by TRAC-BD1 for the bulk of the NO ECC calculation.

In summary, quantitative assessment of the calculated core behavior was difficult due to the coding errors which existed in Version 11. The

ability of the code to calculate the rod temperatures correctly was dependent on the correct calculation of the fluid distribution in the core. The core geometry was complex and difficult to model to the extent that the localized phenomena were not consistently and accurately calculated. However, TRAC-BD1 did a reasonably good job of calculating the global behavior in the core.

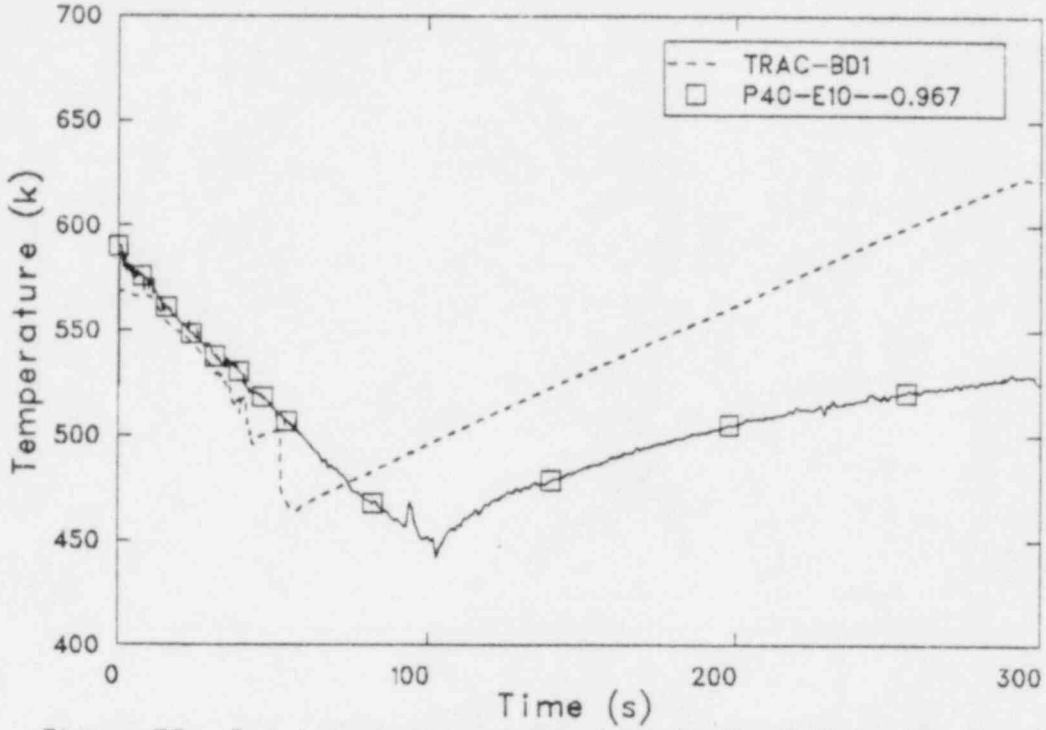

Figure 73. Rod temperature comparison at the 0.25 meter elevation for TLTA Test 6426.

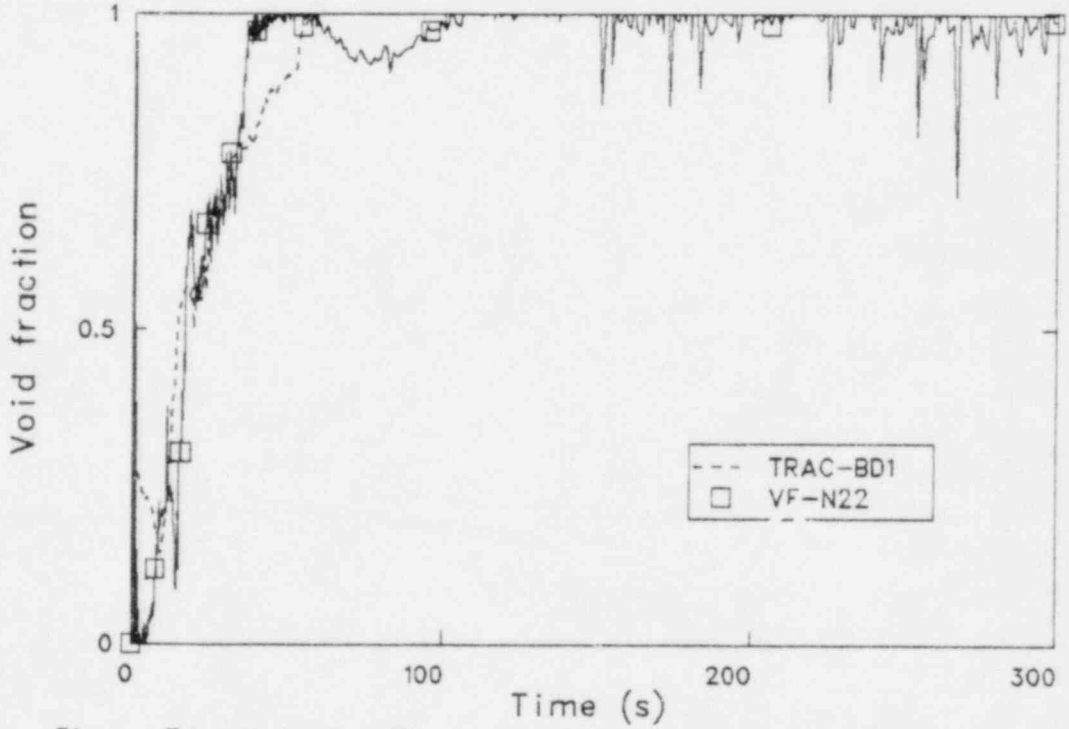

Figure 74. Void fraction comparison at the lowermost heated level in the core for TLTA Test 6426.

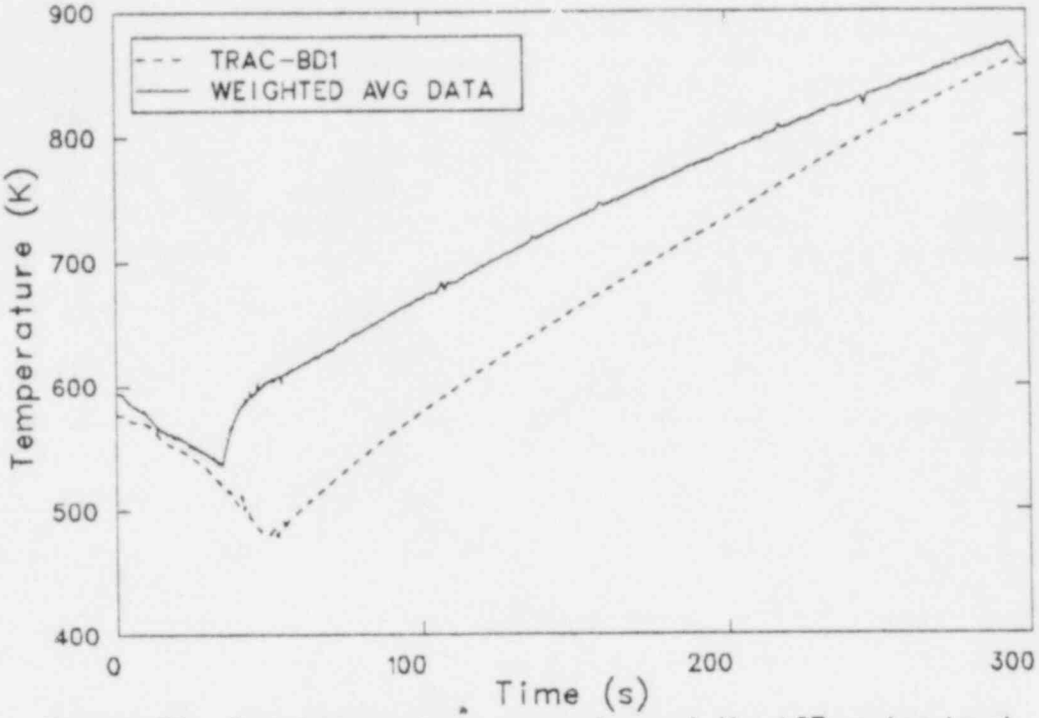

Figure 75. Rod temperature comparison at the 1.27 meter level in the core for TLTA Test 6426.

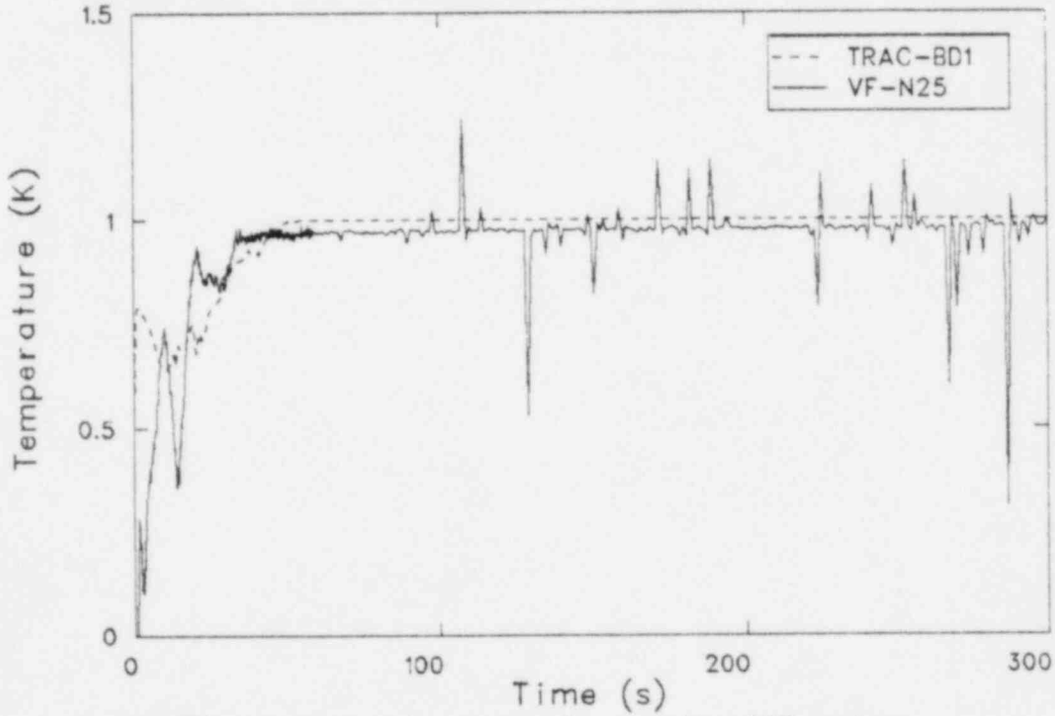

Figure 76. Void fraction comparison at the 1.27 meter elevation in the core for TLTA Test 6426.

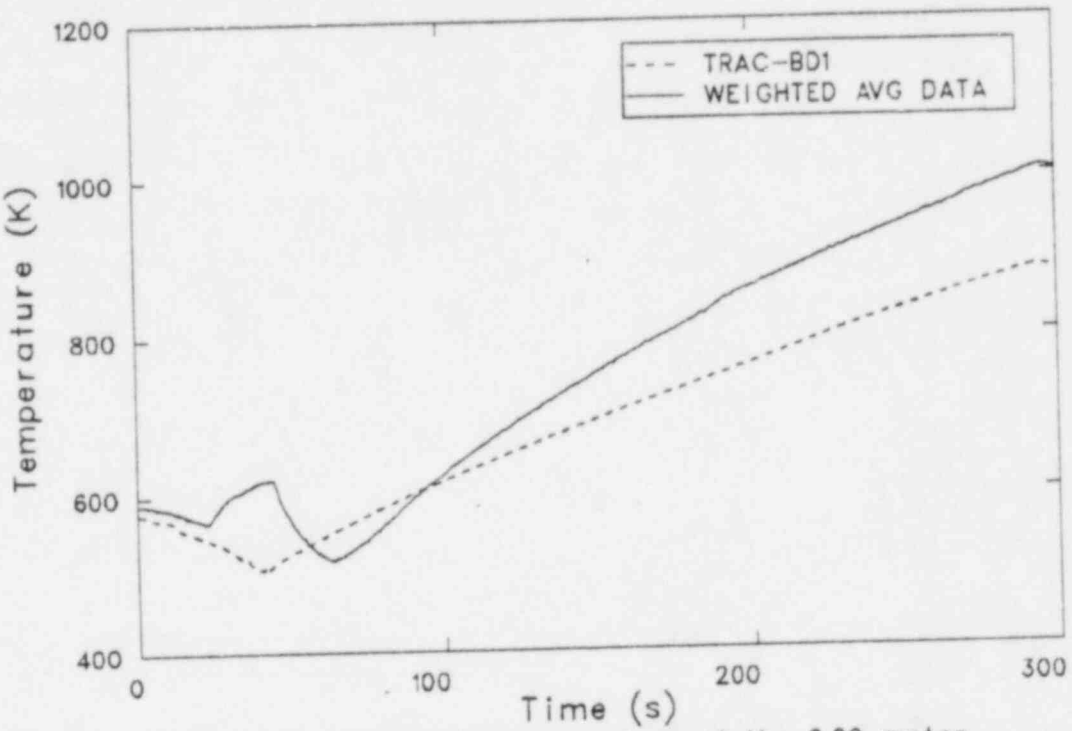

Figure 77. Rod temperature comparison at the 2.29 meter elevation in the core for T_TA Test 6426.

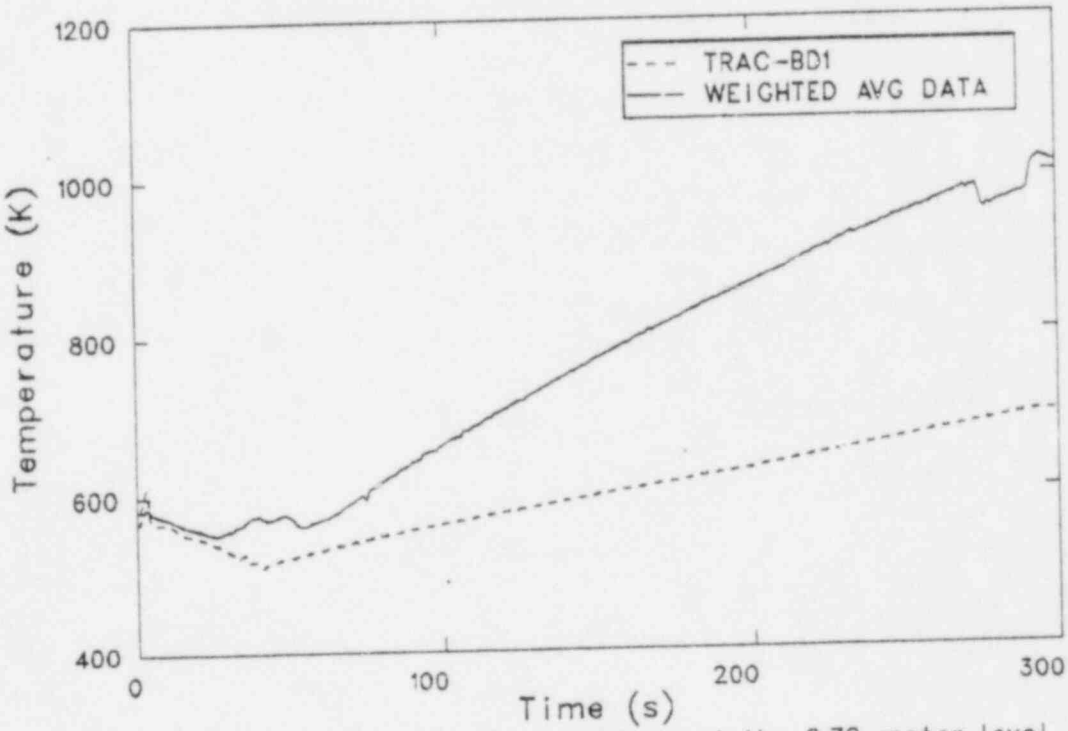

Figure 78. Rod temperature comparison at the 2.72 meter level in the core for TLTA Test 6426.

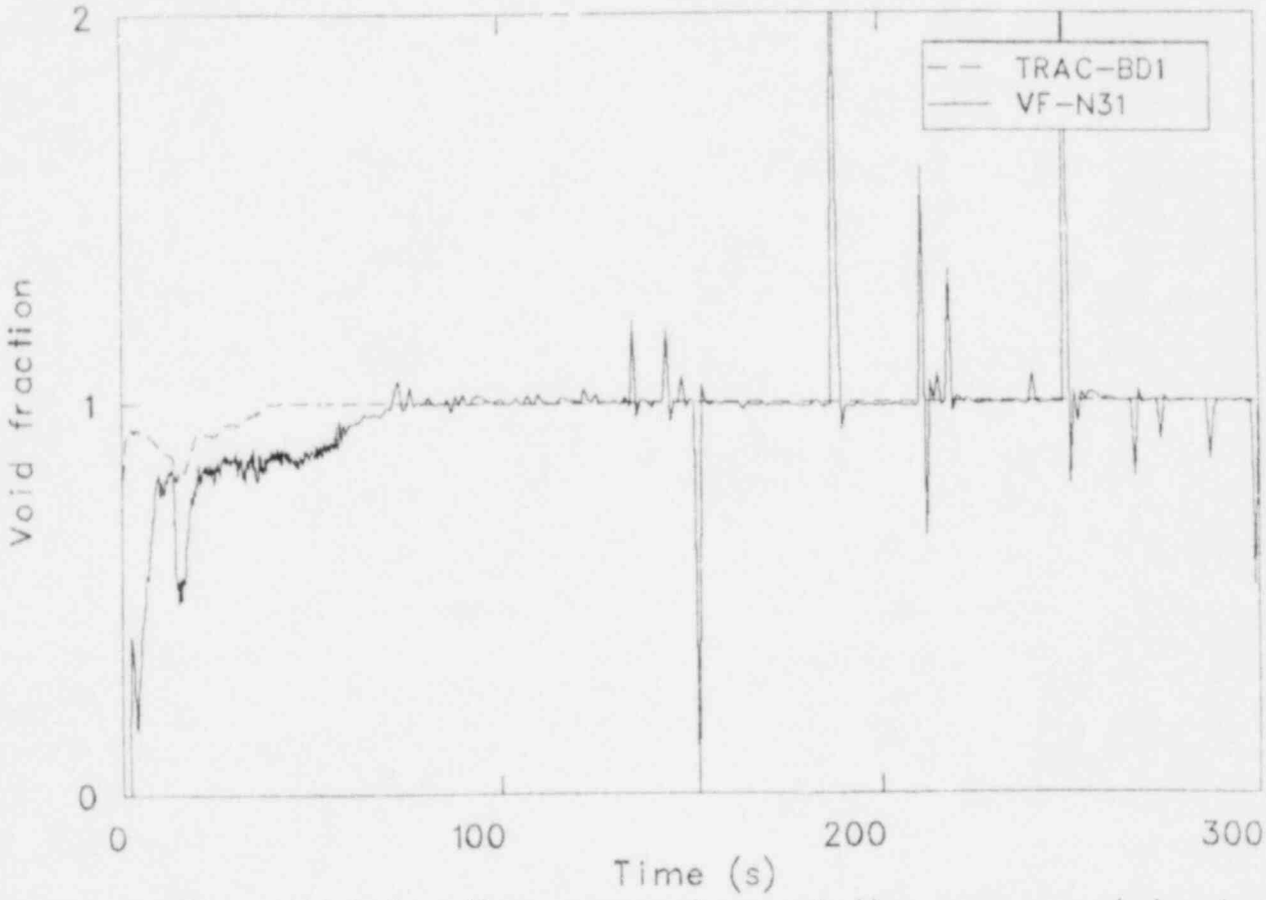

Figure 79. Void fraction comparison at the uppermost heated level in the core for TLTA Test 6426.

5. CONCLUSIONS AND RECOMMENDATIONS

TRAC-BD1 Version 11 was an advancement in the basic capability of best estimate computer codes for BWR safety analyses. The code correctly modeled the qualitative behavior of the subscale TLTA facility. Problems, where they arose, where due to the immaturity of Version 11, to model and input limitations, and to initialization difficulties. These problems are summarized as part of the following conclusions and recommendations.

1. *The differences in the depressurization rates between the two experiments were correctly predicted and resulted from reduced volumetric break flow in the test with ECC.*

   It was found the slower depressurization rate in the ECC test was directly correlatable to the jet pump exit pipe void fraction. As the lower plenum refilled, the liquid carryover to the drive side break was greater. This reduced the volumetric break flow substantially and the ensuing vessel depressurization rate was slower, sufficiently so as to dominate increases in cooling available from penetration of the ECC to the bundle.

2. *The subcooled and two phase break flows calculated by the code were considered inadequate.*

   The subcooled break flow was underpredicted for both simulations. In our opinion, these results contributed to delays in the calculated heater rod dry out. The initial two phase suction side break flow was overcalculated by factors of 1.65 and 1.75, respectively, for the ECC and NO ECC tests. The disagreement between the calculated and measured results decreased as a single phase vapor condition was approached. The effect of the two phase flow overprediction was overprediction of the depressurization rate in both tests and, therefore, early initiation of the ECC in Test 6425.

3. *High void fraction and single phase vapor break flows calculated by the code were considered acceptable.*

The calculated break flows under these conditions showed good agreement with the experiment. The results also showed that use of the choking option for two phase conditions with void fractions exceeding 0.98 produced more accurate results than did the unchoked numerics.

4. *The code heat transfer characterizations for high void fraction conditions were considered to be good.*

The calculated heater rod temperature response in the NO ECC test following dry out generally matched the experimental data, although it was offset in time due to the late dry out.

5. *The code calculated reflood heat transfer may not be adequate.*

The calculated times to peak clad temperature and bundle quench were delayed relative to the ECC experiment. In addition the general heater rod temperature response following dry out exhibited a smaller gradient in the code simulation than in the experiment. The results herein were not sufficient to determine if the stated behavior was dominated by the hydraulic calculations, the heat transfer calculation or a combination of both. In addition, a conservative calculation of the liquid downflow from the upper plenum to the bundle by the CCFL model would help explain the delayed times to peak clad temperature and bundle quench in the ECC test. Similar behavior has been experienced in other code assessments using data from this facility.

6. *Further work is required in the simulation of the injection of subcooled ECC.*

Injection of subcooled ECC into steam filled pipes in the code produced significant and atypical oscillatory behavior using the velocity versus pressure fill model. The results demonstrated this

behavior was driven by the calculation of instantaneous and periodic condensation in the volume just downstream of the injection point. The resulting pressure fluctuations fed back to the ECC injection fills to produce the oscillations. No generally successful modeling solution was found to mitigate this behavior. However, it may be possible to adapt the control system capability of the next version of the code to describe the ECC injection prototypically.

7. *The absence of an automatic initialization feature in the code was considered a significant operational limitation.*

   The results indicated that a high degree of consistency in the initial system conditions was significantly influential to successful code prediction of the subsequent transient. The necessary consistency was not always readily apparent prior to execution of the transient. The manual techniques required to examine a large number of initial parameters and/or to reinitialize after beginning transient calculations were not cost effective. Use of the control system capability of the next version of the code holds promise for improving this situation.

8. *Because the limitations demonstrated in this study are being addressed in TRAC-BD1 (version 12) we recommend this new version be used for further code assessment studies.*

6. REFERENCES

1. J. L. Elliott and D. Dobranich, "TRACNEWS", TRAC-PD2 Newsletter Number 4, Los Alamos National Laboratory, January, 1981.

2. R. G. Hanson, "TRAC-BD1 Assessment Calculations for Marviken Tests 15 and 24," EG&G Idaho Technical Report EGG-CAAD-5705, December 1981.

3. L. S. Lee et al., "BWR Blowdown/Emergency Core Cooling Program - 64-Rod Bundle Core Spray Interaction (BD/ECC1A) Final Report - Volume I, Large Break Tests," General Electric Draft of Final Report GEAP-24912-1, EPRI NP-1783, NUREG/CR 2009, DRF E00-66, March 1981.

4. W. J. Letzring et al., "BWR Blowdown/Emergency Core Cooling Program Preliminary Facility Description Report for the BD/ECC1A Test Phase," NRC-EPRI-GE Cooperative Research and Development Report GEAP-23592, NRC-2, December 1977.

5. G. L. Sozzi, and W. A. Sutherland, "Critical Flow of Saturated and Subcooled Water at High Pressure," General Electric NEDO-13418, Class I, 75NED43, July 1975.

6. J. W. Spore, et al., "TRAC-BD1: An Advanced Best Estimate Computer Program for Boiling Water Reactor Loss-of-Coolant Accident Analysis," NUREG/CR-2178, EGG-2109, October 1981.

APPENDIX A

INITIALIZATION OF THE DOWNCOMER VOID FRACTIONS FOR TLTA TESTS 6425 AND 6426

APPENDIX A
INITIALIZATION OF THE DOWNCOMER VOID FRACTIONS FOR TLTA TESTS 6425 AND 6426

A true steady-state calculation was not performed in this assessment, because steady-state conditions were not established prior to beginning TLTA Tests 6425 and 6426. The most important departure from a steady-state condition was that the vessel water level was falling at the onset of the tests. Thus, the TRAC-BD1 initialization proceeded in the same fashion.

To initialize the TRAC-BD1 calculation, vessel pressure was controlled by Break 19 (see Figure 2 in the main body of the report). Steam discharge from the vessel was regulated by Valve 18. The feedwater mass flow rate from Fill 10 was adjusted so that the water level in the downcomer was correct after the steady-state calculation had been run for a time sufficiently long to render the changes in the calculations very small compared to the property variations anticipated in the early stages of the transient. This time was judged to be about 12 to 15 reactor seconds for this calculation, which yielded a quasi-steady-state in terms of the standard TRAC-BD1 steady-state convergence criteria. The short run time represented a reasonable compromise, done for economy and because of the aforementioned test conditions.

The calculated void fractions used to start the transient were clouded by several things. First, they were determined by the initial void conditions which were input to the steady-state calculation and the duration of the steady-state run. This would not have been true were a steady-state established prior to starting Tests 6425 and 6426. Second, there was a 0.30 meter uncertainty band in the initial liquid level. This translated to a 30 percent uncertainty in the initial void fraction for downcomer Level 6 of the TRAC-BD1 model. Third, the TRAC-BD1 homogenization of the liquid and vapor in a cell made the liquid level difficult to follow with the coarse vessel noding used for this calculation.

Test 6425 proved more difficult to initialize than Test 6426. In Reference 3, General Electric stated that the water level was 1.65 meters above the jet pump support plate. Assuming the top of the support plate to be at 1.43 meters and that it defined the bottom of the downcomer, the initial Test 6425 water level was 3.29 ± 0.15 meters, compared to 3.12 ± 0.15 meters for Test 6426. A water level between 3.14 and 3.44 meters translated to a Level 7 void fraction between 1.0 and 0.72 for Test 6425. To check this water level, the downcomer differential pressures were examined. These are shown in Figure A-1, and they indicated that the water levels were the same for both tests. From DP-9 using the temperature measured by T06 and neglecting the velocity of the falling liquid level, the water level was calculated at 3.13 meters. Applying the GE tolerance of 0.15 meter to this resulted in void fraction ranges from 0.0 to 0.14 in Level 6 of the downcomer and from 1.0 to 0.88 in Level 7.

In Table A-1, the calculated initial void fractions and the degree of subcooling are compared to the data for Test 6426. This test proved easier to initialize than Test 6425, even though instrumentation degradation was observed between Tests 6425 and 6426, and fewer measurements were available for the initialization of the latter. As shown in Table A-1, the calculated subcooling agreed well with the data, and the downcomer void fractions appeared reasonable. The results of the transient calculation would have been improved were the calculated downcomer void fractions lower in Levels 5 and 6 and the calculated lower plenum subcooling greater. However, considering that a steady state water level did not exist in these tests and that TRAC-BD1 did not track a discrete liquid level, the Test 6426 subcooling initialization was quite good. The important result of Table A-1 was that Level 6 was kept as full of liquid as the calculation would allow and Level 7 was essentially full of vapor. This initialization yielded reasonable results in the early stages of the transient calculation and was correct as far as Test 6426 data were concerned.

The results of a downcomer initialization run for Test 6425 are shown in Table A-2. The downcomer void fraction in Level 6 again fell outside the desired range, and indeed this initialization did not produce an accurate transient calculation, as shown in Case A of Figure A-2. The

surprising result was that downcomer voids in the tolerance range established above did not produce good results, either. In fact, the downcomer Level 6 void fraction was set equal to 0.89 for an accurate transient calculation, as shown in Case B of Figure A-2. This last setting was quite arbitrary and in apparently the wrong direction according to the test data. Figure A-2 demonstrated the strong dependence of the transient depressurization calculation on the initial value of the downcomer void fraction. Recognizing this sensitivity, and recognizing the need for a calculational solution for the initial downcomer void fractions as opposed to a manual setting procedure, reinitialization of Test 6425 was attempted.

Several problems were encountered when attempting to reinitialize. First, although the measured condition of saturated liquid at low void fraction in downcomer Level 6 could be calculated by TRAC-BD1, it was at the expense of the correct subcooling in Levels 4 and 5. Second, vapor carryunder was a problem, resulting in calculated void fractions which were too high in Levels 4 and 5.

To make the initialization procedure more objective, the downcomer level trip feature was next employed. Use of this option improved the downcomer void distribution, as shown in Table A-3. However, there was no improvement in the subcooling profile, and the Level 1 calculation was erroneous. Furthermore, the vessel pressure distribution was no longer correct due to the change in water level with the change in the calculated void fraction.

To summarize, manual attempts at effecting a correct downcomer initialization were time consuming, expensive, and they failed. The controls package for TRAC-BD1, now available as part of Version 12, is highly recommended for future initialization calculations on the TLTA configuration provided the experiment to be modeled starts from steady state conditions.

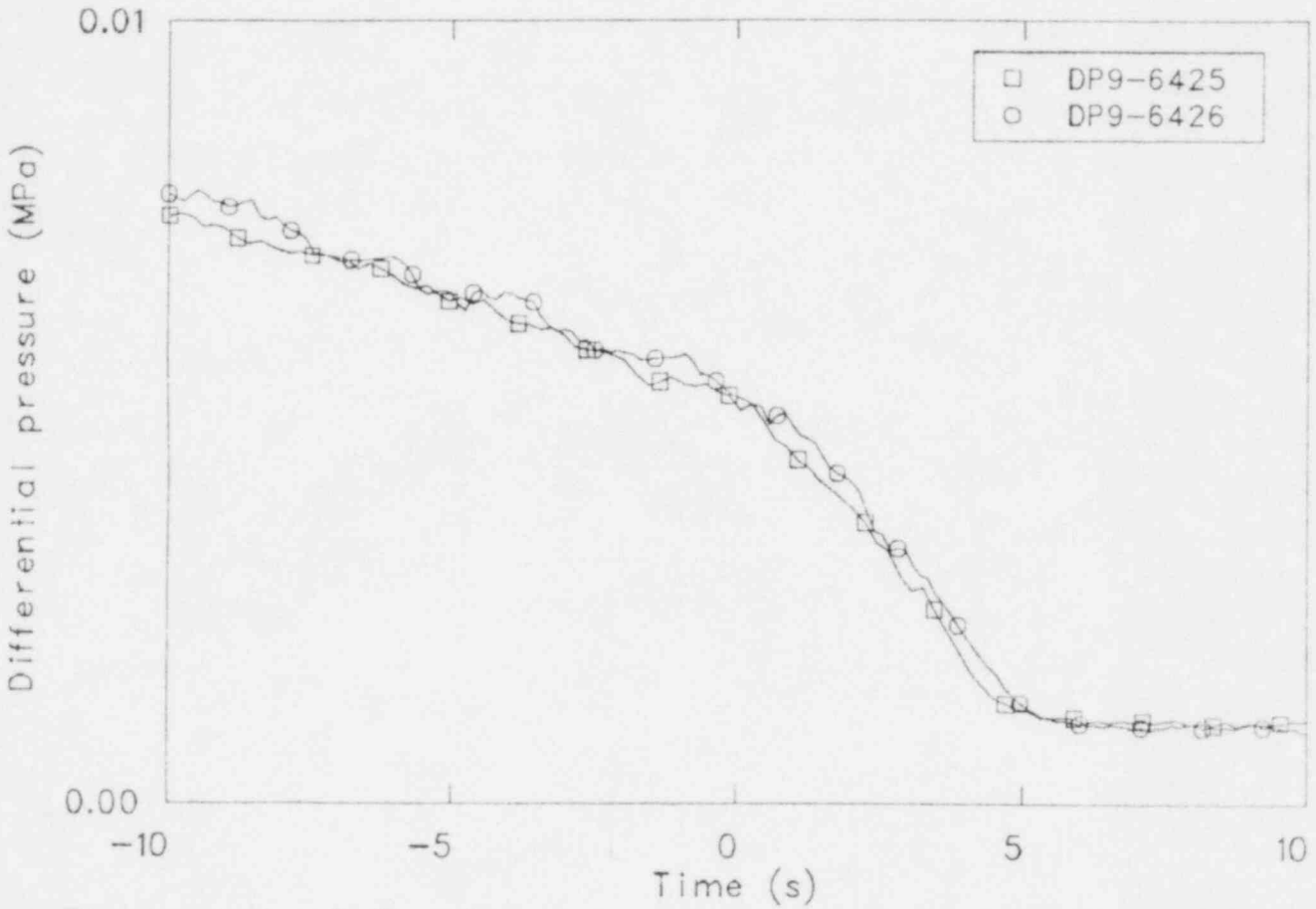

Figure A-1. Collapsing downcomer water levels at the onset of TLTA Tests 6425/6426.

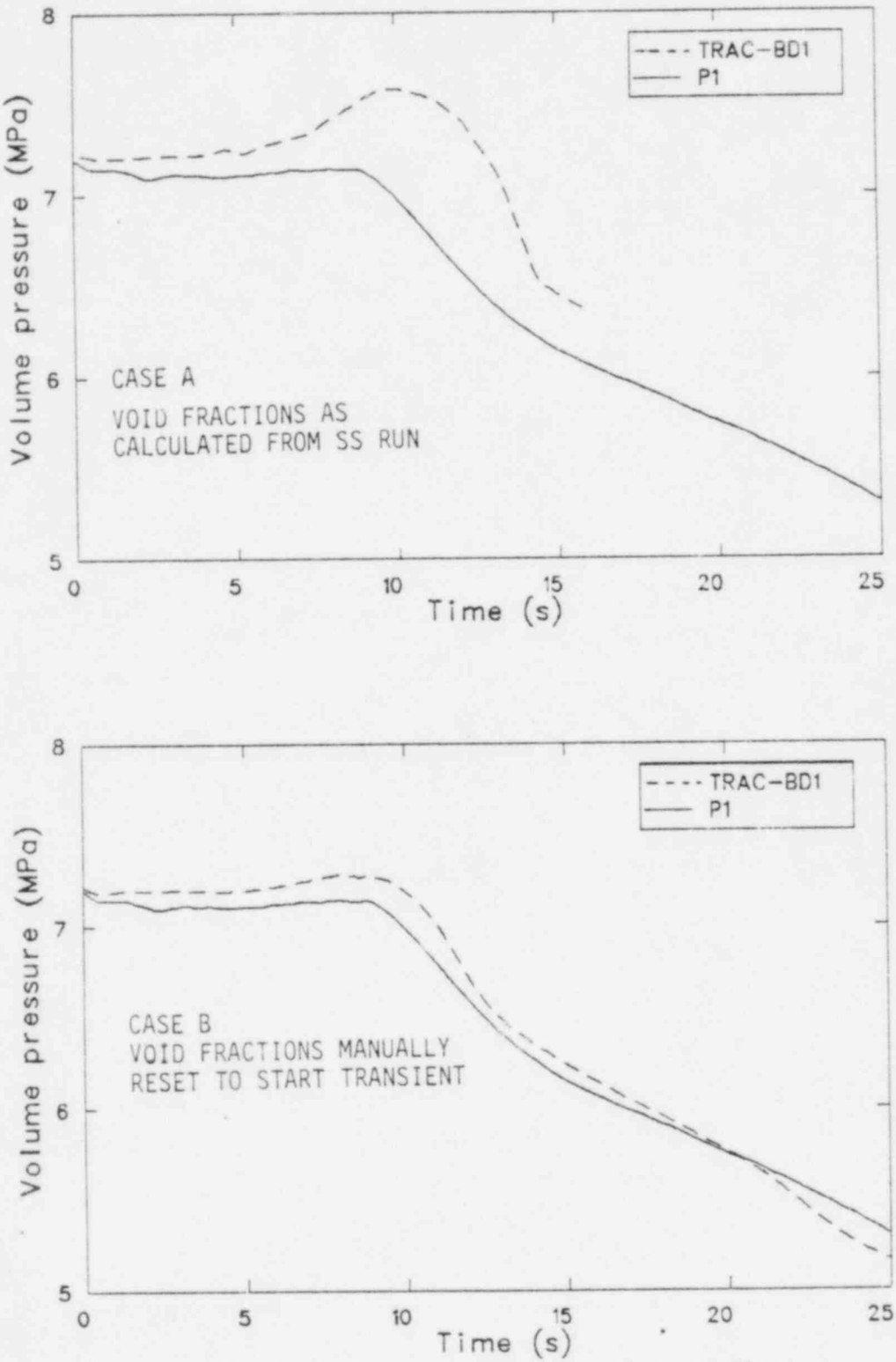

Figure A-2. Effect of downcomer void fractions on the transient calculation.

TABLE A-1. TEST 6426 SUBCOOLING AND VOID DISTRIBUTION INITIALIZATION

Vessel Level	Instrument	Measured Subcooling (K)	Calculated Subcooling (K)	Measured Void Fraction	Calculated Void Fraction
1	T01	14.7	10.9	0.0	0.0
2	T03	15.4	7.8	0.15[a]	0.079
3	T02 (GT)		7.8	0.0-0.15[a]	0.109
4			6.6		0.071
5			5.6	0.0	0.303
6	T07	5.5	5.6	0.0	0.289
7			0		0.906

a. These data are believed to be too high.

TABLE A-2. VOID FRACTION AND DEGREE OF SUBCOOLING IN THE LOWER PLENUM AND DOWNCOMER AS CALCULATED FROM THE STEADY STATE RUN--TLTA TEST 6425

Vessel Level	Instrument	Measured Subcooling (K)	Calculated Subcooling (K)	Derived[a] Void Fraction	Calculated Void Fraction
1	T01	10.9	10.5	0.0	0.0
2	T03	11.2	7.7	.0 - 0.1	0.095
3	T02 (Guidetube)	10.4	9.4	0.0 - 0.3	0.0
3	(Lower plenum)	--	7.6	--	0.135
4	T25 (Bypass)	7.2	7.9	0.0	0.051
5	T05 (Downcomer)	9.1	5.6	--	0.332
6	T06, T07 (2.20 m, 2.51 m)	0.0	5.7	0.0	0.308
	T08 (3.12 m)	0	--	--	--
7		--	0.0	--	0.895

a. These void fractions were derived from DP cell measurements.

TABLE A-3. DOWNCOMER INITIALIZATION FOR TLTA TEST 6425 USING A TRIP ON COLLAPSED LIQUID LEVEL[a]

Vessel Level	Measured Subcooling (K)	Calculated Subcooling (K)	Measured Void Fraction	Calculated Void Fraction
1	10.9	35.2	0.0	0.0
2	11.2	6.5	0.0 - 0.1	0.06
3	10.4	6.6	0.0 - 0.3	0.10
4	7.2	5.2	0.0	0.09
5	9.1	5.1	--	0.21
6	0.0	5.1	0.0	0.20
7	--	0.0	--	0.88

a. Collapsed liquid level set at 2.16 meters above the bottom of the downcomer, run time = 25 seconds reactor time.